

**Crosslinking studies on the conventional  
kinesin of *Neurospora crassa***

Dissertation  
der Fakultät für Biologie der  
Ludwig-Maximilians Universität  
München

vorgelegt von  
Katrin Hahlen  
aus Köln  
2004

## Ehrenwörtliche Versicherung

Diese Dissertation wurde selbständig und ohne unerlaubte Hilfsmittel angefertigt.

Katrin Hahlen

Erstgutachter:	PD Dr. Günther Woehlke
Zweitgutachter:	Prof. Dr. Charles N. David
eingereicht:	30.4.2004
Tag der mündlichen Prüfung:	22.7.2004

Meeting abstracts:

Hahlen K, Woehlke G and Schliwa M (2002)

"Testing kinesin's flexibility by crosslinking: Which domains need to be mobile to allow mobility?"

2nd Munich Symposium on Cell Dynamics

Hahlen K, Woehlke G and Schliwa M (2003)

"Testing kinesin's flexibility by crosslinking: Which domains need to be mobile to allow mobility?"

47th Annual Meeting of the Biophysical Society

Hahlen K, Schäfer F, Schliwa M and Woehlke G (2003)

"The role of the neck in fast kinesins"

Jahrestagung der Gesellschaften für Zellbiologie und Entwicklungsbiologie

Hahlen K, Schliwa M and Woehlke G (2003)

"Crosslinking kinesin's neck-linker to the motor core"

Workshop Molecular Motors and New Microscopic Techniques

The work presented here was carried out in the laboratory of Prof. Dr. Manfred Schliwa (Adolf-Butenandt-Institut of the Ludwig-Maximilians Universität, München) from January 2000 to December 2003. The work was supported by the Deutsche Forschungsgemeinschaft.

---

# Contents

<b>Abbreviations.....</b>	<b>V</b>
<b>1 Introduction.....</b>	<b>1</b>
1.1 Molecular Motors.....	1
1.1.1 Kinesin Superfamily.....	2
1.1.2 Similarities between Kinesins, Myosins and G-Proteins.....	3
1.2 Conventional Kinesins.....	4
1.2.1 Functional Anatomy.....	4
1.2.2 Model of Motion.....	6
1.3 <i>Neurospora crassa</i> Kinesins.....	7
1.4 Goals of the Present Work.....	8
<b>2 Materials and Methods.....</b>	<b>11</b>
2.1 Materials.....	11
2.1.1 Reagents and other Materials.....	11
2.1.2 Vectors.....	11
2.1.3 Bacterial Strains.....	11
2.1.4 Media and Cultivation of <i>E. coli</i> .....	11
2.2 Molecular Biology Methods.....	12
2.2.1 Agarose Gel Electrophoresis.....	12
2.2.2 DNA Extraction from Agarose Gels.....	12
2.2.3 Determination of DNA Concentration.....	12
2.2.4 Preparation of Plasmid DNA.....	12
2.2.5 DNA cleavage with Restriction Endonucleases.....	12
2.2.6 Ligation of DNA into Plasmid Vectors.....	13
2.2.7 Preparation and Transformation of Competent Cells.....	13
2.2.7.1 Preparation of Electrocompetent Cells.....	13
2.2.7.2 Electroporation.....	13
2.2.7.3 Preparation of SEM Competent Cells.....	13
2.2.7.4 Heat Shock Transformation.....	14
2.2.8 Identification of Transformed Clones in <i>E. coli</i> .....	14
2.2.9 Polymerase Chain Reaction (PCR).....	14
2.2.10 Introduction of Point Mutations.....	15
2.2.11 Oligonucleotides.....	15
2.2.11.1 Primers for the Removal or Insertion of Restriction Sites.....	15
2.2.11.2 Primers for the Removal of Cysteine residues 38, 59 and 307.....	15

---

2.2.11.3	Primers for the Insertion of Cysteine residues .....	16
2.2.11.4	Primers for the Construction of Monomeric Constructs .....	17
2.2.11.5	Primer for the Monomeric Human Kinesin Construct .....	17
2.2.11.6	Sequencing Primers .....	17
2.2.12	Generation of Constructs .....	17
2.2.13	Summary of all Measured Constructs.....	21
<b>2.3</b>	<b>Biochemical Methods .....</b>	<b>22</b>
2.3.1	SDS-Polyacrylamide Gel Electrophoresis (PAGE).....	22
2.3.2	Coomassie Staining .....	23
2.3.3	Colloidal Coomassie Staining.....	23
2.3.4	Expression of Kinesin Constructs.....	23
2.3.5	Protein Purification.....	23
2.3.5.1	Purification of Bacterially Expressed NcKin .....	23
2.3.5.2	Purification of Bacterially Expressed HsKin.....	24
2.3.5.3	Purification of Tubulin .....	25
2.3.6	Determination of Protein Concentration.....	27
2.3.7	Polymerisation of Microtubules .....	27
2.3.8	Determination of Microtubule Concentration.....	27
2.3.9	Microscopy .....	28
2.3.9.1	Video Enhanced Light Microscopy.....	28
2.3.9.2	Motility Assay .....	28
2.3.10	ATPase Assays .....	29
2.3.10.1	Basal ATPase Assay .....	29
2.3.10.2	Microtubule-activated ATPase Assay.....	30
2.3.10.3	Calculations for the ATPase Assay.....	31
2.3.11	mantADP Experiments .....	32
2.3.11.1	Loading of Kinesin Motor Domains with mantADP .....	32
2.3.11.2	Stoichiometry of Kinesin·mantADP Complexes .....	33
2.3.11.3	Fluorometric Measurements of mantADP Release.....	33
2.3.12	Sedimentation Assay .....	34
2.3.13	Measurements under Reducing and Oxidising Conditions.....	34
<b>3</b>	<b>Results.....</b>	<b>36</b>
3.1	Rationale for the Design of Crosslinking Mutants.....	36
3.1.1	Wild-type Constructs.....	37
3.1.2	Neck/Neck Crosslinking Constructs.....	38
3.1.3	Neck-Linker/Motor Core Crosslinking Constructs.....	39
3.1.3.1	NcKin .....	39
3.1.3.2	HsKin .....	40

---

3.1.4	$\alpha$ 4/ $\alpha$ 6 Crosslinking Constructs.....	40
3.2	Purification of Bacterially Expressed Kinesin.....	41
3.3	Proof of the Crosslink.....	43
3.3.1	Wild-type Constructs.....	45
3.3.2	Neck/Neck Crosslinking Constructs.....	45
3.3.3	Neck-Linker/Motor Core Crosslinking Constructs.....	46
3.3.4	$\alpha$ 4/ $\alpha$ 6 Crosslinking Constructs.....	47
3.4	Motility and ATPase Measurements.....	47
3.4.1	Wild-type Constructs.....	49
3.4.1.1	Motility.....	49
3.4.1.2	ATPase Activity.....	49
3.4.1.3	Summary of NcKin_wt.....	50
3.4.2	Neck/Neck Crosslinking Constructs.....	50
3.4.2.1	Motility.....	50
3.4.2.2	ATPase Activity.....	51
3.4.2.3	Summary of NcKin_S341C and NcKin_P342C.....	52
3.4.3	Neck-Linker/Motor Core Crosslinking Constructs.....	52
3.4.3.1	NcKin_S3C_A334C.....	52
3.4.3.1.1	Motility.....	52
3.4.3.1.2	ATPase Activity.....	53
3.4.3.1.3	Summary of NcKin_S3C_A334C.....	55
3.4.3.2	NcKin_A226C_E339C.....	56
3.4.3.2.1	Motility.....	56
3.4.3.2.2	ATPase Activity.....	56
3.4.3.2.3	Summary of NcKin_A226C_E339C.....	58
3.4.3.3	HsKin_K222C_E334C.....	59
3.4.3.3.1	ATPase Activity.....	59
3.4.3.3.2	Summary of HsKin_K222C_E334C.....	60
3.4.4	$\alpha$ 4/ $\alpha$ 6 Crosslinking Constructs.....	60
3.4.4.1	Motility.....	60
3.4.4.2	ATPase Activity.....	61
3.4.4.3	Summary of NcKin_T273C_S329C.....	63
3.4.5	Summary of All Constructs.....	64
3.5	Competitive Motility Assays.....	67
3.5.1	Competition of NcKin433_wt and NcKin433_S3C_A334C.....	67
3.5.2	Competition of NcKin433_wt and NcKin433_A226C_E339C.....	68
3.5.3	Summary of Competitive Motility Assays.....	68
3.6	Sedimentation Assays.....	69
3.6.1	Microtubule Affinities of NcKin433_A226C_E339C.....	71

3.6.2	Microtubule Affinities of NcKin343_A226C_E339C.....	72
3.7	Basal ATPase Measurements.....	73
3.7.1	NcKin_wt.....	74
3.7.2	NcKin433_S3C_A334C.....	74
3.7.3	NcKin_A226C_E339C.....	74
3.8	ADP Release Experiments.....	76
3.8.1	NcKin433_A226C_E339C.....	77
<b>4</b>	<b>Discussion .....</b>	<b>81</b>
4.1	Evidence for Crosslinking.....	81
4.2	Validity of Wild-type Constructs.....	82
4.3	Neck/Neck Crosslinking Constructs.....	82
4.3.1	Crosslinking Efficiency.....	82
4.3.2	Characterisation of Motile and Hydrolysis Properties.....	83
4.3.3	Comparison with other Neck/Neck Crosslinking Constructs.....	83
4.3.4	Neck Coiled-Coil Unwinding Hypothesis.....	84
4.4	Neck-Linker/Motor Core Crosslinking Constructs.....	85
4.4.1	Crosslinking Efficiency.....	85
4.4.2	Characterisation of Motility, Hydrolysis and Binding Properties.....	86
4.4.2.1	NcKin_S3C_A334C Constructs.....	86
4.4.2.2	NcKin_A226C_E339C Constructs.....	86
4.4.2.3	HsKin_K222C_E334C Constructs.....	88
4.4.3	Comparison of Neck-Linker/Motor Core Crosslinking Constructs.....	89
4.4.4	Neck-Linker Unzippering Hypothesis.....	90
4.5	$\alpha$ 4/ $\alpha$ 6 Crosslinking Constructs.....	93
4.5.1	Crosslinking Efficiency.....	93
4.5.2	Characterisation of Motile and Hydrolysis Properties.....	93
4.5.3	Rotation of Helix $\alpha$ 4 against the Motor Core.....	94
4.6	Future Prospects.....	95
<b>5</b>	<b>Summary.....</b>	<b>97</b>
5.1	Summary.....	97
5.2	Zusammenfassung.....	98
<b>6</b>	<b>References.....</b>	<b>100</b>
	<b>Acknowledgements.....</b>	<b>108</b>
	<b>Curriculum vitae .....</b>	<b>109</b>

---

## Abbreviations

ACES	N-[2-acetamido]-2-aminoethanesulfonic acid
ADP	adenosine-5'-diphosphate
AMP-PNP	adenosine-5'-[ $\beta,\gamma$ -imido]-triphosphate
ATP	adenosine-5'-triphosphate
bp	base pairs
BRB80	Brinkmann reconstitution buffer
BSA	bovine serum albumin
cpm	counts per minute
D	daltons
DNA	deoxyribonucleic acid
dNTP	deoxyribonucleotide triphosphate
DMSO	dimethylsulfoxide
DTNB	5,5'-dithiobis(2-nitrobenzoic acid)
DTT	dithiothreitol
$E_x$	extinction at wavelength x [nm]
$\epsilon$	extinction coefficient
EDTA	ethylene-diamine-tetraacetic acid
EGTA	ethyleneglycol-bis-(2-aminoethylether)-N,N'-tetraacetic acid
FPLC	fast performance liquid chromatography
g	gravity
GFP	green fluorescence protein
GTP	guanosin-5'-triphosphate
H <sub>2</sub> O	distilled water
hktail	amino acids 342-546 of the tail domain of HsKin
HsKin	conventional kinesin of <i>Homo sapiens</i>
IPTG	isopropyl- $\beta$ -thiogalactopyranoside
$K_{bi,ADP}$	bimolecular binding rate [ $\mu\text{M}^{-1}\text{s}^{-1}$ ]
$K_{bi,ATPase}$	apparent bimolecular binding rate ( $k_{cat} / K_{0.5,MT}$ ) [ $\mu\text{M}^{-1}\text{s}^{-1}$ ]
$K_{bi,ratio}$	chemical processivity ( $K_{bi,ATPase} / K_{bi,ADP}$ )
$k_{cat}$	ATP turnover per second and head

---

$K_d$	dissociation constant
$K_{0.5,MT}$	half maximal activation constant
LDH	lactate dehydrogenase
M	molarity [mol/l]
mantADP	2'-(3')-0-[N-methylanthraniloyl]adenosine-5'-diphosphate
mantATP	2'-(3')-0-[N-methylanthraniloyl]adenosine-5'-triphosphate
MM	molecular mass [D]
$M_r$	molecular weight = relative molecular mass (dimensionless)
mRNA	messenger ribonucleic acid
MT	microtubules
NADH	nicotine adenine dinucleotide
NcKin	conventional kinesin of <i>Neurospora crassa</i>
NEM	N-ethylmaleimide
$OD_x$	optical density at wavelength x [nm]
PAA	polyacrylamide
PAGE	polyacrylamide gel electrophoresis
PCR	polymerase chain reaction
PEP	phosphoenolpyruvate
pH	negative decadic logarithm of proton concentration
PI	protease inhibitor
PIPES	piperazine-N,N'-bis-[2-ethanesulfonic acid]
PK	pyruvate kinase
rpm	revolutions per minute
SDS	sodium dodecyl sulfate
Tris	tris-hydroxymethyl-ammoniummethane
$V_{max}$	maximum extinction rate
v/v	volume per volume

Unless stated otherwise, SI-units, derived units and the decimal multiple of SI-units were used.

# 1 Introduction

## 1.1 Molecular Motors

Random diffusion is far too slow to move molecules over large distances in eukaryotic cells and cannot localise them to specific regions of the cell. Localisation to a site within the cell requires active movement, usually aided by cytoskeletal motor proteins - the myosins, kinesins or dyneins. However, specific directional transport of molecules, vesicles and organelles is only one of the functions of molecular motors. The three large super-families of cytoskeletal motor proteins perform a variety of different tasks in the cell, including muscle contraction, movements involved in cell division (assembly of, and force generation in, the meiotic and mitotic spindle, chromosome alignment and segregation), nuclear fusion, polarised growth and morphogenesis, movement of cilia and flagella, cytoskeletal organisation and dynamics [Schliwa & Woehlke 2003].

Cytoskeletal motor proteins are specially built to perform work in the cell: one region of the protein binds to a filament (F-actin in case of myosins and microtubules in case of kinesins and dyneins), hydrolyses ATP and exerts force onto the filament, while other regions are responsible for achieving the different cellular functions such as attachment to cargo for transport or anchoring for force generation. They coordinate the hydrolysis of ATP with binding to, and movement along, a filament and thus convert the chemical energy derived from ATP hydrolysis directly into mechanical work. How do motors capture the energy released by nucleotide hydrolysis and turn it into work? Motor proteins are apparently capable of sensing, and responding to, the presence or absence of the  $\gamma$ -phosphate in ATP, and then transmit this information along a pathway of increasingly larger conformational changes that culminates in a force-generating event. Thus, an understanding of the motor mechanism requires the identification of the force-producing structural changes in the motor, and the steps in the hydrolysis cycle at which they occur. Molecular motors of the kinesin class have served as favourable models because their motor domain is very small compared to myosins or even dyneins, and can easily be expressed in bacteria.

### 1.1.1 Kinesin Superfamily

Kinesin was first identified in 1985 [Brady; Vale *et al.*] as a microtubule-based vesicle motor. This type of kinesin has been termed conventional kinesin, and has been found in different animal and fungal species [Woehlke & Schliwa 2000]. Shortly afterwards, other proteins were discovered that share a high degree of amino acid identity in their motor domain but are completely unrelated in their non-motor domains. The term motor domain refers to the force-producing element of the protein, which is itself divided into two major parts: One, the globular catalytic core, is conserved throughout the superfamily [Vale & Fletterick 1997]. The second, termed the neck region, consists of ~40 amino acids. It is conserved only within certain kinesin classes and appears to work in concert with the catalytic core to produce movement. Beyond the motor domain, many kinesin proteins contain a long  $\alpha$ -helical coiled-coil domain termed the stalk. Finally, there is often an additional globular domain, the tail. It is thought to target the motor to a particular cargo. The kinesin superfamily already contains more than 400 members [Schoch *et al.* 2003] and can be divided into at least nine subfamilies according to the sequence homology of the motor domains [Hirokawa 1998; Kim & Endow 2000; Lawrence *et al.* 2002; Dagenbach & Endow 2004]. The cellular functions of kinesin-related proteins include transport of mRNA, vesicles and organelles, chromosome alignment and segregation, microtubule sliding and crosslinking, and regulation of microtubule dynamics [Hirokawa 1998; Goldstein & Philp 1999]. Much of this versatility in function can be attributed to the unique structural properties of several forms of the mature kinesin molecule.

Firstly, the kinesin subfamilies can be classified into three major groups corresponding to the position of the catalytic core. The catalytic core of N-type variants is located at the amino terminus of the molecule, while it is positioned at the carboxy terminus for C-type variants and at an internal position for I-type variants [Vale & Fletterick 1997]. The direction that a kinesin moves is dependent upon its neck sequence [Endow 1999]. Thus far, all N-type kinesins move to the microtubule plus-end, while C-type kinesins are minus-end directed [Lawrence *et al.* 2002]. The directional movement of kinesins combined with the fact that microtubules are organised within a normal cell with the minus-ends arranged in the centre and the plus-ends pointing towards the periphery of the cell allows for transport to specific compartments of the cell.

Secondly, kinesins occur in different oligomerisation states. Some kinesin proteins function as a single polypeptide chain (monomer), others assemble into homodimers (two identical polypeptide chains), heterodimers (two distinct polypeptide chains) or even tetrameric

---

structures (four polypeptide chains) [Vale & Fletterick 1997]. In addition, some dimeric forms also contain tightly associated subunits.

### 1.1.2 Similarities between Kinesins, Myosins and G-Proteins

Myosins and kinesins have first been thought to be totally unrelated, because they move along different tracks and their motor domains differ considerably in size (800 amino acids in myosins and 350 amino acids in kinesins [Woehlke & Schliwa 2000]). Additionally, they have virtually no amino acid sequence identity. Thus, the striking structural similarity of the core of their catalytic domains came as a surprise [Kull *et al.* 1996]. Furthermore, several features of the myosin/kinesin core have intriguing similarities to structural elements of G-proteins [Vale 1996]. G-proteins are a diverse group of molecular switches that regulate information flow in signal transduction pathways and orchestrate an orderly sequence of interactions in protein synthesis, protein translocation, and trafficking of vesicles [Vetter & Wittinghofer 2001]. They all are protein machines, hydrolysing either ATP (kinesins and myosins) or GTP (G-proteins). Essential to their mechanism is a nucleotide-dependent conformational change, which enables them to change affinity for target proteins (microtubules or F-actin for motors and various target proteins for G-proteins). The similarity is particularly apparent in the nucleotide active site, which consists of three loops, called the P-loop, switch I and switch II (Figure 1.1). The P-loop is responsible for nucleotide binding, while the  $\gamma$ -phosphate groups are flanked by the switch regions. The switch regions were named so because they can detect whether NTP or NDP is bound to the active site and then respond by undergoing a conformational change that depends on the nucleotide state [Woehlke 2001]. Small movements of the  $\gamma$ -phosphate sensors are transmitted to distant regions of the protein via a long helix (switch II helix or  $\alpha 4$  in kinesin), which interacts with the polymer binding sites and the mechanical elements [Vale & Milligan 2000]. This principle leads to a strict nucleotide dependence of the affinity of kinesin to microtubules. Binding is strongest in the absence of nucleotide or with ATP bound, while it is weak with ADP bound to the nucleotide pocket [Crevel *et al.* 1996]. Vice versa, binding to microtubules strongly accelerates kinesin's ATP turnover. Hence, the communication pathway via helix  $\alpha 4$  between microtubule binding site and nucleotide active site works in both directions [Kull & Endow 2002].

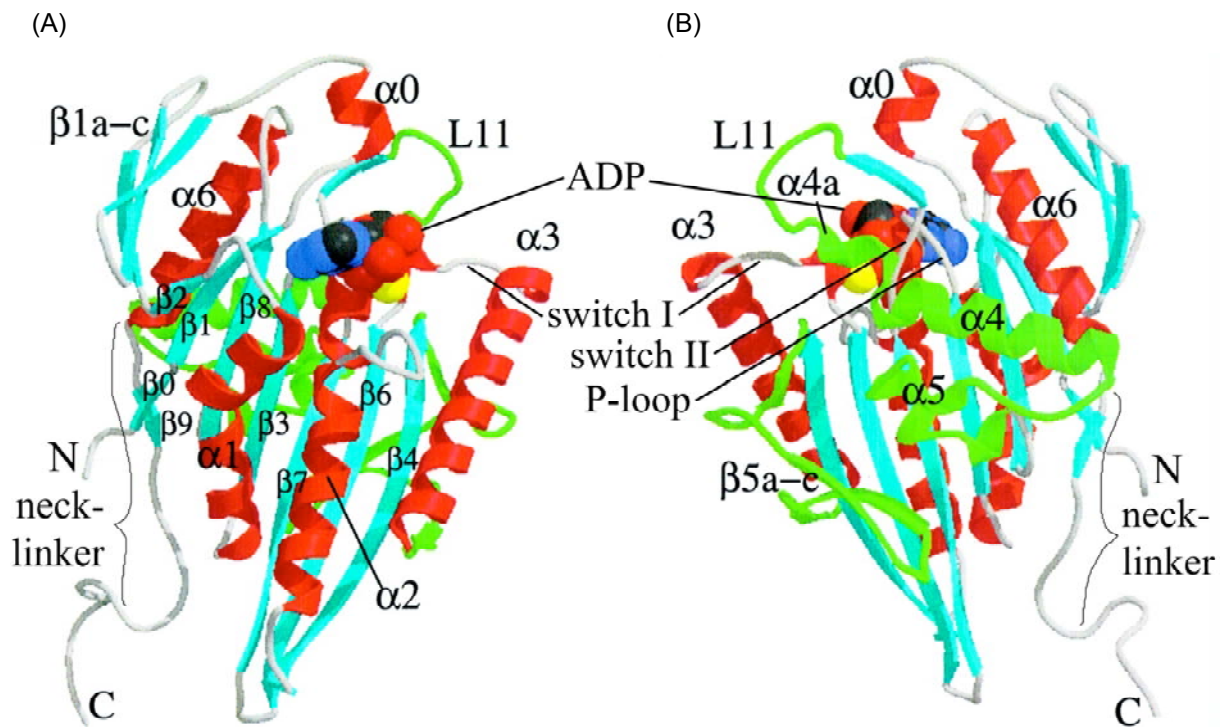


**Figure 1.1:** Crystal structure of monomeric NcKin containing amino acids 1-355 [from Song *et al.* 2001]. (A) front view (B) rear view

It is a globular structure with a central  $\beta$ -sheet of eight strands ( $\beta 1$ - $\beta 8$ ) and three  $\alpha$ -helices on either side ( $\alpha 1$ - $\alpha 6$ ).  $\beta$ -strands are shown in light blue,  $\alpha$ -helices in red. The elements putatively involved in microtubule binding ( $\beta 5$ , L11- $\alpha 4$ -L12- $\alpha 5$ ) are coloured in green. ADP is shown as a space-filling model. Only  $\beta$ -strand 9 of the neck-linker is visible. The rest of the neck-linker and the first two heptads of the predicted neck  $\alpha$ -helix 7 (amino acids 333-355) are unordered.

## 1.2 Conventional Kinesins

### 1.2.1 Functional Anatomy

Native conventional kinesin contains two heavy chains of 110-140 kD and two associated light chains in the size range of 60-80 kD [Schliwa 1989]. The light chains are not essential for kinesin's motility [Yang *et al.* 1990] but probably have regulatory and cargo binding functions [Stenoien & Brady 1997; Gindhart *et al.* 1998; Verhey *et al.* 1998]. They bind to the heavy chains at the coiled-coil tail region [Diefenbach *et al.* 1998]. The domain organisation of the heavy chains is depicted in Figure 1.2. At the N-terminus, ~320 amino acids form the globular catalytic core, also called head domain. It contains the microtubule and nucleotide binding sites [Woehlke *et al.* 1997] and its three-dimensional structure has been solved [Kull *et al.* 1996]. The following neck domain is further divided into the neck-linker and the coiled-coil neck region. In certain crystal structures the neck-linker has an extended structure

consisting of two  $\beta$ -sheets and connects the catalytic core to the following  $\alpha$ -helical coiled-coil domains [Sack *et al.* 1997]. The neck-linker adopts different positions relative to the catalytic core depending on the nucleotide state [Rice *et al.* 1999]. Therefore, it is proposed to be the mechanical transducer element converting the chemical energy of ATP hydrolysis into kinetic energy. The adjacent neck region forms a two-stranded  $\alpha$ -helical coiled-coil which in animal conventional kinesins is sufficient to dimerise the two heavy chains. This was shown by studies on synthetic peptides [Morii *et al.* 1997; Tripet *et al.* 1997], X-ray crystallography of a dimeric kinesin [Kozielski *et al.* 1997] and dimerisation studies on truncated kinesins [Jiang *et al.* 1997]. After the neck domain follows the flexible hinge domain [Seeberger *et al.* 2000]. Further C-terminally, the approximately 50 nm long coiled-coil stalk domain is interrupted by a second flexible region, called the kink [de Cuevas *et al.* 1992]. The kink allows the molecule to bend [Hirokawa *et al.* 1989]. The C-terminus comprises the tail region that is further divided into an approximately 20 nm long coiled-coil region and a final globular domain [Seiler *et al.* 2000]. The tail region has regulatory and cargo binding functions [Coy *et al.* 1999; Friedman & Vale 1999; Kirchner *et al.* 1999a; Hackney & Stock 2000; Seiler *et al.* 2000; Verhey & Rapoport 2001]. The tail coiled-coil either binds its cargo directly or indirectly via the associated light chains. The molecule can fold back, bringing the tail close to the N-terminus. In this folded conformation, ATP turnover is inhibited by the IAK motif in the globular tail.

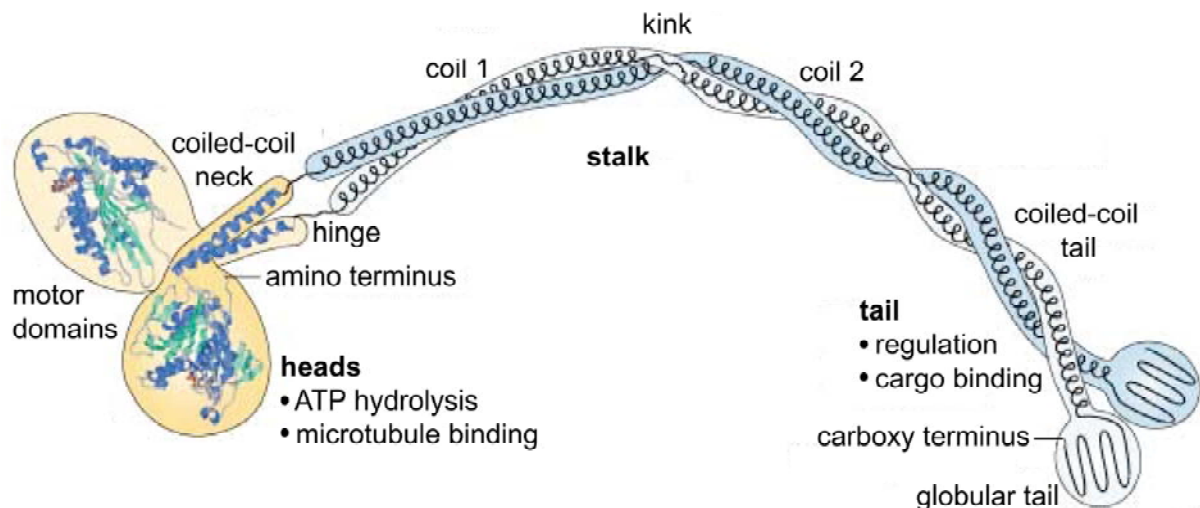


**Figure 1.2: Domain organisation of the conventional kinesin heavy-chain dimer [from Woehlke & Schliwa 2000].**

The crystal structure of a dimeric rat kinesin construct [Kozielski *et al.* 1997] forms the basis of this sketch with respect to the two head (amino acids 1-320) and neck (~ 40 amino acids) domains. The hinge domain has been shown to be flexible [Seeberger *et al.* 2000], while the rodlike stalk regions (~50 nm) form extended coiled-coil structures, separated by a flexible kink [de Cuevas *et al.* 1992]. The tail domain consists of a short coiled-coil (~20 nm) and a globular part [Seiler *et al.* 2000]. The overall length of the molecule is approximately 80 nm [Schliwa 1989].

### 1.2.2 Model of Motion

Conventional kinesin moves along microtubules in 8 nm steps, representing the distance between adjacent tubulin dimers [Svoboda *et al.* 1993]. For each step it hydrolyses one molecule of ATP [Hua *et al.* 1997; Schnitzer & Block 1997]. Thereby it is able to take many sequential steps without falling off the microtubule, a property termed processivity [Howard *et al.* 1989]. Processivity of conventional kinesin requires a dimeric molecule with two motor domains. A motor that possesses just one head, but otherwise has unchanged neck and stalk regions, is still able to maintain motility if several molecules cooperate, but it fails to operate as a single molecule because it seems to fall off after a single step [Berliner *et al.* 1995; Hancock & Howard 1998; Young *et al.* 1998]. Therefore, it is thought that conventional kinesin motility relies on a precise coordination between the two motor domains where one head proceeds to the next binding site while the motor remains tethered to the microtubule by the other, attached head. Conventional kinesin can move processively because, at each time point, at least one head is microtubule-bound. According to the ‘alternating site model’, kinesin uses a nucleotide-dependent change in its affinity for the microtubule to regulate the behaviour of the two heads [Hackney 1994a; Ma & Taylor 1997a; Gilbert *et al.* 1998]. In solution, a kinesin dimer contains one ADP per head. Upon microtubule binding, only one head (light blue in Figure 1.3) locks onto the microtubule and loses its ADP. This head can detach again only if it binds and hydrolyses a new ATP molecule. During this hydrolysis process, the docking of the neck-linker of the leading head is thought to allow the trailing head (dark blue) to bind to the next microtubule binding site, where it loses its ADP and holds on tight [Sablin & Fletterick 2001]. In this intermediate state, both heads are bound to adjacent tubulin binding sites. After finishing hydrolysis in a weakly bound ADP state, the light blue head detaches from the microtubule while the other head holds on. At this point, the heads have exchanged their roles. So processive kinesin movement is achieved by three processes: first, a modulation of microtubule affinity through ATP hydrolysis, second, a mechanism that keeps the two heads out of phase and, third, a ‘power stroke’ linked to the hydrolysis cycle. In conventional kinesin, the power stroke entails conformational changes in the neck-linker region [Rice *et al.* 1999]. This hand-over-hand model is the most widely accepted model for the processive movement of conventional kinesin [Endow & Barker 2003], although there are also other models like the inchworm model [Hua *et al.* 2002]. While the inchworm model can explain certain features of kinesin behaviour, there is mounting evidence supporting the hand-over-hand model [Asbury *et al.* 2003; Kaseda *et al.* 2003; Yildiz *et al.* 2004; Schief *et al.* 2004].

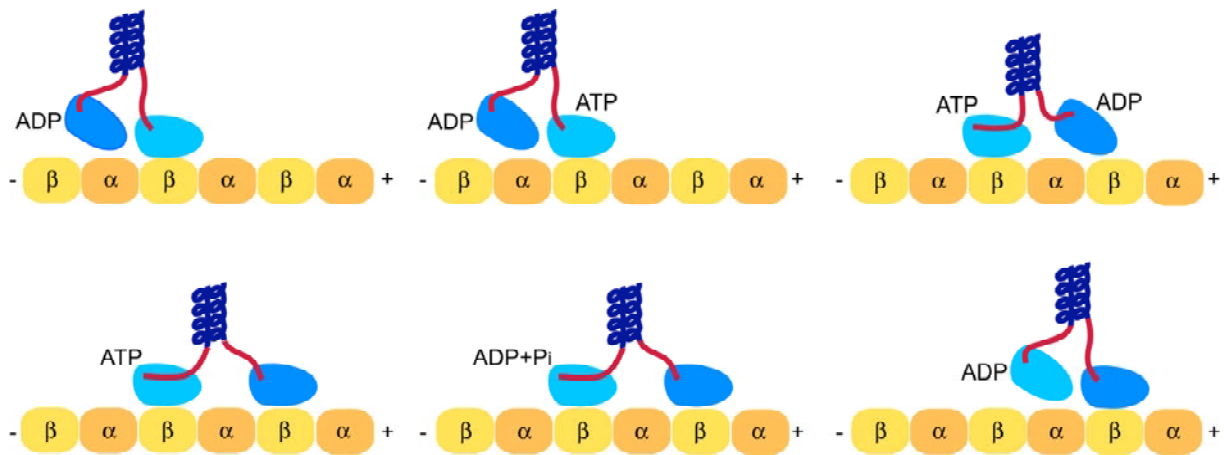


**Figure 1.3:** Scheme of the hand-over-hand model explaining the enzymatic and mechanical cycle of conventional kinesin.

Alternating tubulin subunits ( $\alpha$ ,  $\beta$ ) of a protofilament are coloured in yellow and orange. Polarity of microtubule is indicated by + and -. The kinesin dimer is depicted only up to its coiled-coil neck domain. The neck-linker domain is shown in red and switches between a docked and undocked conformation. The two catalytic motor domains are coloured in different shades of blue to illustrate their alternating relative positions (leading and trailing positions). Explanations see text.

### 1.3 *Neurospora crassa* Kinesins

Filamentous fungi grow in a highly polarised fashion to form extremely elongated hyphae. Long-distance transport mechanisms therefore are indispensable for growth at the tip of hyphae [Xiang & Plamann 2003]. Potential candidates are members of the kinesin superfamily. Different kinesin proteins have been isolated from various filamentous fungi, such as *Aspergillus nidulans* [Enos & Morris 1990; O'Connell *et al.* 1993; Requena *et al.* 2001], *N. crassa* [Steinberg & Schliwa 1995], *Ustilago maydis* [Lehmler *et al.* 1997], *Syncephalastrum racemosum* [Steinberg 1997], *Nectria haematococca* [Wu *et al.* 1998] and *Thermomyces lanuginosus* [Sakowicz *et al.* 1999]. Representatives of almost all known kinesin subfamilies have been found in fungi [Schoch *et al.* 2003]. In *N. crassa* 10 kinesins have been identified [Schoch *et al.* 2003], which is more than in the yeast *Saccharomyces cerevisiae* (6) [Hildebrandt & Hoyt 2000] but substantially less than in human (45) [Miki *et al.* 2001] or the higher plant *Arabidopsis thaliana* (61) [Reddy & Day 2001]. *N. crassa* possesses one conventional kinesin, termed NcKin, that has been discovered in 1995 [Steinberg & Schliwa]. Its domain structure is identical to conventional kinesins from animals [Kirchner *et al.* 1999b], but it lacks associated light chains [Steinberg & Schliwa 1995]. Cargo binding is achieved directly by the coiled-coil tail region, while the globular tail region is responsible for the inactivation of the ATPase activity when no cargo is bound [Kirchner *et*

*al.* 1999a; Seiler *et al.* 2000]. Another difference to animal conventional kinesins is the ~4fold higher velocity of NcKin in *in vitro* motility assays [Kirchner *et al.* 1999b]. Like its animal counterparts NcKin moves processively in discrete 8 nm steps along the microtubule [Crevel *et al.* 1999]. The highly conserved sequence of the catalytic domains of different species is reflected in almost identical secondary and tertiary structures [Kull *et al.* 1996; Sack *et al.* 1997; Song *et al.* 2001]. However, the sequence of the neck region of NcKin diverges from animal conventional kinesins and seems to be fungal-specific [Lehmler *et al.* 1997; Grummt *et al.* 1998; Wu *et al.* 1998; Requena *et al.* 2001]. Studies of synthetic peptides [Deluca *et al.* 2003] and dimerisation studies [Kallipolitou *et al.* 2001] show that in contrast to animal kinesins the neck region of NcKin alone is not sufficient for the maintenance of a stable  $\alpha$ -helical coiled-coil. Fungal conventional kinesins are involved in polarised growth and secretion [Xiang & Plamann 2003]. The cellular function of NcKin has been investigated in a deletion mutant [Seiler *et al.* 1997; Seiler *et al.* 1999]. While knockouts of the kinesin heavy chain in animals were lethal [Saxton *et al.* 1991; Gho *et al.* 1992; Patel *et al.* 1993; Tanaka *et al.* 1998], conventional kinesin is nonessential in fungi [Lehmler *et al.* 1997; Seiler *et al.* 1997; Wu *et al.* 1998]. NcKin null cells exhibited severe alterations in cell morphogenesis [Seiler *et al.* 1997]: Cell growth was reduced but not impeded and growth abnormalities like an increase in hyphal diameter, a convoluted shape and a high incidence of branching occurred. The apical movement of submicroscopic, secretory vesicles to the Spitzenkörper, an organelle in the hyphal tip known to be linked to cell elongation, was defective [Seiler *et al.* 1999]. Though slow and abnormal, growth still persisted, the lack of NcKin thus can be compensated at least partly by other processes.

#### 1.4 Goals of the Present Work

The crystal structure of dimeric rat kinesin [Kozielski *et al.* 1997] does not allow simultaneous binding of both catalytic cores to two adjacent binding sites on the microtubule, which are spaced 8 nm apart. Concurrent binding of both heads is prevented because their microtubule binding regions (i) do not lie in the same plane (the two heads are related by a rotation of ~120°) [Kozielski *et al.* 1997] and (ii) are separated only by roughly 5 nm [Block 1998]. Since a two-heads-bound intermediate is thought to be critical for processive motion [Vale & Milligan 2000], some element in the dimeric kinesin structure must ‘melt’ during the enzymatic cycle [Block 1998]. Two theories have been advanced for this conformational

change (Figure 1.4). The first proposes a partial unwinding of the neck coiled-coil [Tripet *et al.* 1997; Hoenger *et al.* 1998; Thormählen *et al.* 1998]. Transient melting and rewinding of the neck coiled-coil alternates according to two-headed or single-headed binding to the microtubule (Figure 1.4 A). However, exchanging the native neck sequence for a stable coiled-coil sequence does not abolish processivity [Romberg *et al.* 1998; F. Bathe, personal communication]. A crosslinking study also shows that processive movement is not prevented if the two necks are permanently connected [Tomishige & Vale 2000]. These results argue against the neck coiled-coil melting theory. The second theory involves an unzipping of the neck-linker from the motor core [Romberg *et al.* 1998]. Folding of the neck-linker of the leading head from an orientation towards the tip of the head to the opposite broad end of the

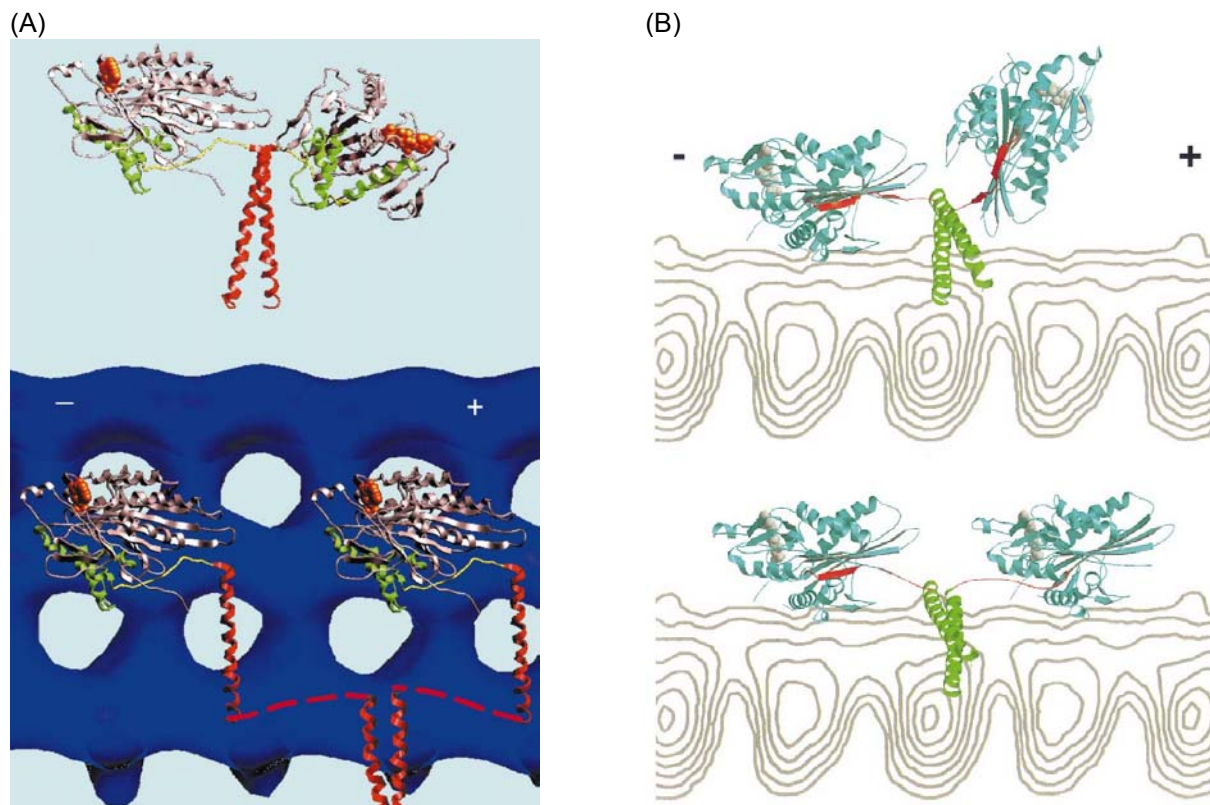


**Figure 1.4:** Two structural models for how the kinesin dimer might span the distance between adjacent  $\alpha/\beta$  tubulin binding sites. (A) Neck coiled-coil unwinding hypothesis [from E. Mandelkow & Johnson 1998] (B) Neck-linker unzipping hypothesis [from Romberg *et al.* 1998]

The upper images show the three-dimensional structure of a dimeric kinesin construct from rat [Kozielski *et al.* 1997] either free in solution (A) or with one head bound to the microtubule (B). In the lower images both heads are modeled onto the microtubule forcing some structural changes in the dimeric molecule. The microtubule plus end is at the right. Colour coding in (A): ADP = orange ball-and-stick model, core motor domain = gray and green, microtubule binding region = green, neck-linker region = yellow, neck helices = red, hinge domain = broken red line, stalk helices = red, microtubule surface = dark blue. Colour coding in (B): ADP = gray ball-and-stick model, core motor domain = blue, neck-linker region = red, neck coiled-coil = green, side view of a microtubule protofilament = gray.

---

head ( $\sim 180^\circ$ ) enables two-headed binding while redocking of the neck-linker onto the tip propels the lagging head to the front (Figure 1.4 B). Crystal structures of the same kinesin construct exist which show the neck-linker either in a docked [Sindelar *et al.* 2002] or disordered [Kull *et al.* 1996] conformation. Additionally, labeling studies reveal switching of the neck-linker between a docked and a mobile state [Rice *et al.* 1999; Sindelar *et al.* 2002]. Kikkawa *et al.* [2001] suggest that positioning of the neck-linker depends on a rotation of the switch II cluster, containing helix  $\alpha 4$ , relative to the motor core.

The goal of the present work was to test these two models for kinesin's processivity in NcKin. Therefore, cysteine residues were introduced in the neck coiled-coil or the neck-linker and the adjacent tip of the motor core. Furthermore, mutants were engineered containing cysteine residues in helices  $\alpha 4$  and  $\alpha 6$ . Under oxidising conditions these cysteine residues were predicted to form disulfide bridges, thereby preventing potential conformational changes in these regions. The effect of crosslinking on the enzymatic and mechanical motor functions was assayed by measuring ATP turnover rates and velocities of motion. Some mutants were characterised further by microtubule co-sedimentation assays and ADP release assays.

---

## 2 Materials and Methods

### 2.1 Materials

#### 2.1.1 Reagents and other Materials

Unless stated otherwise chemicals were obtained from Biorad (München), Fluka (Buchs, Schweiz), Merck (Braunschweig), Roche (Mannheim), Carl Roth (Karlsruhe), Serva (Heidelberg), Sigma-Aldrich (Deisenhofen) and were of p. a. quality. Other materials were supplied mainly by Greiner (Frickenhausen), Nunc (Wiesbaden), Qiagen (Hilden) and Sarstedt (Nümbrecht).

#### 2.1.2 Vectors

for *Neurospora crassa* kinesin constructs: pT 7-7 (Tabor),  
pNk433 [Kallipolitou *et al.* 2001]  
for human kinesin constructs: pET 17b (Novagen, Madison)

#### 2.1.3 Bacterial Strains

*Escherichia coli* strains DH5 $\alpha$  [Sambrook *et al.* 1989] and XL1-Blue (Stratagene, Amsterdam) were used for cloning. *E. coli* strain BL21 CodonPlus (DE)-RIL [Studier *et al.* 1990] (Stratagene) was used for protein expression.

#### 2.1.4 Media and Cultivation of *E. coli*

*E. coli* cells were grown according to standard methods [Sambrook *et al.* 1989] on agar plates or shaking at 240 rpm at 37°C. For protein expression the temperature was reduced to 22°C.

SOB: 2% tryptone, 0.5% yeast extract, 10 mM NaCl, 2.55 mM KCl

LB: 1% tryptone, 0.5% yeast extract, 0.5% NaCl

agar plates: 1.5% agar in LB medium

TPM: 2% bacto-tryptone, 1.5% yeast extract, 0.8% NaCl, 0.2% Na<sub>2</sub>HPO<sub>4</sub>,  
0.1% KH<sub>2</sub>PO<sub>4</sub>, after autoclaving: 0.2% glucose

---

## 2.2 Molecular Biology Methods

### 2.2.1 Agarose Gel Electrophoresis

The separation of DNA fragments according to their size was performed using gels with 0.8% to 2% agarose in TAE buffer. For detection of DNA fragments 0.05 µg/ml ethidium bromide was added to the liquid agarose. Samples were mixed with 1/5 volume of 6x DNA loading dye before loading. Gels were run with 75 V. Bands were detected by UV illumination and documented with the Eagle Eye II CCD camera system (Stratagene, Heidelberg).

50x TAE: 2 M Tris, 0.57% acetic acid, 50 mM EDTA, pH 8.0

6x DNA loading dye: 30% glycerol, 0.25% bromphenol blue, 0.25% xylene cyanol

### 2.2.2 DNA Extraction from Agarose Gels

DNA bands were excised with a scalpel, transferred to sterile Eppendorf vials, weighed and purified with Qiaquick columns (Qiagen, Hilden) following the instructions of the manufacturer.

### 2.2.3 Determination of DNA Concentration

DNA concentration in solutions was determined by measuring the extinction at 260 nm ( $E_{260}$ ) of the diluted sample after calibration of the photometer with a buffer control. An  $E_{260}$  of 1.0 corresponds to 50 µg/ml of doublestranded DNA [Sambrook *et al.* 1989].

### 2.2.4 Preparation of Plasmid DNA

Plasmid DNA was prepared from overnight shaking cultures using the Qiagen-Plasmid-Kit (Qiagen, Hilden). For small scale preparations (3 ml) the manufacturer's manual for 'mini-preps' excluding the Tip20-column was followed, for large scale preparations (100-200 ml) the manual for 'midi-preps'.

### 2.2.5 DNA cleavage with Restriction Endonucleases

Restriction digests were performed using the buffer system and temperature recommended by the manufacturer (New England Biolabs, Frankfurt). Reaction volume was at least 15 µl. 1-5 units enzyme per µg DNA was used. 1 mg/ml casein was added. Incubation time was at least 1 hour. Completion of the digests was analysed on agarose gels (2.2.1).

## 2.2.6 Ligation of DNA into Plasmid Vectors

Vector and DNA fragments were cleaved (2.2.5), separated on agarose gels by electrophoresis (2.2.1), and extracted from agarose gels (2.2.2). DNA fragments were ligated with T4 DNA ligase (New England Biolabs, Frankfurt) in a volume of 15  $\mu$ l at 16°C for 2 hours or overnight using the buffer system supplied by the manufacturer. 50 ng of vector were incubated with no insert (religation control), with equimolar amount of insert and with a fourfold molar excess of insert. 5  $\mu$ l of the reaction was transformed into competent *E. coli* cells (2.2.7.2, 2.2.7.4).

## 2.2.7 Preparation and Transformation of Competent Cells

### 2.2.7.1 Preparation of Electrocompetent Cells

1 l LB medium was inoculated with 10 ml of an *E. coli* overnight culture and grown to an OD<sub>600</sub> of 0.6 at 37°C under vigorous shaking. All flasks and solutions subsequently used were sterilised and cooled to 4°C. Quality of the competent cells depended on a consequent cooling. Cells were harvested by centrifugation (GSA rotor: 4000 rpm, 15 min, 4°C) and resuspended in 1 l H<sub>2</sub>O. After another centrifugation the cells were resuspended in 500 ml H<sub>2</sub>O, pelleted again, washed with 20 ml of 10% glycerol and finally resuspended in 3 ml of 10% glycerol. After aliquotting in 100  $\mu$ l the cells were frozen in liquid nitrogen and stored at -70°C.

### 2.2.7.2 Electroporation

For transformation, electrocompetent cells were thawed on ice. 50  $\mu$ l cells were mixed with 0.5  $\mu$ l vector or 5  $\mu$ l ligation reaction and placed in a precooled, sterile electroporation cuvette (Eurogentec; distance between electrodes 2 mm). After a pulse (2.5 kV, 25 mF and 200 W) 1 ml of SOC medium was added immediately, gently agitated for 45 min at 37°C and plated on LB agar plates with 100  $\mu$ g/ml ampicillin (DH5 $\alpha$  and XL1-Blue) or with 100  $\mu$ g/ml ampicillin and 25  $\mu$ g/ml chloramphenicol (BL21-RIL).

SOC: SOB medium with 10 mM MgSO<sub>4</sub>, 10 mM MgCl<sub>2</sub>, 20 mM glucose

### 2.2.7.3 Preparation of SEM Competent Cells

250 ml SOB medium was inoculated with 3 ml of an *E. coli* overnight culture and grown to an OD<sub>600</sub> of 0.6 at 37°C under vigorous shaking. After the culture was incubated on ice for 10 min the cells were harvested by centrifugation (GSA rotor: 2500 rpm, 10 min, 4°C) and

resuspended in icecold TB solution. After another centrifugation the cells were resuspended in 20 ml TB and 7% DMSO (v/v) was added to the cell suspension. After aliquotting in 100 µl the cells were frozen in liquid nitrogen and stored at -70°C [Inoue *et al.* 1990].

TBsolution: 10 mM PIPES·KOH, pH 6.7, 55 mM MnCl<sub>2</sub>, 15 mM CaCl<sub>2</sub>, 250 mM KCl

#### 2.2.7.4 Heat Shock Transformation

For transformation, electrocompetent cells were thawed on ice. 50 µl cells were mixed with 0.5 µl vector or 5 µl ligation reaction and incubated on ice for 30 min. The mixture was placed in a 42°C waterbath for 30 s, then on ice for 2 min and was plated immediately on LB agar plates with 100 µg/ml ampicillin (DH5α and XL1-Blue) or with 100 µg/ml ampicillin and 25 µg/ml chloramphenicol (BL21-RIL).

#### 2.2.8 Identification of Transformed Clones in *E. coli*

DNA of transformed bacteria was isolated (2.2.4), cleaved with appropriate restriction endonucleases (2.2.5) and analysed on agarose gels (2.2.1). Plasmids with the expected restriction fragments were sequenced by Medigenomix, Martinsried or Biolux, Stuttgart. Sequences were aligned with the Mac molly program.

#### 2.2.9 Polymerase Chain Reaction (PCR)

Amplification of DNA fragments was carried out by ‘polymerase chain reaction’.

The ‘Expand High Fidelity Polymerase Mix’ (Roche, Penzberg) was used for standard PCR reactions. The reactions contained 2 mM MgCl<sub>2</sub>, 2 ng/µl template (final concentration), 200 µM of each dNTP, 0.5 µM 5'- and 3'-primer and 0.5 units per 50 µl expand-polymerase in reaction buffer. Plasmid DNA was used as template. Number of cycles, temperature and duration of denaturation, annealing and elongation phases were chosen according to the supplier’s instructions. The PCR product was isolated from nucleotides and enzyme by the ‘Qiaquick PCR Purification Kit’ (Qiagen, Hilden).

The ‘QuikChange’ (Stratagene Cloning Systems) PCR protocol was used for special mutations. The reactions contained 2 mM MgCl<sub>2</sub>, 0.1-1 ng/µl template (final concentration), 50 µM of each dNTP, 0.2 µM 5'- and 3'-primer and 2.5 units per 50 µl *Pwo*-polymerase in reaction buffer. Plasmid DNA was used as template. Number of cycles, temperature and duration of denaturation, annealing and elongation phases were chosen according to the supplier’s instructions.

### 2.2.10 Introduction of Point Mutations

Mutations that lay close to restriction sites of the vector were introduced by designing primers containing an original restriction site of the vector and the intended mutation. The PCR product was purified, cleaved with the appropriate restriction enzymes and purified again. Then it was ligated into the vector and the ligation mixture was transformed in *E. coli*. The plasmid DNA was prepared and sent for sequencing.

If there were no suitable restriction sites near a desired mutation site, the ‘QuikChange’ (Stratagene Cloning Systems) mutational protocol was followed. Complementary primers containing the mutation and the *Pwo*-polymerase were used. *Pwo*-polymerase has no 5'->3'-exonuclease activity. To get rid of the methylated bacterial template DNA the PCR mixture was cleaved with *DpnI* which is specific for methylated DNA. The PCR product was then transformed in *E. coli* cells. The DNA was prepared, the fragment containing the mutation was cut out by restriction enzymes and ligated into the vector. The ligation mixture was transformed in *E. coli*, the plasmid DNA was prepared and sent for sequencing.

### 2.2.11 Oligonucleotides

Oligonucleotides were purchased from MWG Biotech (Ebersberg), metabion (Martinsried) and ThermoHybaid (Ulm). The following oligonucleotides are given from 5' to 3' end. The mutated bases are highlighted by bold type and restriction sites are underlined.

#### 2.2.11.1 Primers for the Removal or Insertion of Restriction Sites

NkSacI+

AACGCCGAGCTCAGCCCGCCGAGCT**G**AAGCAGATGCTTGCCAAGG

NkSacI-

CCTTGGCAAGCATCTGCTT**C**AGCTCGGCCGGGCTGAGCTCGGCGTT

NkΔKpnISacI+

GGTGGCGAGAC**GGTACCC**AAGGAGAAATGGGTTCACCTTTGGAGCT**G**GCGATCACCCC

NkΔKpnISacI-

GGGGTGATCGCC**C**AGCTCCAAAGGTG**GA**ACCCATTTCTCCTTGGTACCCGTCTCGCCACC

(Primers for cloning plasmid pNk433\_neu)

#### 2.2.11.2 Primers for the Removal of Cysteine residues 38, 59 and 307

Cys59Ser+

ACGCGTCGACGGTAGGCTTGATCGAGAAATCGAAGATGTCGGATTGCTT**G**ATGACATGTCAAAC

Cys38Ser-

TCCAGGGCCGGATACCT**C**TACAGTCGATTCGAAAGAAGCGCAGGGTTCCTTCAC

Cys307Ala+

CGGCATCGTTGTA**A**CTACTGGGTGAAG**C**GTTGATAATGAGTG

Cys307Ala-

CACTCATTATCAAC**G**CTT**C**ACCCAGTAGTTACAACGATGCCG

(Primers for cloning plasmid pNk433\_light)

NkSpI3

CCCTTGACGT**A**CGGACCGCGGTCTT

NkNde5

**C**GGGAGCCATATGTCGTCAAGTGCG

### 2.2.11.3 Primers for the Insertion of Cysteine residues

S341C-

AACGCCGAGCTCTGCCCCGGCCGAGCTGAAGCAGATGCTTGCCAAGG

P342C-

AACGCCGAGCTCAGCT**G**CCCGAGCTGAAGCAGATGCTTGCCAAGG

A226C+

CTGACCGCTCTT**G**CA**C**AGAGCCCGTCTCC

A226C-

GGAGACGGGCTCGT**G**CAAGAGCGGTCAG

E339C+

GGCCGGGCTGAG**A**CAGGCGTTGACTTTC

E339C-

GAAAGTCAACGCCT**G**TCTCAGCCCGGCC

Ser3Cys\_NdeI-

GGAATTCCATATGTCGT**G**TAGTGCGAATAGTATCAAGG

Ala334Cys\_SacI+

CGGGCTGAGCTCGGCGTTGACTTT**G**CATTTGTTCTTGATCG

Thr273Cys+

GGATTTGCCGTC**A**CACAGGGCATTG

Thr273Cys-

CAATGCCCTGT**G**TGACGGCAAATCC

Ser329Cys+

CGCTTTGTTCTTGAT**G**CACTTTGCTCTC



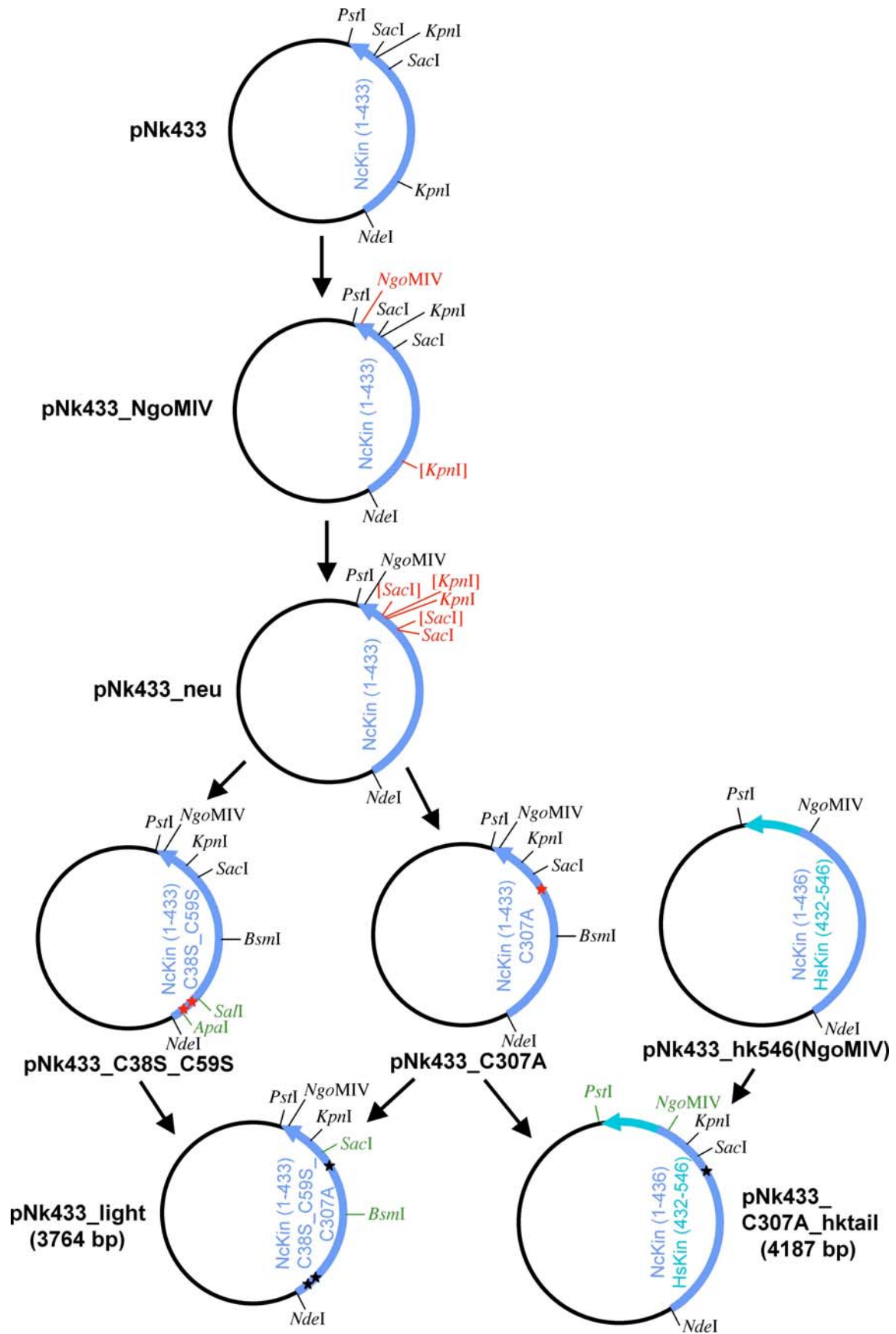


**Figure 2.1: Genealogy of plasmid pNk433\_C307A\_hktail.**

New introduced mutations are depicted in red, restriction sites used for cloning in green. Exchanged cysteine residues are marked with asterisks.

To introduce unique restriction sites in the NcKin gene at the kinesin domain borders, further silent changes in restriction sites lead to plasmid **pNk433\_neu** (Figure 2.1). The restriction site *SacI* at codons 344-345 was shifted to codons 339-340 and another *SacI* site was removed at codons 389-390. The restriction site *KpnI* at codons 384-386 was shifted to codons 378-380. This was done via two PCRs (2.2.9) using the primers NkSacI+ and NkΔKpnISacI-, or NkΔKpnISacI+ and NkSacI- on template pNk433\_NgoMIV. Both PCR products were cleaved with *SacI* and *KpnI*, ligated and sequenced with primer Pk11H. Hence, the kinesin neck domain was flanked by *SacI* and *KpnI*.

Plasmid **pNk433\_light** (Figure 2.1) contains a coding frame for a cysteine-free Nk433 variant. The cysteine residues 38 and 59 were replaced by serine residues via PCR with the primers Cys59Ser+ and Cys38Ser- on template pNk433\_neu. The PCR product was cloned back into pNk433\_neu via the restriction sites *ApaI* and *SallI*, that are located close to the mutations. The new plasmid pNk433\_C38S\_C59S (e) was sequenced with primer NkΔKpnI-. Cysteine residue 307 was replaced by an alanine residue by site directed mutagenesis (2.2.9) with the primers Cys307Ala+ and Cys307Ala- on template pNk433\_neu. The new plasmid **pNk433\_C307A** (2) (Figure 2.1) was sequenced with primer NkΔKpnISacI- and cloned back into pNk433\_C38S\_C59S via the restriction sites *BsmI* and *SacI*. The resulting plasmid pNk433\_light (ii) was then sequenced again with primer NkSacI-.

**pNk433\_light\_S341C**, **pNk433\_light\_P342C**: PCR with primers S341C-, or P342C- and NkΔKpnISacI- on template pNk433\_light, cloned back with *KpnI* and *SacI* into pNk433\_light, sequenced with primer Nk\_A425\_NgoMIV

**pNk433\_light\_A226C\_E339C**: site directed mutagenesis with primers A226C+ and A226C- on template pNk433\_light, cloned back with *SacI* and *SacII* into pNk433\_light, resulting plasmid pNk433\_light\_A226C sequenced with primers NkΔKpnISacI- and S358C+; site directed mutagenesis with primers E339C+ and E339C- on template pNk433\_light\_A226C, cloned back with *KpnI* and *SacII* into pNk433\_light, sequenced with primers Cys307Ala+ and Nk\_A425\_NgoMIV

**pNk433\_C307A\_S341C**, **pNk433\_C307A\_P342C**, **pNk433\_C307A\_A226C\_E339C**: all three cysteine-light plasmids were cleaved with *BamHI* and *PstI* and the small fragment (890 bp) was cloned into pNk433\_neu

**pNk433\_C307A\_hktail** (Figure 2.1), **pNk433\_C307A\_S341C\_hktail**, **pNk433\_C307A\_P342C\_hktail**, **pNk433\_C307A\_A226C\_E339C\_hktail**: the plasmid pNk433\_hk546(NgoMIV) (Figure 2.1) containing NcKin to amino acid 436 followed by amino acids

432 to 546 from HsKin was cleaved with *NgoMIV* and *PstI* and the small fragment containing hktail (450 bp) was cloned into all four plasmids pNk433\_C307A..., sequenced with primer T7-7reverse

**pNk343\_C307A\_A226C\_E339C:** PCR with primers Nk343\_E339C- and T7-7forward on template pNk433\_C307A\_A226C\_E339C, PCR product (1110 bp) cleaved with *BamHI* and *PstI*, bigger fragment (590 bp) cloned back into pNk433\_C307A\_A226C\_E339C, sequenced with primers Pk11H and Cys307Ala+

**pNk343\_C307A\_E339C:** PCR with primers Nk343\_E339C- and T7-7forward on template pNk433\_C307A, PCR product (1110 bp) cleaved with *BamHI* and *PstI*, bigger fragment (590 bp) cloned back into pNk433\_C307A, sequenced with primers Pk11H and Thr273Cys+

**pNk343\_C307A:** resulted from cloning pNk343\_C307A\_E339C as a wrong clone not containing the desired mutation of residue 339 from glutamic acid to cysteine as sequencing with primers Pk11H and Thr273Cys+ showed

**pNk433\_C307A\_A226C\_hktail, pNk343\_C307A\_A226C:** site directed mutagenesis with primers A226C+ and A226C- on templates pNk433\_C307A\_hktail and pNk343\_C307A, respectively, sequenced with primers NkBam-, PK11H, NkSpl3 and Cys307Ala-

**pNk433\_C307A\_E339C\_hktail:** site directed mutagenesis with primers E339C+ and E339C- on template pNk433\_C307A\_hktail, sequenced with primers NkBam-, PK11H, T7-7forward and Thr273Cys-

**pNk433\_C307A\_S3C\_A334C\_hktail:** PCR with primers Ala334Cys\_SacI+ and Ser3Cys\_NdeI- on template pNk433\_C307A, PCR product (1000 bp) cleaved with *SacI* and *NdeI*, cloned back into pNk433\_C307A\_hktail, sequenced with primers S358C+ and T7-7forward

**pNk343\_C307A\_S3C\_A334C:** pNk433\_C307A\_S3C\_A334C\_hktail was cleaved with *SacI* and *NdeI*, the small fragment (1000 bp) was cloned back into Nk343\_C307A

**pNk433\_C307A\_S3C\_hktail:** pNk433\_C307A\_S3C\_A334C\_hktail was cleaved with *BamHI* and *XbaI*, the small fragment (480 bp) was cloned back into pNk433\_C307A\_hktail

**pNk433\_C307A\_A334C\_hktail:** pNk433\_C307A\_hktail was cleaved with *BamHI* and *XbaI*, the small fragment (480 bp) was cloned back into pNk433\_C307A\_S3C\_A334C\_hktail

**pNk433\_C307A\_T273C\_hktail, pNk343\_C307A\_T273C, pNk433\_C307A\_S329C\_hktail,**

**pNk343\_C307A\_S329C:** site directed mutagenesis with primers Thr273Cys+ and Thr273Cys-, or rather Ser329Cys+ and Ser329Cys- on template pNk433\_C307A, sequenced with primers S358C+ and NkBam-, cloned back with *SacI* and *SacII* into pNk433\_C307A\_hktail and pNk343\_C307A

**pNk433\_C307A\_T273C\_S329C\_hktail**, **pNk343\_C307A\_T273C\_S329C**: site directed mutagenesis with primers Thr273Cys+ and Thr273Cys- on template pNk433\_C307A\_S329C\_hktail, sequenced with primer S358C+, cloned back with *SacI* and *SacII* into pNk433\_C307A\_hktail and pNk343\_C307A

**pHk560\_light\_K222C\_E334C\_GFP\_6his**: (gift of Michio Tomishige) contains HsKin to amino acid 560, followed by a GFP (green fluorescence protein) and a his-tag consisting of six histidine residues. All surface exposed cysteine residues have been exchanged [Tomishige & Vale 2000] and codons 222 and 334 have been mutated from lysine or rather glutamic acid to cysteine coding codons.

**pHk339\_light\_K222C\_E334C\_8his**: PCR with primers Hk339h8\_E334C and T7-7forward on template pHk560\_light\_K222C\_E334C\_GFP\_6his, PCR product (1110 bp) cleaved with *XhoI* and *NcoI*, bigger fragment (690 bp) cloned back into pHk560\_light\_K222C\_E334C\_GFP\_6his (3.5 kb fragment, without GFP), sequenced with primer pet17b\_vorn

### 2.2.13 Summary of all Measured Constructs

Vector Name	Protein Name	Construct
pNk433_C307A_hktail	NcKin433_wt	dimeric NcKin 'wild-type'
pNk343_C307A	NcKin343_wt	monomeric NcKin 'wild-type'
pNk433_C307A_S341C_hktail	NcKin433_S341C	dimeric NcKin neck/neck
pNk433_C307A_P342C_hktail	NcKin433_P342C	dimeric NcKin neck/neck
pNk433_C307A_A226C_E339C_hktail	NcKin433_A226C_E339C	dimeric NcKin neck-linker/core
pNk343_C307A_A226C_E339C	NcKin343_A226C_E339C	monomeric NcKin neck-linker/core
pNk433_C307A_A226C_hktail pNk433_C307A_E339C_hktail pNk343_C307A_A226C pNk343_C307A_E339C	NcKin433_A226C NcKin433_E339C NcKin343_A226C NcKin343_E339C	dimeric and monomeric NcKin controls
pNk433_C307A_S3C_A334C_hktail	NcKin433_S3C_A334C	dimeric NcKin neck-linker/core
pNk343_C307A_S3C_A334C	NcKin343_S3C_A334C	monomeric NcKin neck-linker/core

Vector Name	Protein Name	Construct
pNk433_C307A_S3C_hktail pNk433_C307A_A334C_hktail	NcKin433_S3C NcKin433_A334C	dimeric NcKin controls
pNk433_C307A_T273C_S329C_hktail	NcKin433_T273C_S329C	dimeric NcKin $\alpha 4/\alpha 6$
pNk343_C307A_T273C_S329C	NcKin343_T273C_S329C	monomeric NcKin $\alpha 4/\alpha 6$
pNk433_C307A_T273C_hktail pNk433_C307A_S329C_hktail pNk343_C307A_T273C pNk343_C307A_S329C	NcKin433_T273C NcKin433_S329C NcKin343_T273C NcKin343_S329C	dimeric and monomeric NcKin controls
pHk560_light_K222C_E334C_GFP_his	HsKin560_K222C_E334C	dimeric HsKin neck-linker/core
pHk339_light_K222C_E334C_his	HsKin339_K222C_E334C	monomeric HsKin neck-linker/core

## 2.3 Biochemical Methods

### 2.3.1 SDS-Polyacrylamide Gel Electrophoresis (PAGE)

Proteins were separated on discontinuous SDS-polyacrylamide gels [Laemmli 1970]. 10% polyacrylamide (PAA) gels were prepared. The gels were run with the ‘Multigel-Long-System’ (Biometra, München) at 50 V for the first 30 min and after that at 90 V. Probes and high molecular weight standard (Sigma) were mixed with 1/5 volume 6x Laemmli sample buffer [Laemmli 1970], incubated at 95°C for 5 min and immediately loaded onto the gel.

PAA solution: 30% acrylamide, 0.8% bisacrylamide (Biorad)

running buffer: 25 mM Tris·HCl, 0.1% SDS, 192 mM glycine

10x buffer for stacking gel: 500 mM Tris·HCl, pH 6.8, 0.4% SDS

10x buffer for separating gel: 1.5 M Tris·HCl, pH 8.8, 0.4% SDS

6x Laemmli sample buffer: 300 mM Tris·HCl, pH 6.8, 15 mM EDTA, 12% SDS,  
30% glycerol, 15%  $\beta$ -mercaptoethanol, 0.06% bromphenol blue

Nonreducing SDS-PAGE was carried out to prove inter- and intra-molecular disulfide bridges in NcKin constructs. These crosslinks are covalent bonds which are not disrupted by heat but



In the meantime the FPLC was prepared. First, the pumps, tubes and column were washed with H<sub>2</sub>O. For calibration of the conductivity meter the column was washed with buffer B to calibrate 100% ionic strength and then with buffer A to calibrate 0% ionic strength and to equilibrate the column.

The supernatant was diluted 3.5fold with H<sub>2</sub>O containing 5 mM MgCl<sub>2</sub>, 1 mM DTT, 0.5 mM EGTA, 10 μM ATP to reduce the salt concentration to 20 mM. This mixture immediately was loaded onto the column by a peristaltic pump (Amersham Pharmacia Biotech, 4 ml/min). The column was washed with buffer A until most unbound protein had eluted. Proteins were detected photometrically by measuring the E<sub>280</sub>. Kinesin was eluted with a manual step gradient from 50 mM to 1 M NaCl and collected in 1.5 ml fractions. Peak fractions of active kinesin were identified by an ATPase assay (2.3.10.2) and their purity checked by SDS-PAGE (2.3.1). NcKin elutes between 50 and 200 mM NaCl, depending on the construct. The peak fractions were pooled, supplemented with 1/10 volume of glycerol, frozen in liquid nitrogen in small aliquots and stored at -70°C.

lysis buffer: buffer A with 50 mM NaCl, 0.5 μM Pefabloc, 1x protease inhibitor (PI),  
1 mM DTT, 0.5 mM EGTA, a pinch each of lysozyme and DNase I

100x PI: 1 mg/ml soybean trypsin inhibitor, 1 mg/ml TAME, 250 μg/ml leupeptine,  
100 μg/ml pepstatine A, 100 μg/ml aprotinin

buffer A: 20 mM NaPO<sub>4</sub>, pH 7.4, 5 mM MgCl<sub>2</sub>, 10 μM ATP

buffer B: buffer A with 1 M NaCl

Buffers A and B were filtered to get rid of gas and particles.

### 2.3.5.2 Purification of Bacterially Expressed HsKin

Purification of HsKin constructs was carried out in a two step chromatographic process [M. Tomishige, personal communication]. First, the protein was accumulated via its histidin tag on a Ni NTA (Qiagen) column. Second, the eluat was further purified with a 5 ml HiTrap Q-Sepharose column on a FPLC system (both Amersham Pharmacia Biotech).

10 g frozen cells were resuspended in 40 ml lysis buffer. The suspension was sonicated (4x 30 s with 60 s break in between for cooldown, output: 4, duty cycle: constant, Branson Sonifier 250) and spun clear of debris (Beckmann rotor 42.1: 42000 rpm, 45 min, 4°C).

In the meantime, 6 ml of packed Ni NTA resin was equilibrated. The resin was resuspended in 15 ml lysis buffer without ATP and imidazole, rocked for 10 min at 4°C and sedimented (Heraeus Minifuge RF: 500 rpm, 2 min, 4°C). This procedure was repeated once. Then the protein was bound to the resin by rocking for 45-60 min at 4°C. The mixture was loaded onto

a Qiagen disposable column and washed with 50 ml Ni wash buffer until the eluate showed an  $E_{280}$  less than 0.1. Elution was carried out with 10x 1 ml fractions of Ni elution buffer. The fractions with the highest  $E_{280}$  were pooled and diluted 4fold with MonoQ buffer A with 1 mM DTT.

The FPLC was prepared as in (2.3.5.1) and equilibrated with 10% MonoQ buffer B (100 mM ionic strength). The diluted Ni NTA eluate was immediately loaded onto the column by a peristaltic pump (Amersham Pharmacia Biotech, 4 ml/min). The column was washed with 10% MonoQ buffer B until most unbound protein was washed out. Proteins were detected photometrically by measuring the  $E_{280}$ . Kinesin was eluted with a manual step gradient from 150 mM to 1 M NaCl and collected in 1.5 ml fractions. The peak fractions of active kinesin were identified by an ATPase assay (2.3.10.2) and their purity checked by SDS-PAGE (2.3.1). HsKin elutes between 150 and 300 mM, depending on the construct. The peak fractions were pooled, supplemented with 1/10 volume of glycerol, frozen in liquid nitrogen in small aliquots and stored at  $-70^{\circ}\text{C}$ .

lysis buffer:	50 mM $\text{NaPO}_4$ , pH 8.0, 250 mM NaCl, 2 mM $\text{MgCl}_2$ , 1 mM ATP, 20 mM imidazole, 10 mM $\beta$ -mercaptoethanol, 0.5 $\mu\text{M}$ Pefabloc, 1x PI
Ni wash buffer:	50 mM $\text{NaPO}_4$ , pH 6.0, 250 mM NaCl, 1 mM $\text{MgCl}_2$ , 0.1 mM ATP, 10 mM $\beta$ -mercaptoethanol
Ni elution buffer:	50 mM $\text{NaPO}_4$ , pH 7.2, 250 mM NaCl, 1 mM $\text{MgCl}_2$ , 0.1 mM ATP, 500 mM imidazole, 10 mM $\beta$ -mercaptoethanol
MonoQ buffer A:	25 mM PIPES $\cdot$ KOH, pH 6.8, 2 mM $\text{MgCl}_2$ , 1 mM EGTA, 0.1 mM ATP
MonoQ buffer B:	MonoQ buffer A with 1 M NaCl

### 2.3.5.3 Purification of Tubulin

Pig brain tubulin was purified in three successive steps of polymerisation and depolymerisation followed by an ion exchange chromatography step [E.-M. Mandelkow *et al.* 1985]. Fresh pig brain halves were obtained at the local slaughterhouse and put on ice immediately. In the cool room they were separated from blood vessels and connective tissue. 700 ml buffer A was added to 700 g of brain. The mixture was homogenised in a warring blender (Braun) and centrifuged (GSA-rotor, 13000 rpm,  $4^{\circ}\text{C}$ , 70 min). The supernatant was inoculated with 25% glycerol (final concentration v/v, Roth 3783.1) and 2 mM ATP (final concentration). To polymerise the tubulin, this mixture was incubated slightly shaking at  $35^{\circ}\text{C}$

for 30 min. The microtubules were sedimented at 32°C (prewarmed centrifuges and Beckmann rotors 35: 35000 rpm, 50 min and TI 45: 42000 rpm, 45 min). The pellets were resuspended in 100 ml buffer C and homogenised on ice in dounce homogenisers (Wheaton). The microtubules were allowed to depolymerise on ice for 25 min and centrifuged again (precooled centrifuge and Beckmann rotor 42.1: 36000 rpm, 30 min, 4°C). After addition of 2 mM ATP the supernatant was polymerised once more at 35°C for 30 min and pelleted again (prewarmed centrifuge and Beckmann rotor 42.1: 33000 rpm, 60 min, 32°C). The pelleted microtubules were weighed, frozen in liquid nitrogen and stored at -70°C.

To remove last traces of microtubule-binding proteins, the tubulin was passed through a phosphocellulose column. The activated phosphocellulose (P-11, Whatman) was equilibrated to pH 4.0 and 50 ml of the column material (150 ml total volume) was packed into a column (Pharmacia). For equilibration, the column was loaded with 3 volumes of buffer D at 1 ml/min. In the meantime microtubules were thawed and homogenised on ice in 50-100 ml buffer B. The mixture was incubated on ice for 25 min for microtubule depolymerisation. After centrifugation (precooled centrifuge and Beckmann rotor 42.1: 36000 rpm, 30 min, 4°C) the supernatant was inoculated with 10% DMSO and 2 mM ATP and polymerised at 35°C for 30 min. The microtubules were pelleted (prewarmed centrifuge and Beckmann rotor 42.1: 33000 rpm, 60 min, 32°C) and resuspended in 5-7 ml buffer D, again homogenised and depolymerised on ice for 25 min. After centrifugation (precooled centrifuge and Beckmann rotor TI 70.1: 34200 rpm, 30 min, 4°C) the supernatant was applied to the column by a peristaltic pump (Pharmacia, Amersham). After the probe had entered the column completely, the column was washed with buffer D with 0.16 ml/min. Under these buffer conditions tubulin does not bind to the phosphocellulose in contrast to microtubule associated proteins. 1 ml fractions were collected. Peak fractions were identified by mixing 2 µl with 400 µl H<sub>2</sub>O and 100 µl Bradford reagent. The fractions with the highest protein concentration were pooled and frozen in liquid nitrogen after the addition of 0.1 mM GTP. Tubulin was stored at -70°C.

buffer A: 0.1 M PIPES·NaOH, 2 mM EGTA, 1 mM MgSO<sub>4</sub>, 1 mM DTT, 100 µM ATP

buffer B: 0.5 M PIPES·NaOH, 1 mM EGTA, 1 mM MgSO<sub>4</sub>, 1 mM DTT, 1 mM ATP

buffer C: 0.1 M PIPES·NaOH, 1 mM EGTA, 1 mM MgSO<sub>4</sub>, 1 mM DTT, 1 mM ATP

buffer D: 0.1 M PIPES·NaOH, 1 mM EGTA, 1 mM MgSO<sub>4</sub>, 1 mM DTT, 50 µM ATP

All buffers were adjusted to pH 6.9 at 4°C.

### 2.3.6 Determination of Protein Concentration

The protein concentration was determined with Bradford reagent (Biorad, 500-0006) [Bradford 1976]. For each measurement, a reference curve with bovine serum albumine (BSA) was measured in parallel. Measurement of the absorption at  $E_{630}$  with an microplate reader (Dynatech MR 5000) produced the protein concentration. Kinesin concentrations are given in monomer concentrations.

In case of unclean preparations (bacterial proteins or degradation products) SDS-PAGE was carried out with different amounts of protein (0.15-1.2  $\mu\text{g}$ ). The gels were stained with Coomassie Blue and imaged using a CCD camera (Eagle Eye System, Stratagene). A density profile was generated in the MacIntosh program NIH Image, and analysed for its relative content of kinesin. The concentration of the Bradford test was corrected accordingly.

### 2.3.7 Polymerisation of Microtubules

For some measurements the microtubule concentration had to be determined accurately. Therefore, aggregated tubulin had to be removed. Tubulin was thawed and aggregated tubulin was pelleted (precooled centrifuge and Beckmann rotor TLA 100.3: 80000 rpm, 4°C, 10 min). The supernatant was inoculated with 1 mM GTP and incubated at 37°C for 10 min. 20  $\mu\text{M}$  taxol (paclitaxel, Sigma T-7402) was added for stabilisation of microtubules and incubated at 37°C for 20 min. After polymerisation the microtubules were centrifuged (prewarmed centrifuge and Beckmann rotor TLA 120.1: 80000 rpm, 25°C, 10 min) through 40% sucrose in 12A25+ buffer (2.3.10.2) to remove unpolymerised tubulin. The pelleted microtubules were washed with 12A25+ buffer containing 20  $\mu\text{M}$  taxol and then resuspended in this buffer. The volume was chosen to achieve a final concentration of 100  $\mu\text{M}$  tubulin dimer.

For motility assays the microtubule concentration was irrelevant. Tubulin was thawed, polymerised after addition of 1 mM GTP for 10 min and after addition of 20  $\mu\text{M}$  taxol for another 20 min at 37°C. The microtubules were diluted 10-50fold with BRB80 (2.3.9.2) containing 20  $\mu\text{M}$  taxol.

### 2.3.8 Determination of Microtubule Concentration

The concentration of microtubule suspensions was determined after denaturation in guanidium·HCl by measuring the  $E_{280}$  in the photometer.

blank: 90  $\mu\text{l}$  6.6 M guanidium·HCl + 10  $\mu\text{l}$  12A25+ with 20  $\mu\text{M}$  taxol

samples: 90  $\mu\text{l}$  6.6 M guanidium·HCl + 10  $\mu\text{l}$  MT-dilution

Microtubules were diluted 1:10 and 1:5 in 12A25+ with 20  $\mu\text{M}$  taxol.

Microtubule concentration was calculated with the following formula [Huang & Hackney 1994]:

$$(E_{280} / 1.03) * \text{final dilution of MT (100 or 50)} = \text{g/l MT}$$

The molar concentration of microtubules was calculated via the molar mass of a tubulin dimer (~100000 g/mol):

$$\text{g/l} = 10^{-5} \text{ mol/l} = 10 \mu\text{M}$$

## 2.3.9 Microscopy

### 2.3.9.1 Video Enhanced Light Microscopy

Light microscopy was carried out with a Zeiss Axiophot microscope and a 63x oil immersion lens (Zeiss, Oberkochen) that was temperature controlled (25°C) by a connected waterbath. Microtubules were observed in phase contrast with a Newicon C2400-7 camera (Hamamatsu). The image was transferred via a 'DVS 1000 Image Processing System' (Hamamatsu) to a monitor (Sony) and recorded on videotape (Fuji). The 'DVS 1000 Image Processing System' was used for contrast enhancement and background subtraction. For velocity measurements, the time a microtubule needed for movement between two marked points on the monitor was measured manually. Distances on the monitor were calibrated by an object micrometer. At least ten calculated velocities were averaged and standard deviations determined.

### 2.3.9.2 Motility Assay

The velocity of kinesin constructs was measured in a microscopic motility assay [Paschal & Vallee 1993]. Microtubules were polymerised (2.3.7). 1.25  $\mu\text{g}$  kinesin were applied to a coverslip that was kept for 1-2 min in a wet chamber to allow the kinesin tail to bind to the glass surface. Casein buffer was added to a final volume of 5  $\mu\text{l}$ . Then 1  $\mu\text{l}$  BRB80 with 100 mM KCl, 1  $\mu\text{l}$  100 mM  $\text{MgCl}_2$ , 1  $\mu\text{l}$  100 mM ATP and 1  $\mu\text{l}$  microtubules were added. The coverslip was put onto a glass slide and sealed with a mixture of paraffin, lanolin and vaseline (1:1:1). This slide was observed under a microscope, and moving microtubules were analysed as described above (2.3.9.1). The motor density bound to the glass is very high (statistically in the centre of the coverslip at least 27555 kinesin dimers per  $\mu\text{m}^2$ ), causing a microtubule (on average between 1-10  $\mu\text{m}$  long) to being moved by thousands of kinesin molecules acting in concert. Therefore, it is also called a multiple motor assay.

BRB80 buffer: 80 mM PIPES·KOH, pH 6.8, 5 mM  $\text{MgCl}_2$ , 1 mM EGTA

casein buffer: BRB80 with 0.1 M glucose, 2.5 mg/ml casein

Calculation of motor density:

$$1.25 \mu\text{g kinesin} = \frac{1.25 \mu\text{g}}{M_m} = \frac{1.25 \mu\text{g} * \text{mol}}{2 * 60864 * 10^6 \mu\text{g}} = 10.27 \text{ pmol kinesin dimer}$$

$$10.27 \text{ pmol kinesin dimer} * N_A = 6.2 * 10^{12} \text{ kinesin dimers}$$

$$\text{area of coverslip} = 1.5 \text{ cm} * 1.5 \text{ cm} = 2.25 \text{ cm}^2 = 2.25 * 10^8 \mu\text{m}^2$$

$$\text{motor density} = \frac{\text{number of dimers}}{\text{area of coverslip}} = \frac{6.2 * 10^{12} \text{ kinesin dimers}}{2.25 * 10^8 \mu\text{m}^2} = 27555 \frac{\text{kinesin dimers}}{\mu\text{m}^2}$$

$M_m$ : molar mass of a kinesin dimer (NcKin433\_wt) = 2\*60864 g/mol

$N_A$ : Avogadro constant =  $6.02 * 10^{23} \text{ mol}^{-1}$

## 2.3.10 ATPase Assays

### 2.3.10.1 Basal ATPase Assay

The basal ATPase activity of kinesin in the absence of microtubules was measured with radioactive  $[\gamma\text{-}^{32}\text{P}]\text{ATP}$  (Amersham, Pharmacia) [Shimizu *et al.* 2000]. The  $[\gamma\text{-}^{32}\text{P}]\text{ATP}$  was diluted 1:100 in 100 mM ATP to achieve 30000 cpm per mM ATP. For each construct three measurements under reducing conditions and three under oxidising conditions were performed. In these measurements the amount of kinesin was varied. The control reaction contained no kinesin, the others 1-3  $\mu\text{M}$  or 2-6  $\mu\text{M}$  kinesin. The reactions were carried out in 120  $\mu\text{l}$  of 12A25+ buffer (2.3.10.2) to allow to remove five 20  $\mu\text{l}$  aliquots at different time intervals. By addition of 1 mM ATP- $[\gamma\text{-}^{32}\text{P}]\text{ATP}$  working solution the reactions were started and 20  $\mu\text{l}$  samples taken after 10 s, 60 s, 5, 10 and 20 min. These were mixed with 80  $\mu\text{l}$  0.3 M perchloric acid in 1 mM  $\text{NaH}_2\text{PO}_4$  to stop the reaction. Then 100  $\mu\text{l}$  charcoal (100 mg/ml) was added to absorb free ATP and ADP and the suspension was centrifuged (13000 rpm, 1 min, 22°C) to pellet the charcoal. 100  $\mu\text{l}$  supernatant containing the free  $\gamma$ -phosphate  $[\text{}^{32}\text{P}]$  were then transferred into a fresh scintillation counting vial and mixed with 3 ml scintillation solution ‘Quickscint1’ for aqueous solutions (Zinsser Analytic) to measure Cerenkov radiation. The radioactivity of these samples and appropriate standard solutions (1 mM  $[\gamma\text{-}^{32}\text{P}]\text{ATP}$ ) was measured in a scintillation counter (Canberra Packard, Frankfurt/Main). The amount of released phosphate ( $\mu\text{M}$ ) was calculated from the measured radioactivity (counts per minute) of the samples with the help of the standard solutions and plotted against the reaction time. The basal ATPase activity was derived from the slopes of linear fits of the time traces.

### 2.3.10.2 Microtubule-activated ATPase Assay

The microtubule-stimulated steady state ATP turnover was measured in a coupled enzymatic assay under saturating ATP conditions and with varying microtubule concentrations. In this assay, ATP turnover is coupled to the oxidation of NADH to NAD<sup>+</sup> by the enzymes lactate dehydrogenase (LDH) and pyruvate kinase (PK) (Figure 2.2) [Huang & Hackney 1994]. PK requires phosphoenolpyruvate (PEP) as co-substrate. The rate of NADH oxidation can be observed in the photometer (Kontron Uvicon 930, Lohhof) by a decrease in extinction at 340 nm.

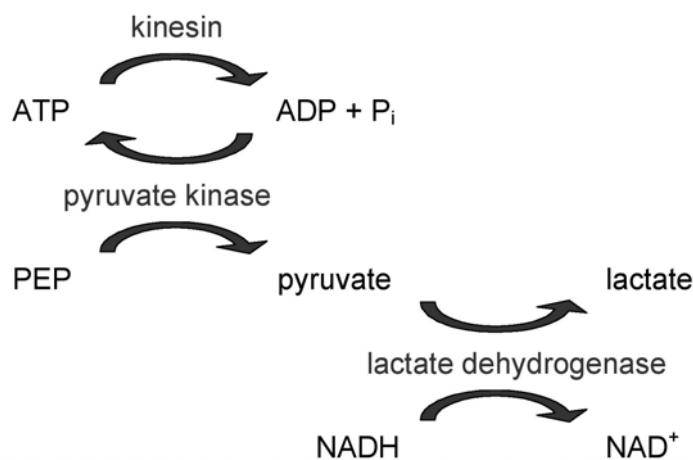


**Figure 2.2: Principle of the coupled ATPase assay.**

ATP hydrolysis by kinesin is coupled to the oxidation of NADH by the enzymes pyruvate kinase (PK) and lactate dehydrogenase (LDH). PK regenerates ATP by converting PEP into pyruvate, which in turn is transformed into lactate by LDH, whereby NADH is oxidised to NAD<sup>+</sup>.

A microtubule stock solution with a known tubulin concentration was prepared (2.3.7, 2.3.8). For each measurement 4  $\mu$ l ATP, 4  $\mu$ l NADH, 4  $\mu$ l PEP, 2  $\mu$ l enzyme mix and 0-20  $\mu$ M microtubules (final concentration) were mixed. The volume was filled up to 79  $\mu$ l with 12A25+ and the reaction was started by addition of 1  $\mu$ l kinesin. The kinesin was diluted 1:1 to 1:100, depending on the construct and the assay conditions, to prevent the enzymatic activities of LDH and PK to become rate-limiting. The reaction mixture was transferred quickly into a 50  $\mu$ l quartz cuvette (Hellma). The extinction  $E_{340}$  was recorded for 1 min in the photometer (time drive mode). Its initial slope was determined and plotted against the corresponding microtubule concentration. The entire set of extinction rates ( $-\Delta E/\text{min}$ ) acquired at different microtubule concentrations was fitted to a hyperbolic curve and used for the determination of the maximal extinction rate  $-\Delta E_{\text{max}}$  ( $V_{\text{max}}$ ) and the half maximal

activation constant ( $K_{0.5,MT}$ ), using the computer program Kaleidagraph (Synergy Software, Macintosh). The hyperbola was defined by the Michaelis-Menten equation:

$$V = \frac{V_{\max} * [MT]}{[MT] + K_{0.5, MT}}$$

12A25+ buffer:	12 mM ACES·KOH, pH 6.8, 25 mM K-acetate, 2 mM Mg-acetate, 0.5 mM EGTA
ATP:	20 mM ATP in 12A25+, pH 7.0
NADH:	4 mM nicotine adenine dinucleotide (Sigma) in 12A25+
PEP:	4 mg/ml phosphoenolpyruvate (mono potassium salt, Sigma) solution in 12A25+, pH 7.0 with 1 M KOH
enzyme mix:	30 $\mu$ l lactate dehydrogenase (5.5 U/ $\mu$ l, glycerol solution, Roche), 30 $\mu$ l pyruvate kinase (2 U/ $\mu$ l, glycerol solution, Roche), 90 $\mu$ l 12A25+
dilution buffer:	buffer A (2.3.5.1) with 1 mg/ml BSA, 275 mM NaCl, 10 $\mu$ M ATP

### 2.3.10.3 Calculations for the ATPase Assay

The conversion of the decrease of extinction rates ( $-\Delta E/t$ ) in change of the ATP concentration per time was carried out with the Lambert-Beer law:

$$\Delta E / t = d * \epsilon * \Delta [NADH] / t$$

$\Delta E/t$ : change of extinction per time ( $V_{\max}$ )

d: thickness of the cuvette (1 cm)

$\epsilon$ : extinction coefficient for NADH (6.22/mM\*cm)

By transformation and insertion of the variables, following equation for the decrease of NADH concentration arises:

$$\begin{aligned} \frac{\Delta [NADH]}{t} &= \frac{\Delta E}{t} * \frac{1}{d * \epsilon} = \frac{\Delta E_{\max}}{\text{min}} * \frac{\text{mM} * \text{cm}}{1 \text{ cm} * 6.22} = \frac{\Delta E_{\max}}{60 \text{ s}} * \frac{\text{mM}}{6.22} = \frac{V_{\max}}{373.2} * \frac{10^{-3} \text{ M}}{\text{s}} \\ &= \frac{V_{\max}}{373200} * \frac{\text{M}}{\text{s}} \end{aligned}$$

As NADH oxidation and ATP turnover are coupled 1:1 in the assay, the decrease of NADH equals the decrease of ATP over time.

$$\Delta [ATP] / \text{s} = V_{\max} / 373200 \text{ M/s}$$

The amount of kinesin in the assay is calculated from the volume that was used in the assay and its concentration:

$$[\text{kinesin}] = \frac{\text{kinesin conc.}}{M_m} * \frac{\text{vol}}{80 \mu\text{l}} = \frac{\text{kinesin conc.}}{M_m} * \frac{1 \mu\text{l}}{80 \mu\text{l}} = \frac{\text{kinesin conc.}}{M_m * 80}$$

[kinesin]: kinesin concentration in the assay [M]

kinesin conc.: concentration of the kinesin dilution used in the assay [g/l]

$M_m$ : molar mass of the kinesin construct [g/mol]

vol: volume kinesin per 80  $\mu\text{l}$  assay [1  $\mu\text{l}$ ]

The catalytic constant  $k_{\text{cat}}$ , represents the maximal turnover of substrate molecules per single kinesin motor head per time and therefore is a characteristic value for an enzyme. It can be calculated by dividing the change of ATP concentration in time ( $\Delta[\text{ATP}]/\text{s}$ ) by the kinesin monomer concentration in the assay ([kinesin]):

$$k_{\text{cat}} = \frac{\Delta[\text{ATP}]}{\text{s} * [\text{kinesin}]} = \frac{V_{\text{max}} * M}{373200 * \text{s}} * \frac{M_m * 80}{\text{kinesin conc.}} = 2.1436 * 10^{-4} * \frac{V_{\text{max}} * M_m}{\text{kinesin conc.}} * \frac{M}{\text{s}}$$

Hence, the  $k_{\text{cat}}$  value [1/s] is the maximal amount of ATP which is hydrolysed by one kinesin head per second.

### 2.3.11 mantADP Experiments

#### 2.3.11.1 Loading of Kinesin Motor Domains with mantADP

To exchange of the ADP that is bound in the catalytic site of kinesin with the fluorescent analogue mantADP, kinesin was incubated with a 3fold excess of mantATP (2'-(3')-O-(N-methylanthraniloyl)adenosine-5'-triphosphate, Molecular Probes, M-12417) at room temperature in the dark for 15 min. This procedure leads to a mantADP-charged kinesin because mantATP is hydrolysed even in the absence of microtubules. Unbound mantATP was removed by gel filtration over a MicroSpin G-25 column (Amersham Pharmacia Biotech). The column was pre-treated with 300  $\mu\text{l}$  of 1 mg/ml BSA in 12A25+ for 30 min, and then equilibrated with 5-6 column volumes of 12A25+. 50  $\mu\text{l}$  of the kinesin mantATP mixture were loaded onto the column and centrifuged with 3000 rpm for 2 min. The eluate contained mostly kinesin·mantADP complexes (modified after [Kallipolitou *et al.* 2001]).

### 2.3.11.2 Stoichiometry of Kinesin·mantADP Complexes

The concentration of the kinesin·mantADP complexes was determined photometrically with the help of an absorption spectrum from 250 to 450 nm. The maximal protein absorption is present around 280 nm, the absorption maximum of the methylanthraniloyl group (mant) lies at 356 nm. Therefore, the protein concentration and the concentration of mant were calculated from the absorption spectra at 280 and 356 nm and their known extinction coefficients. The extinction coefficient of kinesin was calculated using the program Isoelectric from the GCG program package, the extinction coefficient of mantATP was taken from manufacturer's information.

$$\begin{aligned} \text{Extinction coefficients:} \quad \epsilon_{356}(\text{mant}) &= 5800 / \text{M} \cdot \text{cm} \\ \epsilon_{280}(\text{Nk433\_C307A\_hktail}) &= 29360 / \text{M} \cdot \text{cm} \\ \epsilon_{280}(\text{ADP}) &= + 2250 / \text{M} \cdot \text{cm} \\ \epsilon_{280}(\text{Nk433\_C307A\_hktail} \cdot \text{mantADP}) &= 31610 / \text{M} \cdot \text{cm} \end{aligned}$$

### 2.3.11.3 Fluorometric Measurements of mantADP Release

The ADP release from the motor domain of free kinesin is very slow. It is strongly accelerated by binding of kinesin to microtubules. The fluorescent ATP analogue mantATP was used to observe the ADP release. The fluorescence of methylanthraniloyl-nucleotides is more intense when they are bound to protein than in solution. Their absorption maxima lie at 356 nm. MantATP is bound to the kinesin head like ATP and hydrolysed to mantADP. The mantADP release can be observed by a decrease of fluorescence [Hackney 1995; Ma & Taylor 1997a, b].

Kinesin was loaded with mantATP (2.3.11.1) and the kinesin and mantADP concentrations were established (2.3.11.2). Microtubules were polymerised (2.3.7) and their concentration determined (2.3.8). Measurements were carried out with a spectro fluorometer (Aminco Bowman, model AB2) in 1 ml cuvettes (Greiner, 613101). Absorption wavelength was 365 nm, emission wavelength 445 nm with bandwidths of 4 nm. Sensitivity of the measurement could be adjusted by a photomultiplier. It was set at 700 to 850 V to obtain an output signal of about 3V. The reaction (1 ml) contained approximately 100 nM kinesin in 12A25+ buffer (2.3.10.2). After addition of a surplus of 1 mM ATP and substoichiometric amounts of microtubules (0 to 20 nM) the decrease of fluorescence was observed in the fluorometer over time. The curves were imported into the computer program Kaleidagraph and fitted to single or double exponential functions. The rates of these curve fits were plotted

against the microtubule concentration and fitted to a linear function. The slope of this line gives the bimolecular binding rate ( $K_{bi,ADP}$ ) of the kinesin microtubule association [Hackney 1995].

### 2.3.12 Sedimentation Assay

This assay gives information about the microtubule affinity of the NcKin constructs in the presence of AMP-PNP (nonhydrolysable ATP analogue) or ADP. A microtubule stock solution with a known tubulin concentration was prepared (2.3.7, 2.3.8). Ten different final concentrations of microtubules between 0 and 70  $\mu$ M, depending on the construct and the conditions, were mixed with either 1 mM AMP-PNP or ADP and 0.3  $\mu$ M kinesin. The reaction buffer was 12A25+ (2.3.10.2) in a total volume of 80  $\mu$ l. The samples were centrifuged in a prewarmed Beckman Optima centrifuge and prewarmed rotor TLA 100.3 at 80000 rpm for 5 min. 50  $\mu$ l of each supernatant were transferred into fresh reaction vials. Pellets were washed with 12A25+ and resuspended in 80  $\mu$ l 12A25+. Supernatant and pellet samples were supplemented with 66 ng BSA as a loading control and then analysed on SDS-PAA gels (2.3.1) to determine the amount of unbound and bound kinesin. The gels were stained, photographed (2.3.2) and analysed with the program NIH Image (Macintosh). BSA bands were used for standardisation of sample bands. The percentage of protein present in the pellet was plotted against the microtubule concentration and the curve fit gives the dissociation constant  $K_d$ , which is the microtubule concentration where half of the protein is bound.

### 2.3.13 Measurements under Reducing and Oxidising Conditions

All types of measurements for biochemical characterisation of the different kinesin constructs were carried out under several conditions. Following the different incubation methods are outlined:

- Under buffer conditions (without DTT or other reducing agents) cysteine residues are subject to air oxidation. Here kinesin was used in assays as it was purified.
- Under reducing conditions the formation of disulfide bridges by cysteine residues is prevented. This was accomplished by incubating kinesin with 1 mM DTT on ice for 2 h prior to measuring.
- Under oxidising conditions cysteine residues tend to form disulfide bridges. To cause the formation of disulfide bridges, kinesin was therefore incubated on ice with 0.2 mM

---

DTNB for 5 min before starting the assays. DTNB consists of two identical parts linked by a dithiole bond. A DTNB molecule first reacts with the thiol group of one cysteine, forming a disulfide bond and releasing the reduced half of the DTNB molecule. If there is a second cysteine in close proximity, the remaining part of the DTNB molecule reacts with the thiol group of this cysteine. This results in a disulfide bridge between the two cysteine residues and release of the second reduced half of the DTNB molecule [Riddles *et al.* 1983].

- As a control, NEM was used to mimick the addition of DTNB to one cysteine. In contrast to DTNB, NEM only has one reactive group which is able to bind to a thiol group. However, a positive control of a NEM reaction lacks. Therefore, it is not confirmed whether a NEM molecule has the same reactivity for thiols as a DTNB molecule. Kinesin was incubated on ice with 0.2 mM NEM for 15 min, then the excess NEM was quenched with 5 mM DTT. Thus treated the protein was used in assays.
- To show reversibility of the crosslinking, kinesin was first oxidised by 0.2 mM DTNB for 5 min on ice and then reduced again by incubation on ice with 5 mM DTT for 4 h before measuring. Measurements performed after this treatment were called 'rescue'.

For nonreducing SDS-PAGE (2.3.1), untreated, reduced, oxidised, rescued and NEM incubated kinesin constructs were used.

Gliding velocities (2.3.9.2) of kinesin constructs were measured under buffer, reducing, oxidising, rescue and NEM control conditions. The corresponding reagents also were added to the casein buffer such that their final concentration in the whole assay was identical to the incubation conditions.

Basal ATPase assays (2.3.10.1) were carried out under reducing and oxidising conditions.

Microtubule-activated ATP turnover rates (2.3.10.2) of kinesin constructs were measured under buffer, reducing, oxidising, rescue and NEM control conditions.

Binding rates in the fluorometer (2.3.11.3) were measured under reducing and oxidising conditions.

Sedimentation assays (2.3.12) were carried out under reducing and oxidising conditions.

---

## 3 Results

### 3.1 Rationale for the Design of Crosslinking Mutants

To investigate the flexibility of different parts of the kinesin molecule and its functional importance, constructs were created in which parts of the molecule could be reversibly connected. This was achieved by introducing reversible disulfide bridges in suitable regions of the motor domain. The positions of cysteine insertion were selected by carefully analysing the known crystal structures of rat [Kozielski *et al.* 1997] and human conventional kinesin [Kull *et al.* 1996] and, as soon as it was solved, of NcKin [Song *et al.* 2001]. The introduced cysteine residues needed to be in close proximity to allow their thiol groups to form a disulfide bridge (the length of a disulfide bond is 0.2 nm) under oxidising conditions and they must not replace any essential amino acid.

NcKin is composed of 928 amino acids. The NcKin constructs used in this work are C-terminally truncated. They either consist of amino acids 1 to 433, containing head, neck and hinge domains, or of amino acids 1 to 343, containing only the head domain. These truncated constructs were chosen as they are more stable and lead to higher expression levels than full length NcKin [A. Kallipolitou & G. Woehlke, personal communication]. Furthermore, they do not contain the tail domain, which regulates motor activity [Coy *et al.* 1999; Friedman & Vale 1999; Hackney & Stock 2000; Seiler *et al.* 2000]. In addition, they allow for comparison of single and double headed kinesin constructs as NcKin up to amino acid 433 is dimeric while NcKin up to amino acid 343 is monomeric [Kallipolitou *et al.* 2001]. NcKin truncated after amino acid 433 does not differ in motile or catalytic properties from full length NcKin [Kallipolitou *et al.* 2001]. However, without labeling it cannot be used in motility assays as it is missing the tail domain, which adheres unspecifically to glass surfaces. Usually, a cys-tag is C-terminally attached to the truncated constructs. This reactive cysteine can be conjugated with biotin-maleimide, which in turn can bind to streptavidin-coated glass surfaces. This procedure could not be used here as reactive cysteine residues already were required for the formation of disulfide bridges. The introduced cysteine residues would be biotinylated, too, and crosslinking would be impossible. To overcome this problem, part of the HsKin tail domain (hktail: amino acids 432-546) was added after amino acid 436 of NcKin, henceforth called NcKin433. The hktail did not contain any cysteine residues and lacked the tail region

responsible for regulating motor activity (the IAK motif). Just increasing the length of the NcKin construct to the corresponding length (amino acid 550) does not result in a construct which adheres to glass [G. Woehlke, personal communication].

Figure 3.1 summarises all mutations engineered in this study.

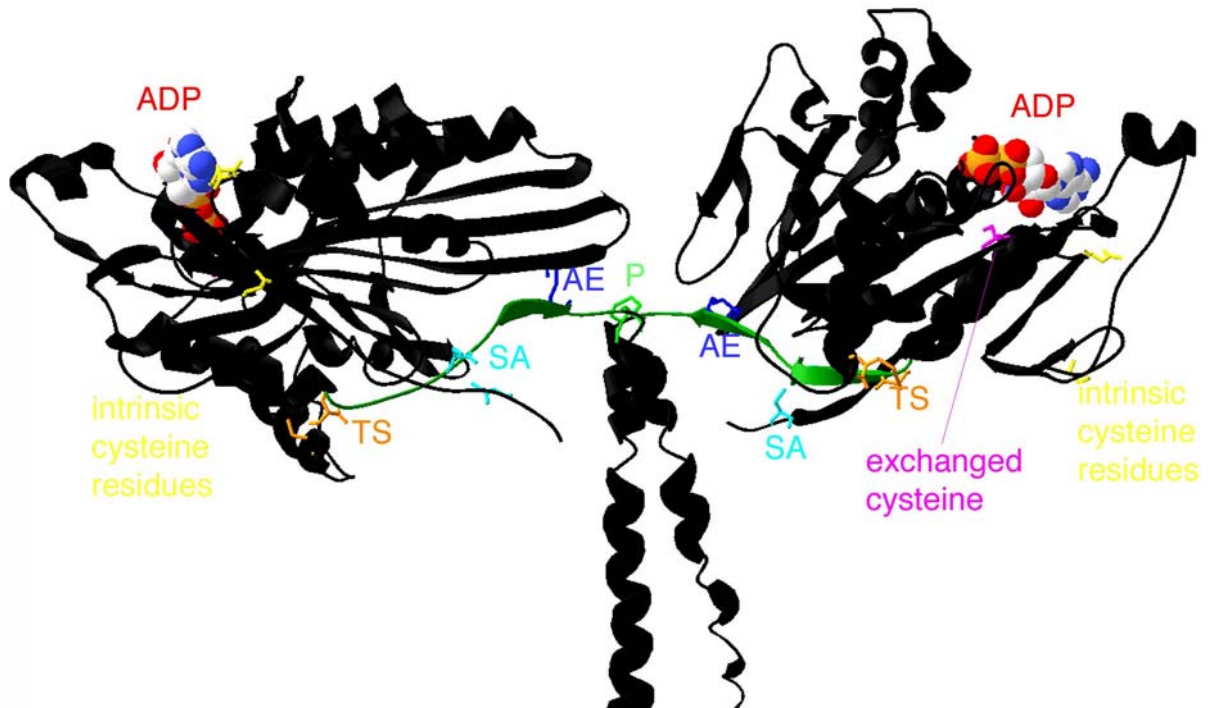


**Figure 3.1:** Overview of mutated residues in a ribbon diagram of the three-dimensional structure of dimeric rat kinesin [from Kozielski *et al.* 1997].

Mutated amino acid residues are shown with their respective sidechains in colour. Exchanged cysteine residue 307 is purple, remaining cysteine residues are marked in yellow. Introduced cysteine residues of the neck/neck crosslinking construct are light green. For neck-linker/motor core crosslinking constructs introduced cysteine residues are marked in light and dark blue, and for  $\alpha 4/\alpha 6$  crosslinking constructs in orange. The neck-linker is depicted in green. ADP is shown in a space-filling model.

### 3.1.1 Wild-type Constructs

A NcKin construct entirely free of endogenous cysteine residues (NcKin433\_light) would serve best as ‘wild-type’ reference, as effects of intrinsic cysteine residues and unspecific interactions with introduced cysteine residues could be excluded. pNk433 only codes for three cysteine residues in the head domain (amino acids 38, 59 and 307), which were exchanged into serine or alanine residues (2.2.12). However, neither was pNk433\_light expressed by *E. coli*, nor pNk433\_C38S\_C59S. Therefore, pNk433\_C307A\_hktail and pNk343\_C307A were taken as a basis for the following constructs. Their corresponding proteins NcKin433\_wt and NcKin343\_wt that still contain endogenous cysteine residues at amino

acid 38 and 59 were used as wild-type references. The intrinsic cysteine residues of the head domain of NcKin do not react with rhodamine-maleimide [G. Woehlke, personal communication] indicating that they are not solvent exposed.

### 3.1.2 Neck/Neck Crosslinking Constructs

To investigate whether unwinding of the neck coiled-coil is a prerequisite for simultaneous binding of both heads to the microtubule [Tripet *et al.* 1997; Hoenger *et al.* 1998; Thormählen *et al.* 1998], a disulfide bridge was introduced between the N-terminal position of the two neck domains of a dimeric NcKin molecule. This will lead to an intermolecular crosslink between the two subunits of NcKin. As the crystal structure of NcKin is not ordered in the neck region [Song *et al.* 2001], two dimeric constructs in which serine residue 341 (pNk433\_C307A\_S341C\_hktail) or proline residue 342 (pNk433\_C307A\_P342C\_hktail) were replaced by cysteine residues (2.2.12) were tested in neck/neck crosslinking studies, coding for proteins **NcKin433\_S341C** and **NcKin433\_P342C**, respectively (Figure 3.2).

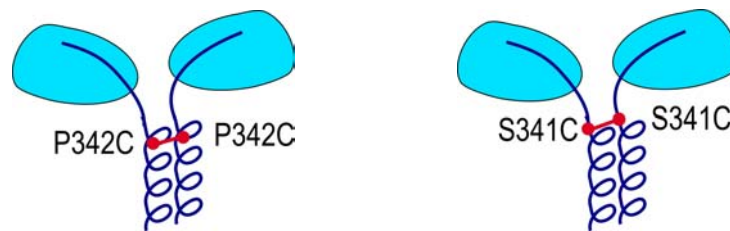


**Figure 3.2:** Sketch of the neck/neck crosslinking constructs **NcKin433\_P342C** and **NcKin433\_S341C**.

The red line indicates the reversible disulfide bridge between the two neck domains of a single kinesin molecule.

These residues are located at the C-terminal end of the neck-linker (amino acid 341) and the N-terminal start of the neck domain (amino acid 342) (Figure 3.3), leading to a juxtaposition of two cysteine residues in a dimeric kinesin construct. Proline residue 432 was chosen as it occupies the 'a' position of the first heptad repeat of the neck coiled-coil in an alignment with animal kinesins (Figure 3.3). The *a* and *d* positions are preferred for disulfide bond formation [Zhou *et al.* 1993]. Additionally, a NcKin neck peptide could be crosslinked at residue P342C which increased the propensity of the peptide to fold as a supercoil [Deluca *et al.* 2003]. Nonetheless, the second construct was made because it was uncertain that the neck coiled-coil started right at amino acid 342. Peptide studies revealed a reduced coiled-coil stability of the NcKin neck domain compared with animal neck domains [Morii *et al.* 1997; Tripet *et al.* 1997; Kallipolitou *et al.* 2001] and the crystal structure of NcKin shows no evidence for a

coiled-coil neck conformation [Song *et al.* 2001]. Therefore, serine residue 341 was also tried for crosslinking the neck regions.

	320	330	342				376
				<i>abcde</i> <b><i>fga</i></b>	<i>bcde</i> <b><i>fgabcd</i></b>	<i>efg</i> <b><i>abcde</i></b> <i>fg</i>	<b><i>abcde</i></b> <i>fg</i>
NcKin	TLRFGMRAKS	IKNK <b>A</b> KVNA <b>E</b>	L <b>S</b> PAELKQML	AKAKTQITSF	ENYIVNLESE	VQVWRGG	
HsKin	TLLFGQRAKT	IKNTV <b>C</b> VNV <b>E</b>	L <b>T</b> AEQWKKKY	EKEKEKNKIL	RNTIQWLENE	LNRWRNG	
RnKin	TLMFGQRAKT	IKNTVSVNLE	L <b>T</b> AEEWKKKY	EKEKEKNKAL	KSVIQHLEVE	LNRWRNG	
	motor core	neck-linker		coiled-coil neck			

**Figure 3.3: Amino acid sequence alignment of neck-linker and neck domains of *N. crassa*, human and rat conventional kinesin.**

Numbering as in NcKin (HsKin numbers -5 and RnKin numbers -3). Domain borders are marked. The predicted heptad repeats (a-b-c-d-e-f-g)<sub>n</sub> are indicated. Mutated residues are coloured green for neck/neck crosslinks (amino acids 341 and 342) and blue or purple for neck-linker/motor core crosslinks (amino acids 334 and 339).

### 3.1.3 Neck-Linker/Motor Core Crosslinking Constructs

#### 3.1.3.1 NcKin

The second hypothesis for the simultaneous binding of both heads to the microtubule, the unzipping of the neck-linker from the motor head [Romberg *et al.* 1998] can be tested by forming disulfide bridges between the neck-linker and adjacent parts of the catalytic core of the same peptide of a NcKin molecule. This will lead to intramolecular crosslinks within the subunits of NcKin. Two types of constructs were made for neck-linker/motor head crosslinking studies: A226C/E339C and S3C/A334C (Figure 3.4).

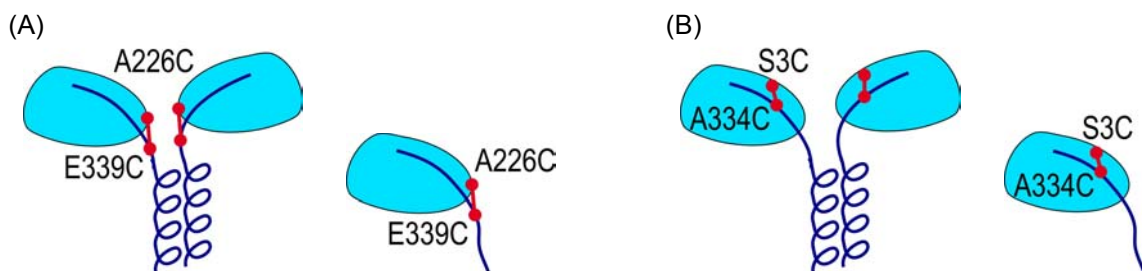


**Figure 3.4: Sketches of the neck-linker/motor core crosslinking constructs (A) NcKin\_A226C\_E339C (B) NcKin\_S3C\_A334C.**

The red line indicates the reversible disulfide bridge between the neck-linker and the motor core domains within single kinesin subunits.

Glutamic acid residue 339 is located at the C-terminal end of the neck-linker (Figure 3.3) and in close proximity to alanine residue 226, which is located in the tip of the motor core (loop 10) (Figure 3.1). By connecting these sites via a disulfide bridge, the end of the neck-linker is docked onto the motor core, causing its complete loss of freedom to move. This pair of cysteine residues was introduced in both the dimeric and monomeric wild-type construct,

resulting in the two constructs pNk433\_C307A\_A226C\_E339C\_hktail and pNk343\_C307A\_A226C\_E339C (2.2.12), coding for the proteins **NcKin433\_A226C\_E339C** and **NcKin343\_A226C\_E339C**, respectively.

Alanine residue 334 is located at the N-terminal start of the neck-linker (Figure 3.3) and adjacent to serine residue 3, right at the N-terminus of the motor head. This crosslink causes docking of the beginning of the neck-linker onto the motor core, thereby allowing for some degree of flexibility in the neck-linker. This pair of cysteine residues also was introduced in the dimeric and monomeric wild-type constructs, resulting in the two constructs pNk433\_C307A\_S3C\_A334C\_hktail and pNk343\_C307A\_S3C\_A334C (2.2.12), coding for **NcKin433\_S3C\_A334C** and **NcKin343\_S3C\_A334C**.

All constructs contain the two intrinsic cysteine residues of the motor domain (C38 and C59). To determine any possible interaction of the introduced cysteine residues with these remaining cysteine residues, single mutants were generated. These mutants only contain one introduced cysteine. If these single mutants react like wild-type, but the double mutants not, the effect can be assigned to the newly introduced cysteine residues. The following single mutants were examined: **NcKin433\_A226C** coded by pNk433\_C307A\_A226C\_hktail, **NcKin433\_E339C** coded by pNk433\_C307A\_E339C\_hktail, **NcKin343\_A226C** coded by pNk343\_C307A\_A226C, **NcKin343\_E339C** coded by pNk343\_C307A\_E339C, **NcKin433\_S3C** coded by pNk433\_C307A\_S3C\_hktail and **NcKin433\_A334C** coded by pNk433\_C307A\_A334C\_hktail (2.2.12).

### 3.1.3.2 HsKin

To decide whether the effects of the neck-linker/motor core crosslink are unique for NcKin, a comparison between NcKin and HsKin neck-linker/motor core constructs was necessary. Therefore, the corresponding double mutants of the NcKin A226C/E339C constructs were investigated in HsKin. In HsKin lysine residue 222 and glutamic acid residue 334 align with alanine residue 226 and glutamic acid residue 339 in NcKin. This led to the following constructs pHk560\_light\_K222C\_E334C\_GFP\_his and pHk339\_light\_K222C\_E334C\_his (2.2.12) or rather proteins **HsKin560\_K222C\_E334C** and **HsKin339\_K222C\_E334C**.

### 3.1.4 $\alpha$ 4/ $\alpha$ 6 Crosslinking Constructs

According to a crystallographic model, positioning of the neck-linker may be regulated by a torsion of helix  $\alpha$ 4 with respect to the motor core, including helix  $\alpha$ 6 [Kikkawa *et al.* 2001].

Inhibiting this rotation by introducing a crosslink between helices  $\alpha 4$  and  $\alpha 6$  therefore might generate similar effects as immobilisation of the neck-linker. To test this hypothesis, a pair of cysteine residues was introduced in the C-terminal portions of helices  $\alpha 4$  and  $\alpha 6$  whose crosslink was predicted to prevent the relative motion of these two helices. Kinesin crystal structures revealed amino acid residues threonine (273) and serine (329) as best candidates for the amino acid exchange. Both amino acids were exchanged for cysteine residues in the dimeric and monomeric wild-type construct, resulting in the two constructs pNk433\_C307A\_T273C\_S329C\_hktail and pNk343\_C307A\_T273C\_S329C (2.2.12), coding for **NcKin433\_T273C\_S329C** and **NcKin343\_T273C\_S329C** (Figure 3.5).

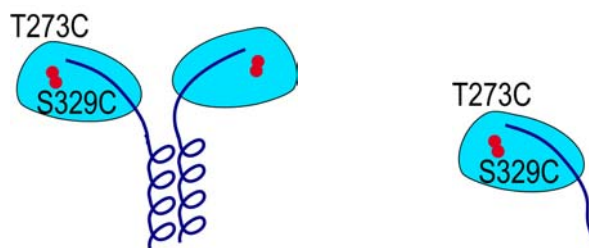


**Figure 3.5: Sketch of the  $\alpha 4/\alpha 6$  crosslinking constructs NcKin\_T273C\_S329C.**

The red circles indicate the reversibly crosslinking disulfide bridge between the two helices  $\alpha 4$  and  $\alpha 6$  in the motor domain of single kinesin subunits.

Any interaction of the introduced cysteine residues with the two remaining intrinsic cysteine residues was highly unlikely because they are positioned too far away from each other. Single mutants containing only one introduced cysteine were needed nevertheless in order to exclude effects directly due to the amino acid exchanges and possible monovalent reactions of the cysteine residues. The following single mutants were examined: **NcKin433\_T273C** coded by pNk433\_C307A\_T273C\_hktail, **NcKin433\_S329C** coded by pNk433\_C307A\_S329C\_hktail, **NcKin343\_T273C** coded by pNk343\_C307A\_T273C and **NcKin343\_S329C** coded by pNk343\_C307A\_S329C (2.2.12).

### 3.2 Purification of Bacterially Expressed Kinesin

All NcKin and HsKin constructs could be expressed in *E. coli* (2.3.4), except for the pNk433\_light and pNk433\_C38S\_C59S constructs (2.2.12).

NcKin constructs were isolated by a single chromatographic purification step (2.3.5.1). Elution peaks appeared for dimers at 200 mM NaCl, for monomers at 50-100 mM NaCl. The peak fractions were very clean, except for NcKin433\_wt (Figure 3.6 A, B). Protein concentrations ranged from 0.22 to 3.0 mg/ml.

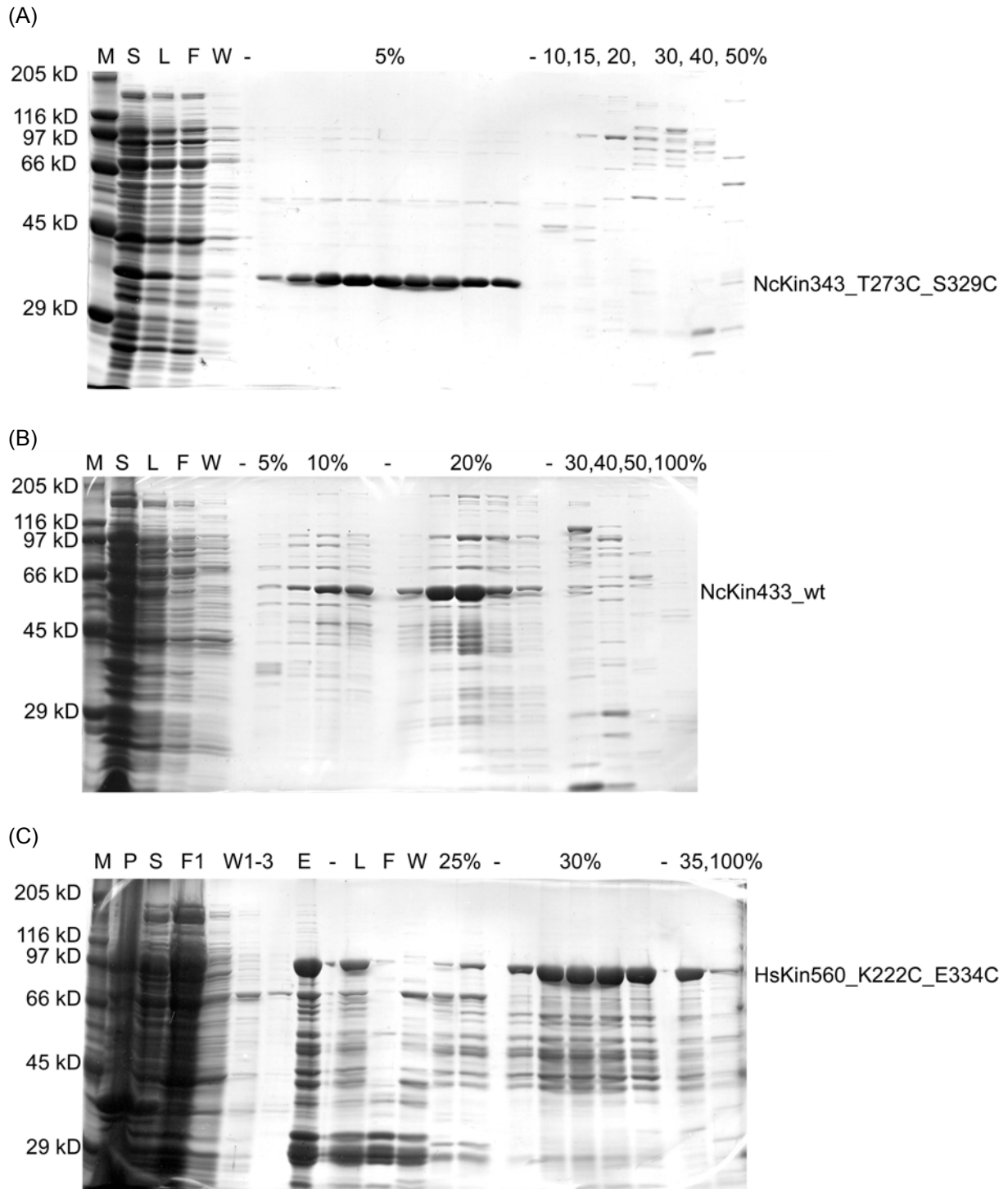


**Figure 3.6: SDS-gels of three protein purifications. (A), (B) NcKin (C) HsKin**

(A) Most NcKin preparations were more than 95% pure, comparable to NcKin343\_T273C\_S329C in panel A. (B) NcKin433\_wt preparations contained significant amounts of impurities, only 49% of total protein was kinesin (C) HsKin560\_K222C\_E339C preparations also contained significant amounts of impurities, 60% of total protein was kinesin. M = molecular mass standard, P = bacterial pellet after ultracentrifugation, S = bacterial supernatant after ultracentrifugation, F1 = flow through Ni-NTA column, W1-3 = wash of Ni-NTA column, E = eluate of Ni-NTA column, L = load to sepharose column, F = flow through sepharose column, W = wash of sepharose column, 5-100% = protein fractions eluted at 50 mM to 1 M NaCl from sepharose column

HsKin constructs were purified by a two step chromatographic process (2.3.5.2). Elution peaks appeared for the dimer at 300 mM NaCl, for the monomer at 150 mM NaCl. After the second purification step the peak fractions of the dimeric construct still were considerably contaminated (Figure 3.6 C). Protein concentrations were 0.25 and 2.9 mg/ml for the dimer and monomer, respectively.

Protein concentrations of the pooled fractions were measured photometrically (2.3.6). For preparations of NcKin433\_wt and HsKin560\_K222C\_E334C that still contained significant amounts of contaminations, the measured total protein concentration was adjusted by comparison of the intensities of the kinesin band with the contaminating bands (2.3.6). The proportion of kinesin in the total protein content was 49% and 60% for NcKin433\_wt and HsKin560\_K222C\_E339C, respectively.

The contaminated protein preparations exhibited normal wild-type behaviour when measured under reducing conditions. This implies that the contamination consists of inactive degradation products or unrelated protein which does not influence the measurements carried out in this study.

### 3.3 Proof of the Crosslink

All NcKin and HsKin constructs were tested for crosslinking by nonreducing SDS-PAGE (2.3.1). Thereby proteins are separated according to their mass. To prevent influences of their structure, proteins are denatured prior to loading by heat and the detergent SDS, interrupting all noncovalent interactions. Disulfide bridges are preserved as they are covalent bonds and disrupted only by reducing agents like  $\beta$ -mercaptoethanol or DTT.

Under reducing conditions, i.e. after incubation with DTT (2.3.13), all constructs run as expected from their molecular mass calculated from their amino acid composition (Figure 3.7). The molecular masses per polypeptide chain of the different types of constructs are listed below.

NcKin433_wt, etc.	= 60.9 kD	HsKin560_K222C_E334C	= 91.2 kD
NcKin433 (without hktail)	= 47.2 kD		
NcKin343_wt, etc.	= 37.4 kD	HsKin339_K222C_E334C	= 38.8 kD

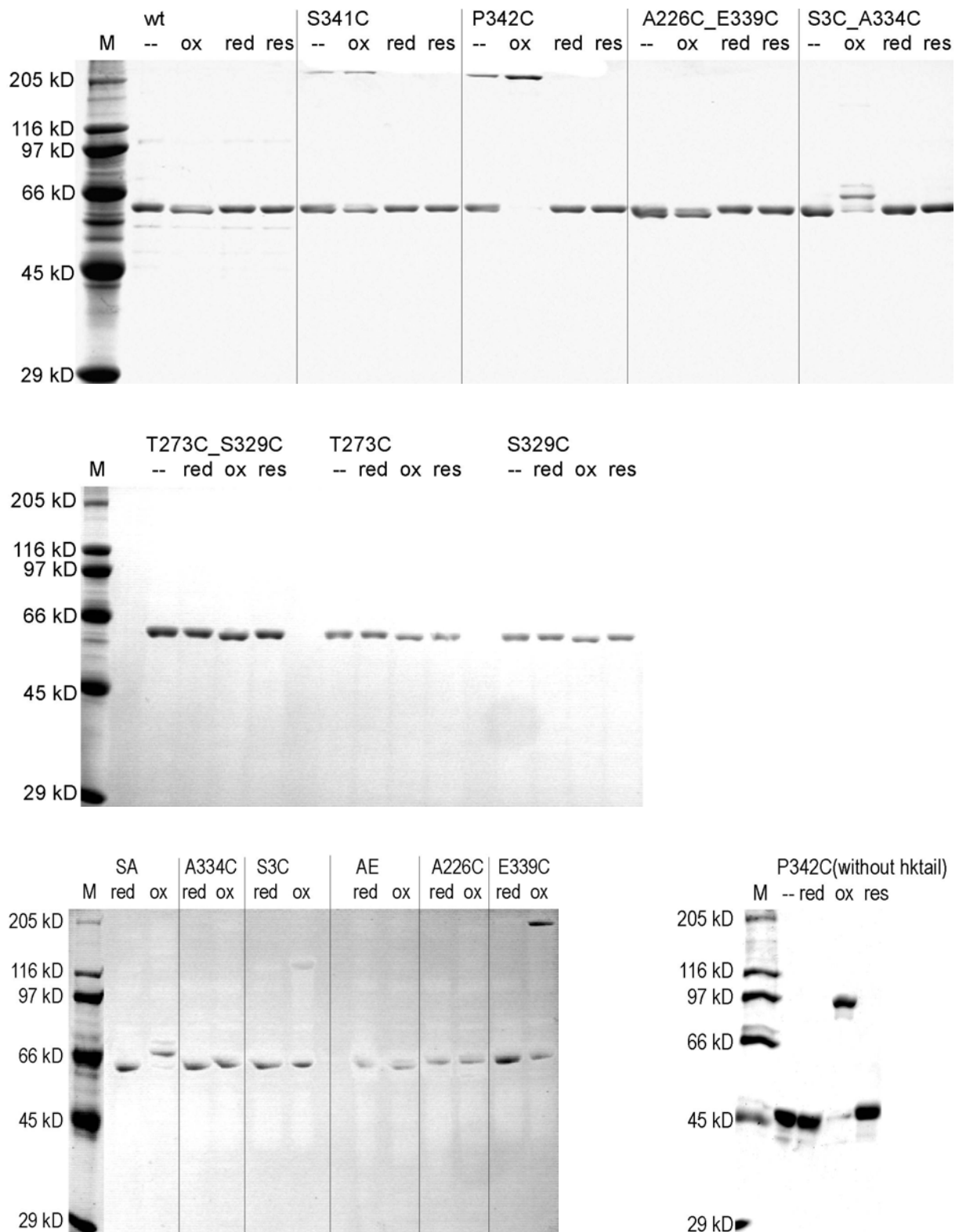


**Figure 3.7: Nonreducing SDS-gels of dimeric NcKin constructs as proof of crosslinks.**

Protein names are given without the prefix NcKin433\_, some are abbreviated further: SA = S3C\_A334C, AE = A226C\_E339C; M = molecular mass standard, -- = untreated protein, red = reduced protein, ox = oxidised protein, res = protein under rescue conditions. NcKin433\_wt: unaffected; NcKin433\_S341C: faintly crosslinked; NcKin433\_P342C: fully crosslinked and rescued; NcKin433\_A226C\_E339C: partly crosslinked and fully rescued, NcKin433\_A226C: unaffected, NcKin433\_E339C: partly crosslinked; NcKin433\_S3C\_A334C: mostly crosslinked and fully rescued, NcKin433\_S3C: faintly crosslinked, NcKin433\_A334C: unaffected; NcKin433\_T273C\_S329C, NcKin433\_T273C and NcKin433\_S329C: probably unaffected (minimal band shift)

### 3.3.1 Wild-type Constructs

Protein bands of the dimeric wild-type NcKin construct do not shift after incubation with oxidising or reducing agents (Figure 3.7). For each condition (buffer, DTNB, DTT and rescue (2.3.13)) the protein shows a band at ~60 kD. This confirms the assumption that the two remaining cysteine residues cannot react with each other.

Nonreducing gels of all monomeric constructs were hard to interpret as strange double bands occurred. But the data of the dimeric constructs allow to infer a behaviour similar to that of the monomers.

### 3.3.2 Neck/Neck Crosslinking Constructs

If the neck/neck crosslinking constructs NcKin433\_S341C and NcKin433\_P342C form disulfide bridges under oxidising conditions, this intermolecular crosslink should result in a protein band at a position representing the mass of two polypeptide chains, namely at 122 kD. For both constructs a band around 200 kD appeared under oxidising conditions (Figure 3.7). This mass rather corresponds to three polypeptide chains linked together, but it is hard to imagine, how a third polypeptide should attach to the dimeric molecule. The difference between the mass of two crosslinked polypeptides and the observed band may be explained by structural influences on the running behaviour. The disulfide bridge between the two chains may force them into a disadvantageous shape, thereby reducing its mobility in the gel. However, under oxidising conditions the same constructs without hktail show a new band at roughly 90 kD (Figure 3.7), matching the mass of the dimeric constructs. Apparently, the combination of the crosslink and the hktail together cause the observed strange running behaviour. This may be due to a problem with SDS association. Any unspecific crosslink between one introduced and one intrinsic cysteine residue is highly improbable, as the neck region of one polypeptide would have to fold back to the head of the other polypeptide to somehow reach the intrinsic cysteine residues. These observations suggest that indeed disulfide bridges are formed by the introduced cysteine residues.

The extent of crosslinking varies among the two constructs and the procedure used for oxidation. In general, the bands of the two crosslinked polypeptide chains are weaker in case of air oxidation, i.e. under buffer conditions, than oxidation with DTNB (2.3.13). Under oxidising conditions NcKin433\_S341C shows only very weak 200 kD bands and the prevailing amount of protein still is located at the 60 kD band, implying that the efficiency of this disulfide bond formation is rather low and most of the protein always is uncrosslinked.

The proportion of crosslinked protein is much higher for NcKin433\_P342C. After oxidation with DTNB the entire protein band is shifted to 200 kD, representing a completely crosslinked protein population. The much higher crosslinking efficiency of NcKin433\_P342C is in accordance with proline residue 342 holding an 'a' position of a coiled-coil neck region (3.1.2). The crosslinks of both constructs are fully reversible as the bands at 200 kD disappear under rescue conditions.

### 3.3.3 Neck-Linker/Motor Core Crosslinking Constructs

If the dimeric and monomeric neck-linker/motor core crosslinking constructs form disulfide bridges under oxidising conditions, this intramolecular crosslink should result in a looping of the polypeptide chains. These partly folded polypeptides have not changed their mass but their conformation, leading to a slight shift of the corresponding protein bands.

This band shift to ~67 kD is unambiguously visible and almost complete for NcKin433\_S3C\_A334C after incubation with DTNB (Figure 3.7), suggesting a crosslinking efficiency of about 90%. An additional weak band upon oxidation at ~70 kD cannot be explained while the faint band at ~120 kD probably is due to an intermolecular crosslink via cysteine residue 3 (compare single mutant NcKin433\_S3C). The single control mutant NcKin433\_A334C does not show a band shift when incubated with oxidising or reducing agents, whereas the other single control mutant NcKin433\_S3C shows an additional weak band at ~120 kD after DTNB incubation. This band corresponds to the mass of two polypeptide chains linked together, suggesting an intermolecular crosslink. The introduced cysteine is located right at the N-terminus of the polypeptide chains, which probably is quite mobile. This flexibility may allow the formation of a disulfide bridge between the introduced cysteine residues of a dimer. In this case the connecting covalent bond is right at the end of two polypeptide chains, therefore increasing its length but not interfering with unfolding. This might explain why this crosslinked construct runs as expected from its size in contrast to other constructs which are crosslinked in the middle of two polypeptide chains. As this band is very weak, this crosslink occurs only rarely in the single mutant and therefore the proportion of crosslinked protein is negligible. In addition, this faint band does not always occur in the double mutant, showing that the formation of the disulfide bridge between residues 3 and 334 is very much favoured.

The electrophoretic mobility of NcKin433\_A226C\_E339C is slightly increased under buffer and DTNB conditions (2.3.13) leading to a band at ~58 kD (Figure 3.7). The bands of the crosslinked protein are stronger than the ones of the uncrosslinked protein, indicating a

crosslinking efficiency of about 75%. The single control mutant NcKin433\_A226C does not show a band shift in response to incubation with oxidising or reducing agents, whereas the other single control mutant NcKin433\_E339C shows an additional band at ~200 kD after DTNB incubation. The crosslinked NcKin433\_E339C exhibits the same electrophoretic mobility as the crosslinked neck/neck constructs (3.3.2), indicating an intermolecular crosslink. The introduced cysteine is located at the end of the neck-linker, only two residues N-terminal to the introduced cysteine of NcKin433\_S341C. Because of the proximity to the coiled-coil neck region, the two residues 339 of the two polypeptide chains of a dimer are next to each other. Together with the intrinsic flexibility of the neck-linker a disulfide bridge between the introduced cysteine residues of a dimer may form. By comparing the strength of the crosslinked and uncrosslinked bands a crosslinking efficiency of about 60% can be estimated. As this crosslinked band does not occur in the double mutant, the formation of the disulfide bridge between residues 226 and 339 is apparently very much favoured.

### 3.3.4 $\alpha 4/\alpha 6$ Crosslinking Constructs

If the  $\alpha 4/\alpha 6$  crosslinking constructs form disulfide bridges under oxidising conditions, this intramolecular crosslink should result in a slight shift of the corresponding protein bands as seen for the neck-linker/motor core crosslinking constructs (3.3.3). However, the electrophoretic mobility of NcKin433\_T273C\_S329C changes only minimally with respect to reducing or oxidising conditions (2.3.13). After oxidation a slight band shift to ~59 kD may be induced (Figure 3.7). However, the same holds for both single control mutants NcKin433\_T273C and NcKin433\_S329C, which cannot be crosslinked due to the spatial separation of their cysteine residues. Therefore, probably no crosslink is formed in either construct.

## 3.4 Motility and ATPase Measurements

For all dimeric constructs gliding velocities (2.3.9.2) and microtubules stimulated ATP turnover rates (2.3.10.2, 2.3.10.3) were determined. Performing motility assays with monomeric constructs is not possible as these constructs lack a tail region which is necessary for binding the molecule to the coverslip. Therefore, for all monomeric constructs only microtubule-stimulated ATPase assays were performed.

In Figure 3.8 two typical ATPase measurements for dimeric and monomeric constructs are depicted. Data points show a hyperbolic dependence of the ATPase activity on the

microtubule concentration. By curve-fitting to the Michaelis-Menten-Equation the kinetic parameters  $k_{\text{cat}}$  and  $K_{0.5, \text{MT}}$  were determined. The ATP turnover rate  $k_{\text{cat}}$  signifies the amount of ATP hydrolysed per kinesin head domain per second. The  $K_{0.5, \text{MT}}$  equals the concentration of tubulin dimers that produce half-maximal ATPase activity. It corresponds to the Michaelis-Menten constant  $K_m$  for microtubules. For Michaelis-Menten enzymes the  $K_m$  is the dissociation constant of the complex of enzyme and substrate. Enzymes with a high affinity to the substrate have a low  $K_m$ . In the case of dimeric kinesin, the  $K_{0.5, \text{MT}}$  does not only reflect the affinity of kinesin and microtubules, because the reaction is not limited by the rate of kinesin-microtubule complex formation but by the steady-state turnover rate. Once a dimeric kinesin has docked onto the microtubule, the processive mechanism of motility ensures that the kinesin-microtubule complex is maintained for several reaction cycles. That is why the half maximal activation constant  $K_{0.5, \text{MT}}$  is much smaller than expected from kinesin's affinity to microtubules. Monomeric kinesins cannot work according to the alternating head mechanism and fall off the microtubule after one catalytic cycle. Therefore, here the  $K_{0.5, \text{MT}}$  reflects the affinity of kinesin and microtubules. Any changes in the  $K_{0.5, \text{MT}}$  of a monomeric kinesin mutant thus are likely to be due to an altered microtubule affinity. Any changes in the  $K_{0.5, \text{MT}}$  of dimeric mutants, however, may also be due to a disturbed processive mechanism of motility [Hackney 1995]. Values of  $K_{0.5, \text{MT}}$  measured here were quite variable, therefore, they indicate tendencies rather than quantitative evidence.

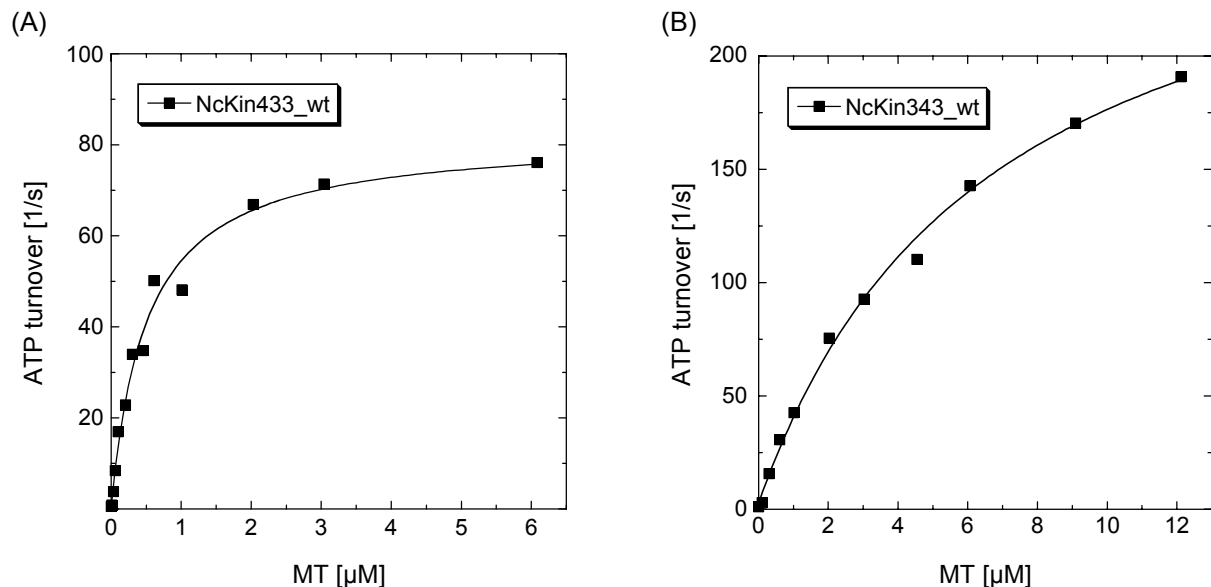


**Figure 3.8: ATPase activity of (A) NcKin433\_wt and (B) NcKin343\_wt as a function of microtubule concentration.**

Data points were fitted according to the hyperbolic equation  $y = B + k_{\text{cat}} * [\text{MT}] / (K_{0.5, \text{MT}} + [\text{MT}])$ . B = background activity

### 3.4.1 Wild-type Constructs

#### 3.4.1.1 Motility

Gliding velocities measured for the dimeric wild-type construct (NcKin433\_wt) did not differ from previously reported velocities of full length NcKin. For full length wild-type NcKin, isolated from *N. crassa*, gliding velocities of 2.5-3.8  $\mu\text{m/s}$  have been reported [Steinberg & Schliwa 1995] and for the same protein expressed by *E. coli*, 2.6  $\mu\text{m/s} \pm 0.3$  have been measured [Majdic 1999]. Velocities measured for NcKin433\_wt under the different reducing and oxidising conditions lay in the range of 2.4-2.8  $\mu\text{m/s}$  with standard deviations up to 10% (Figure 3.9 and Table 3.1 on page 64-66). Therefore, NcKin433\_wt indeed shows wild-type gliding behaviour and its velocity is not influenced by different incubation methods.

#### 3.4.1.2 ATPase Activity

Catalytic ATP turnover of NcKin433\_wt in the presence of microtubules under all but NEM conditions (72-74  $\text{s}^{-1}$  with standard deviations up to 20% (Figure 3.9 and Table 3.1)) was only slightly higher than for the bacterially expressed full length NcKin (57  $\text{s}^{-1} \pm 8$ ) [Majdic 1999] and bacterially expressed NcKin433 without hktail (61  $\text{s}^{-1} \pm 8$ ) [Kallipolitou *et al.* 2001]. However, the turnover rate under NEM conditions (128  $\text{s}^{-1}$ ) diverged profoundly from the values of the other conditions and from the previously reported values. As the NEM value is based on a single measurement it has not been confirmed. Therefore, NcKin433\_wt also is suitable as a wild-type reference in regard of ATP turnover.  $K_{0.5,MT}$  were in the normal range for dimers varying between 0.27-0.35  $\mu\text{M} \pm 0.28$ .

For the monomeric wild-type construct (NcKin343\_wt) the ATP turnover rate under the different reducing and oxidising conditions lay in the range of 242-302  $\text{s}^{-1}$  with standard deviations up to 6% (Figure 3.9 and Table 3.1). This corresponds well with a  $k_{\text{cat}}$  of 260  $\text{s}^{-1} \pm 74$ , measured by Kallipolitou *et al.* [2001].  $K_{0.5,MT}$  varied between 4.8-5.4  $\mu\text{M} \pm 2.4$ , which are usual values for monomers.

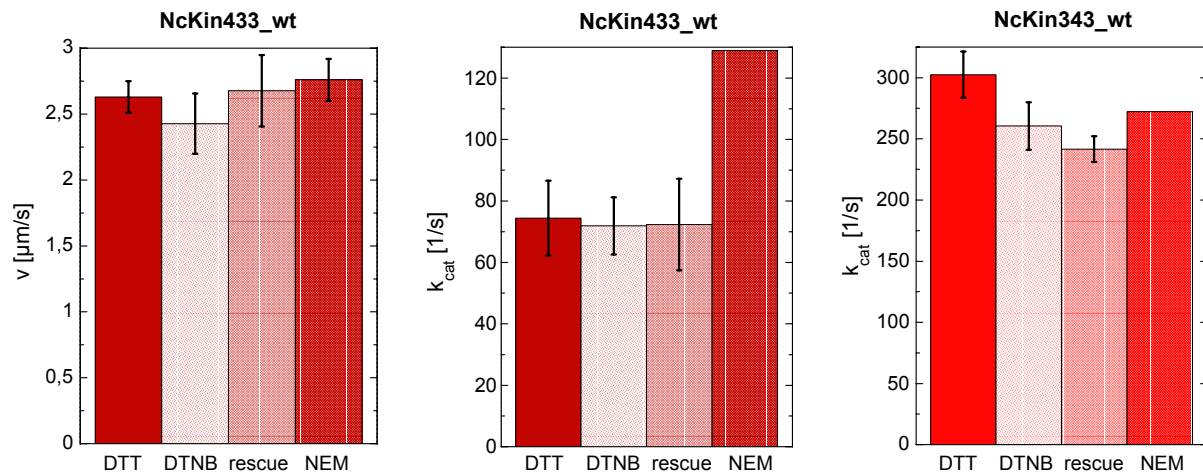


**Figure 3.9: Motility and ATPase properties of NcKin\_wt constructs.**

Bar charts of mean values and their standard deviations of gliding velocities and ATP turnover rates ( $k_{\text{cat}}$ ) of wild-type constructs.

### 3.4.1.3 Summary of NcKin\_wt

Measurements of wild-type constructs were obtained from two independent preparations each. In conclusion, it can be said that both wild-type constructs act as suitable wild-type references concerning gliding velocity and ATPase measurements. Both wild-type constructs are not affected by different incubation methods apart from the  $k_{\text{cat}}$  of NcKin433\_wt under NEM conditions, which is extremely high. This value represents a single measurement only and therefore is unconfirmed. Furthermore, a similar effect was not observed in the monomeric wildtype construct. Thus, it can be excluded that neither the exchange of cysteine 307 in alanine nor the attachment of part of the human tail region (hktail) affect the hydrolysis or stepping mechanism of NcKin.

## 3.4.2 Neck/Neck Crosslinking Constructs

### 3.4.2.1 Motility

NcKin433\_S341C showed a reduction of 20-25% in gliding velocities for DTNB and rescue conditions (1.7 and 1.8  $\mu\text{m/s}$ , respectively) compared with its velocities for DTT and NEM conditions (Figure 3.10 and Table 3.1). Velocities under DTT and NEM conditions (2.1 and 2.4  $\mu\text{m/s}$ , respectively) are slightly below the mean values of measurements under all conditions of the dimeric wild-type (2.6  $\mu\text{m/s} \pm 0.24$ ).

For NcKin433\_P342C gliding velocities of 2.5  $\mu\text{m/s}$  were measured for DTT, NEM and rescue conditions and 2.1  $\mu\text{m/s}$  for DTNB conditions (Figure 3.10 and Table 3.1). All values lie within the tolerance.

### 3.4.2.2 ATPase Activity

ATP turnover rates of NcKin433\_S341C varied between different conditions (Figure 3.10 and Table 3.1). The rescue experiment yielded the lowest  $k_{\text{cat}}$  of  $56 \text{ s}^{-1}$ , the NEM experiment the highest  $k_{\text{cat}}$  of  $82 \text{ s}^{-1}$ .  $K_{0.5, \text{MT}}$  varied between  $0.17\text{-}0.33 \text{ }\mu\text{M}$ , which is quite normal.

Turnover rates of NcKin433\_P342C under all conditions lay between  $63\text{-}66 \text{ s}^{-1}$  (Figure 3.10 and Table 3.1), which is slightly below the mean value of all dimeric wildtype measurements ( $73 \text{ s}^{-1} \pm 10$ ).  $K_{0.5, \text{MT}}$  were average values ranging between  $0.30\text{-}0.44 \text{ }\mu\text{M} \pm 0.25$ .

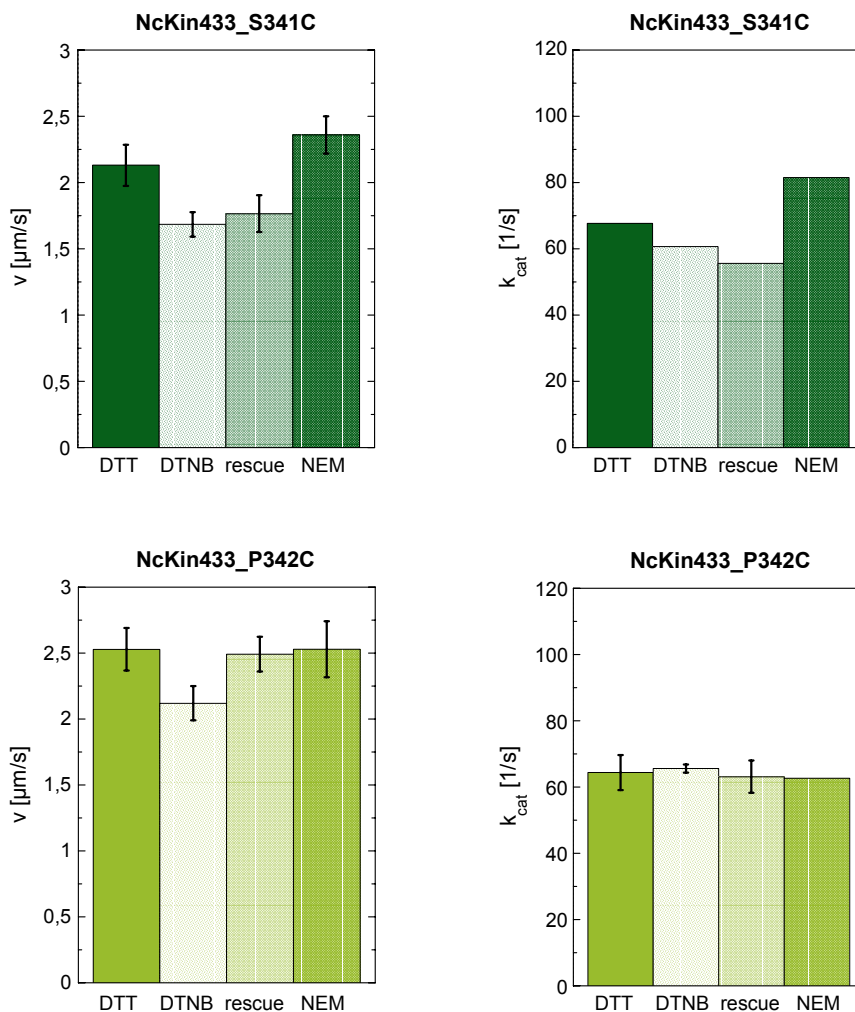


**Figure 3.10: Motility and ATPase properties of NcKin\_S341C and NcKin\_P342C constructs.** Bar charts of mean values and their standard deviations of gliding velocities and ATP turnover rates ( $k_{\text{cat}}$ ) of neck/neck crosslinking constructs.

### 3.4.2.3 Summary of NcKin\_S341C and NcKin\_P342C

Only one preparation of NcKin433\_S341C was examined. Here both ATPase and motility measurements showed some degree of variation. It is noteworthy that the protein slowed down under DTNB and rescue conditions by 20-25% and that its catalytic activity showed a peak under NEM conditions.

All ATP turnover rates and gliding velocities measured for two independent preparations of NcKin433\_P342C are comparable to NcKin433\_wt results (3.4.1) and previously measured values of wild-type NcKin [Steinberg & Schliwa 1995; Majdic 1999; Kallipolitou *et al.* 2001]. The results of both assays were independent of reducing or oxidising conditions.

These findings suggest that melting of the neck coiled-coil of NcKin is not necessary to allow for normal hydrolysis and multiple motor gliding behaviour.

## 3.4.3 Neck-Linker/Motor Core Crosslinking Constructs

### 3.4.3.1 NcKin\_S3C\_A334C

#### 3.4.3.1.1 Motility

Gliding velocities of NcKin433\_S3C\_A334C under DTT and rescue conditions (2.3 and 2.2  $\mu\text{m/s}$ , respectively) were indistinguishable from wild-type values (Figure 3.11 and Table 3.1). However, after incubation with DTNB there was hardly any movement (0.07  $\mu\text{m/s}$ ). The NEM-treated sample showed a reduced velocity of 1.7  $\mu\text{m/s}$ .

The single mutant NcKin433\_S3C exhibited normal gliding velocities of 2.6-2.7  $\mu\text{m/s}$  for NEM, DTT and rescue conditions and slowed down to 2.1  $\mu\text{m/s}$  after DTNB incubation (Figure 3.11 and Table 3.1). For NEM and DTNB a strange effect was detected. Microtubule gliding significantly slowed down if a given site on the slide was observed for some time. Gliding velocities at different sites of the same slide measured thereafter first were normal and then also decreased with increasing observation time. The effect was more pronounced for DTNB, decreasing the velocity to 0.7  $\mu\text{m/s}$ , than for NEM, resulting in a lowest velocity of 1.8  $\mu\text{m/s}$ . A heating effect can be excluded as the temperature of the sample was regulated by cooling or heating the objective and thus the part of the slide which is under observation. Possibly, the effect can be assigned to influences of light as it occurs only at sites which have been observed for some time.

Similar gliding behaviour was observed for the other single mutant NcKin433\_A334C. Here, NEM and DTNB results (2.2 and 2.0  $\mu\text{m/s}$ , respectively) differed from DTT and rescue

results (2.5 and 2.7  $\mu\text{m/s}$ , respectively), which matched wild-type velocity (Figure 3.11 and Table 3.1). Here likewise a temporal decline of gliding velocities under NEM (to 1.1  $\mu\text{m/s}$ ) and DTNB (to 0.8  $\mu\text{m/s}$ ) conditions occurred. A recovery of fast gliding at the beginning of observation at a new site could not clearly be shown.

#### 3.4.3.1.2 ATPase Activity

ATP turnover rates of NcKin433\_S3C\_A334C under all conditions were relatively high (Figure 3.11 and Table 3.1). They varied between 86  $\text{s}^{-1}$  for rescue and 97  $\text{s}^{-1}$  for DTNB conditions. These values are at the upper extreme of the mean value of all dimeric wild-type ATPase measurements ( $73 \text{ s}^{-1} \pm 10$ ).  $K_{0.5,MT}$  values were in the normal range for dimers varying between 0.17-0.38  $\mu\text{M} \pm 0.26$ , but for DTNB conditions, where it was significantly lower at 0.13  $\mu\text{M} \pm 0.1$ .

The single mutant NcKin433\_S3C showed some variability in the  $k_{\text{cat}}$  values for the different types of incubation (Figure 3.11 and Table 3.1). For DTT the highest rate of 99  $\text{s}^{-1}$  was measured, for rescue 81  $\text{s}^{-1}$  and for NEM and DTNB 70  $\text{s}^{-1}$  and 67  $\text{s}^{-1}$ , respectively. All these measurements were complicated by a rapid decrease of ATPase activity within the short duration of the assay (approximately 30 min). The reagents used in the assay were not responsible as subsequent assays performed with the same reagents but different aliquots of kinesin in the beginning exhibited normal ATPase activity. Apparently, the construct loses activity during the time of the assay.  $K_{0.5,MT}$  ranged within normal values of 0.22-0.32  $\mu\text{M}$ .

The catalytic activity of the single mutant NcKin433\_A334C under all conditions showed more constancy (Figure 3.11 and Table 3.1). It ranged between 92  $\text{s}^{-1}$  and 99  $\text{s}^{-1}$ .  $K_{0.5,MT}$  values were a little high for dimers ranging between 0.52-0.70  $\mu\text{M}$ .

NcKin343\_S3C\_A334C exhibited similar high turnover rates as the monomeric wild-type construct (Figure 3.11 and Table 3.1).  $K_{\text{cat}}$  was highest under DTT conditions (283  $\text{s}^{-1}$ ), followed by rescue (246  $\text{s}^{-1}$ ), NEM (234  $\text{s}^{-1}$ ) and DTNB conditions (231  $\text{s}^{-1}$ ).  $K_{0.5,MT}$  values were in the lower range for monomers varying between 1.7-2.1  $\mu\text{M}$ , dropping even further to 1.1  $\mu\text{M}$  for NEM measurements.

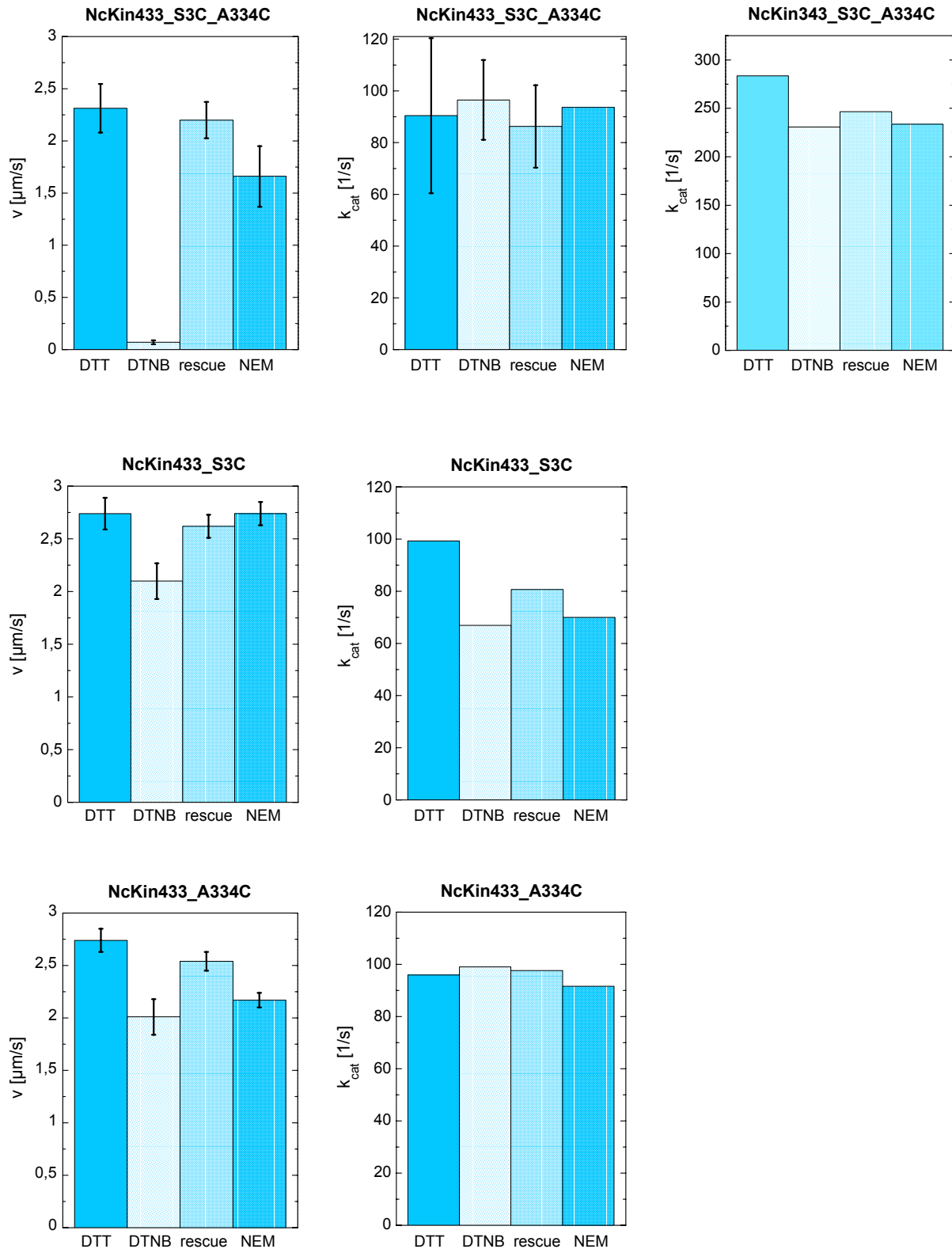


**Figure 3.11: Motility and ATPase properties of NcKin\_S3C\_A334C constructs.**

Bar charts of mean values and their standard deviations of gliding velocities and ATP turnover rates ( $k_{\text{cat}}$ ) of partial neck-linker/motor core crosslinking constructs. Gliding velocities of both single mutants decreased during the motility assay under DTNB and NEM conditions. NcKin433\_S3C additionally lost ATPase activity under all conditions while measuring. In these cases only the very first measurements have been used for the determination of gliding velocities and ATP turnover rates.

### 3.4.3.1.3 Summary of NcKin\_S3C\_A334C

ATP turnover rates and gliding velocities have been measured in two independent preparations of NcKin433\_S3C\_A334C. While oxidation had a pronounced effect on its gliding velocity, almost completely abolishing movement, ATP turnover was not affected at all. Thus, energy gained by ATP hydrolysis was not transduced into movement any more. Hydrolysis and motility were uncoupled. In the NEM control the velocity was reduced by 26%, which might be attributable to sterical clashes impeding stepping when NEM is bound to the cysteine in the neck-linker (compare results of the single mutant NcKin433\_A334C). Apparently these sterical clashes do not interfere with hydrolysis. The  $K_{0.5,MT}$  value was smaller for the oxidised protein, indicating an increased dwell time on the microtubule which may be caused by an impaired microtubule release.

Only one preparation each of the single mutants and the monomer was examined.

Single mutant NcKin433\_S3C showed a reduction of gliding velocity by 23% after oxidation. This slowed movement could be due to the small amount of protein crosslinked at residues 3 (3.3.3). ATP turnover rates for DTNB and NEM also were reduced by 29-33%. In both measurements complications arose. For gliding assays only NEM and DTNB conditions were affected, exhibiting a decrease of velocity, possibly induced by light, while the hydrolysis rate was subject to inactivation during the measuring period of 30 min under all conditions. These observations are difficult to explain. Any slow oxidation effect can be ruled out because measurements with a high concentration of DTT were affected, too. Presumably, this protein preparation was somehow sensitive leading to an instable protein.

Gliding velocity of the single mutant NcKin433\_A334C slowed down for NEM and DTNB by 21-27%, while the catalytic activity was not influenced. These effects probably were caused by binding of the reagent (NEM or DTNB) to residue 334 resulting in sterical clashes which impede movement. Similar complications as for NcKin433\_S3C arose for NEM and DTNB conditions in the gliding assays. Microtubule gliding slowed down with time. But there is no coherent reason apparent. Its  $K_{0.5,MT}$  values were quite high, especially for DTT and rescue conditions, indicating a decrease of microtubule affinity or processivity.

The ATPase activity of the monomer was highest under reducing conditions and 13-19% reduced for the other conditions. Under NEM conditions the  $K_{0.5,MT}$  was extremely low, suggesting an unusually high microtubule affinity of the monomer.

It can be concluded that NcKin cannot transduce the energy of ATP hydrolysis into movement if its neck-linker is partially immobilised.

### 3.4.3.2 NcKin\_A226C\_E339C

#### 3.4.3.2.1 Motility

NcKin433\_A226C\_E339C exhibited normal gliding velocities of 2.3-2.4  $\mu\text{m/s}$  for NEM, DTT and rescue conditions, but drastically slowed down to 0.4  $\mu\text{m/s}$  after DTNB incubation (Figure 3.12 and Table 3.1).

Gliding velocities of the single mutant NcKin433\_A226C under NEM, DTT and rescue conditions (2.9  $\mu\text{m/s}$ ) were high (Figure 3.12 and Table 3.1) compared with the mean value of all wild-type motility measurements (2.6  $\mu\text{m/s} \pm 0.24$ ). After incubation with DTNB its velocity was back to average (2.5  $\mu\text{m/s}$ ).

The other single mutant NcKin433\_E339C showed slightly fluctuating gliding velocities for all different types of incubation (Figure 3.12 and Table 3.1). They ranged from 2.3-2.7  $\mu\text{m/s}$ .

#### 3.4.3.2.2 ATPase Activity

ATP turnover rates of NcKin433\_A226C\_E339C under NEM, DTT and rescue conditions were relatively low (Figure 3.12 and Table 3.1). They varied between 26-34  $\text{s}^{-1}$  and thus were significantly lower than the mean value of all dimeric wild-type ATPase measurements (73  $\text{s}^{-1} \pm 10$ ). Upon oxidation, the  $k_{\text{cat}}$  dropped to 4  $\text{s}^{-1}$ .  $K_{0.5, \text{MT}}$  values were normal (0.20-0.35  $\mu\text{M} \pm 0.25$ ), but rose to 0.99  $\mu\text{M} \pm 0.31$  for DTNB measurements.

The catalytic activity of the single mutant NcKin433\_A226C was quite constant under all conditions (Figure 3.12 and Table 3.1). It ranged between 61  $\text{s}^{-1}$  and 66  $\text{s}^{-1}$ .  $K_{0.5, \text{MT}}$  values were a little high for dimers ranging between 0.46-0.54  $\mu\text{M}$ , especially for DTNB conditions, where it reached 1.03  $\mu\text{M}$ .

The same holds for the other single mutant NcKin433\_E339C for all but DTT conditions (Figure 3.12 and Table 3.1).  $K_{\text{cat}}$  values of 68-71  $\text{s}^{-1}$  have been measured except for the DTT value of 95  $\text{s}^{-1}$ .  $K_{0.5, \text{MT}}$  ranged between totally normal values of 0.37-0.45  $\mu\text{M}$ .

The following monomers again exhibited very high ATPase activity, comparable to the previously described monomers (3.4.1.2, 3.4.3.1.2).

$K_{\text{cat}}$  of NcKin343\_A226C\_E339C for NEM and DTT ranged between 195-205  $\text{s}^{-1}$  (Figure 3.12 and Table 3.1), which is rather low for monomeric constructs (mean of all monomeric wild-type values = 269  $\text{s}^{-1} \pm 28$ ). Incubation with DTNB greatly reduced it to 7  $\text{s}^{-1}$ . Rescue was incomplete, recovering to a  $k_{\text{cat}}$  of 121  $\text{s}^{-1} \pm 52$ .  $K_{0.5, \text{MT}}$  values ranged between 4.4-5.8  $\mu\text{M}$ , but increased to 7.2 and 7.7  $\mu\text{M}$  under NEM and rescue conditions, respectively.

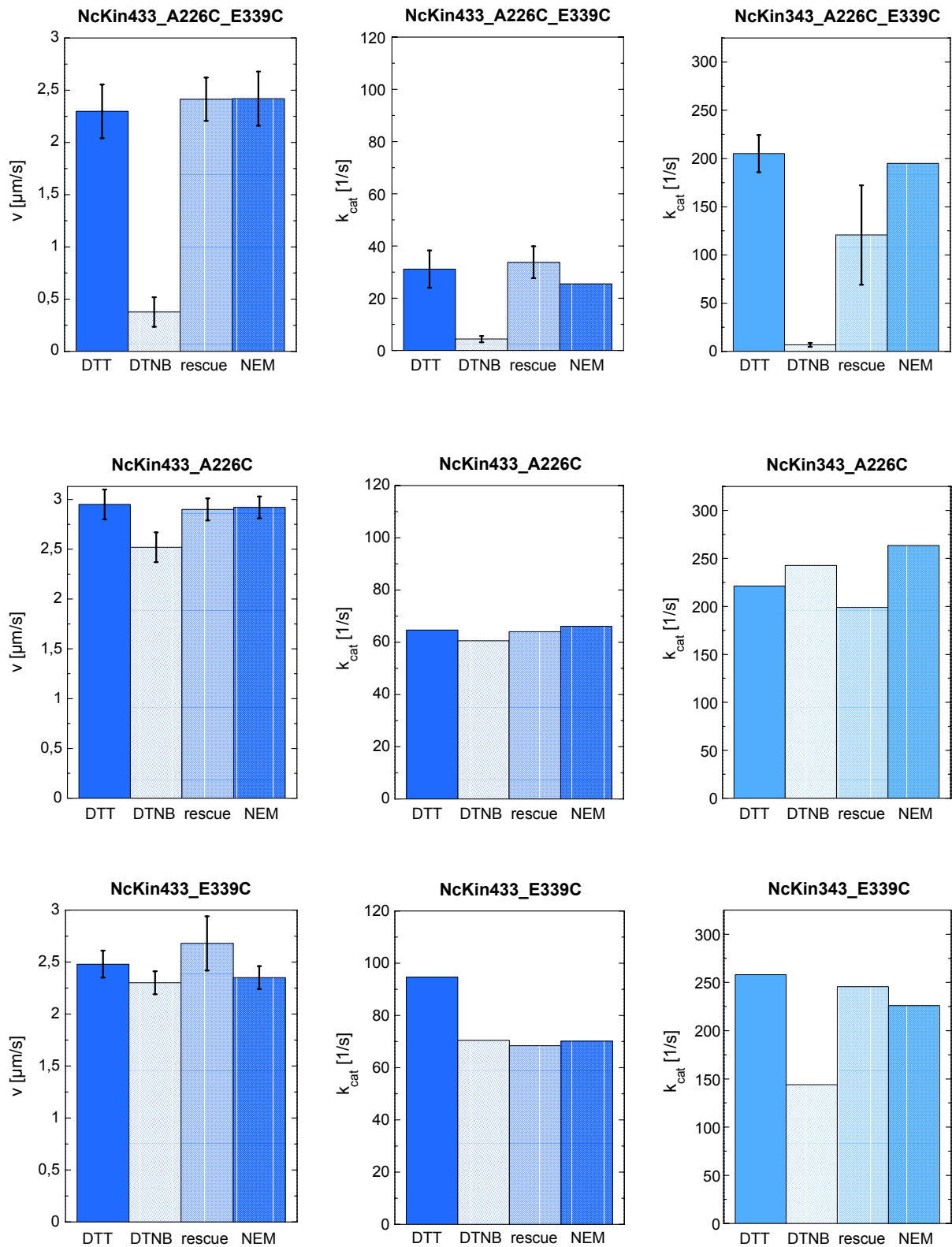


**Figure 3.12: Motility and ATPase properties of NcKin\_A226C\_E339C constructs.**

Bar charts of mean values and their standard deviations of gliding velocities and ATP turnover rates ( $k_{cat}$ ) of complete neck-linker/motor core crosslinking constructs.

Single mutant NcKin343\_A226C exhibited relatively variable turnover rates (Figure 3.12 and Table 3.1). The lowest of  $199\text{ s}^{-1}$  occurred under rescue conditions, increasing to  $221\text{ s}^{-1}$  under DTT, to  $243\text{ s}^{-1}$  under DTNB and to  $263\text{ s}^{-1}$  under NEM conditions. Normal  $K_{0.5,MT}$  values between  $2.2\text{--}2.8\text{ }\mu\text{M}$  were measured except for DTNB conditions ( $7.5\text{ }\mu\text{M}$ ).

For the other single mutant NcKin343\_E339C  $k_{cat}$  values varied between  $226\text{--}258\text{ s}^{-1}$  for all but DTNB conditions, where it decreased to  $144\text{ s}^{-1}$  (Figure 3.12 and Table 3.1).  $K_{0.5,MT}$  values were normal ( $4.3\text{--}5.4\text{ }\mu\text{M}$ ) apart from an extremely high value for DTNB conditions ( $23\text{ }\mu\text{M}$ ).

#### 3.4.3.2.3 Summary of NcKin\_A226C\_E339C

ATP turnover rates and gliding velocities have been measured for two independent preparations of NcKin433\_A226C\_E339C. Oxidation had a pronounced effect both on its gliding velocity and ATP turnover, reducing its velocity and turnover rate by 83% and 86%, respectively. This implies an effective inactivation of all motor functions. The  $K_{0.5,MT}$  value was three times bigger for the oxidised protein. Together with the observation that microtubule binding to the coverslip coated with oxidised protein is weak to non-existent, a dramatically decreased affinity to microtubules can be suspected. Furthermore, its ATPase activity under nonoxidising conditions was less than half of the dimeric wild-type and its two single mutants. This indicates partly inactive protein preparations because it is unlikely that the combined exchange of residues 226 and 339 should result in a reduced hydrolysis but the separate exchanges should not. Inactivated protein could be due to an inability to completely reduce the construct so that part of the protein was permanently crosslinked. But this is unlikely as in the nonreducing gels no second band is visible except upon oxidation.

Only one preparation of each single mutant was examined.

Single mutant NcKin433\_A226C showed rather high gliding velocities for nonoxidised conditions, but the difference to the average was not significant. Its ATPase activity was not influenced, while overall its  $K_{0.5,MT}$  values were quite high. Under DTNB conditions it doubled further, indicating a decrease of microtubule affinity or processivity.

The other single mutant NcKin433\_E339C exhibited slightly fluctuating velocities and a 27% increased  $k_{cat}$  when reduced. This could be attributable to the occurrence of an intermolecular crosslink for more than half of the protein (3.3.3). But there is no explanation why the effect of the crosslink is not reversible and can be imitated by the binding of NEM. Thus, the high ATP turnover value might rather be assigned to a single strongly deviating measurement.

Measurements of two independent preparations of NcKin343\_A226C\_E339C have been averaged for ATPase results. Oxidation led to a 97% decrease of ATP turnover, which could be rescued to 60% of the initial value. The extent of rescue diverged dramatically between preparations, leading to a standard deviation of 43%. Thus, breaking of the crosslink seems to be more difficult in the monomer than dimer. Its  $K_{0.5,MT}$  values were unusually high for NEM and rescue conditions, indicating lower microtubule affinity.

Again, only one preparation of each single mutant was examined.

$K_{cat}$  values of the single mutant NcKin343\_A226C were relatively broadly distributed. Under oxidising conditions the  $K_{0.5,MT}$  was threefold higher, suggesting an unusually low microtubule affinity.

The catalytic activity of the other single mutant NcKin343\_E339C was nearly halved by oxidation. This must be attributed to the formation of an intramolecular crosslink between cysteine 339 and one of the remaining intrinsic cysteine residues. Probably, the neck-linker in the monomers is totally flexible as it is not restrained by the neck region that follows it as in the dimers. Therefore, it might be able to fold back towards the broad end of the motor core and thereby reach cysteine 38 or 59. Additionally, its  $K_{0.5,MT}$  was extremely high (5x bigger than under the other conditions), suggesting a dramatically reduced microtubule affinity.

These findings indicate that immobilisation of the complete neck-linker of NcKin prevents both hydrolysis and motility.

### 3.4.3.3 HsKin\_K222C\_E334C

#### 3.4.3.3.1 ATPase Activity

$K_{cat}$  values measured for HsKin560\_K222C\_E334C under buffer and DTT conditions (28-30  $s^{-1}$ ) (Figure 3.13 and Table 3.1) perfectly matched values reported for the wild-type protein of the same length (31  $s^{-1}$ ) [Case *et al.* 2000] and the same protein (cysteine-light construct) lacking the two mutations (30-32  $s^{-1}$ ) [Tomishige & Vale 2000]. However, for the identical protein containing the two introduced cysteine residues, they report a  $k_{cat}$  of only 12-13  $s^{-1}$  under buffer and NEM conditions. A turnover rate of 6.8  $s^{-1}$ , which they describe for oxidising conditions, agrees with measurements of 5  $s^{-1}$  in this study. Catalytic activity could not be rescued, it remained low at 7  $s^{-1}$ . Compared with the NcKin constructs its  $K_{0.5,MT}$  values were rather low (0.08-0.12  $\mu M$ ), increasing 3fold after oxidation (0.25  $\mu M$ ).

The ATP turnover of HsKin339\_K222C\_E334C under buffer and DTT conditions ranged between 56-66  $s^{-1}$  (Figure 3.13 and Table 3.1). These data fit very well with a previously

reported value of  $60 \text{ s}^{-1}$  for a monomeric human wild-type kinesin consisting of the first 332 amino acids [Ma & Taylor 1997b]. Oxidation dramatically reduced the  $k_{\text{cat}}$  to  $4 \text{ s}^{-1}$ , recovering under rescue conditions to  $18 \text{ s}^{-1}$ .  $K_{0.5, \text{MT}}$  values were extremely low for a monomeric construct ( $0.23\text{-}0.40 \text{ }\mu\text{M}$ ), increasing 3-4fold after oxidation ( $1.16 \text{ }\mu\text{M}$ ).

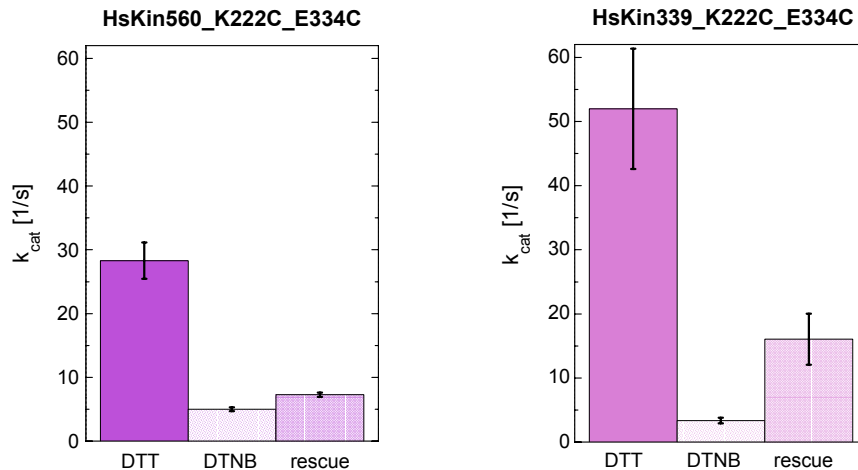


**Figure 3.13: Motility and ATPase properties of HsKin\_K222C\_E334C constructs.**

Bar charts of mean values and their standard deviations of gliding velocities and ATP turnover rates ( $k_{\text{cat}}$ ) of human neck-linker/motor core crosslinking constructs.

#### 3.4.3.3.2 Summary of HsKin\_K222C\_E334C

Both HsKin constructs were purified only once and these preparations were measured twice.

Oxidation of dimer and monomer reduced the ATPase activity by 82% and 93%, respectively.

The turnover rates of both proteins could not be rescued. They only reached 26% and 32% of the initial values of dimer and monomer, respectively. Especially the monomer exhibited extremely low  $K_{0.5, \text{MT}}$  values, indicating unusually high microtubule affinity. Both oxidised constructs showed an about 3fold increase of  $K_{0.5, \text{MT}}$ .

These results show that a completely immobilised neck-linker causes the total loss of enzymatic activity also in HsKin. Therefore, the need of mobility of the neck-linker for motor function is not unique for NcKin but rather a general feature of conventional kinesins.

### 3.4.4 $\alpha 4/\alpha 6$ Crosslinking Constructs

#### 3.4.4.1 Motility

Average gliding velocities of NcKin433\_T273C\_S329C of  $2.2\text{-}2.3 \text{ }\mu\text{m/s}$  were measured for NEM and DTT (Figure 3.14 and Table 3.1). They decelerated to  $0.4\text{-}0.5 \text{ }\mu\text{m/s}$  under oxidising and rescue conditions.

Single mutant NcKin433\_T273C exhibited normal gliding velocities of 2.4-2.6  $\mu\text{m/s}$  for all but DTNB conditions, where it was only 1.0  $\mu\text{m/s}$  (Figure 3.14 and Table 3.1). With increasing observation time the velocity decreased from 1.3 to 0.75  $\mu\text{m/s}$ .

The other single mutant NcKin433\_S329C showed constant velocities between 2.4-2.6  $\mu\text{m/s}$  for all incubation methods (Figure 3.14 and Table 3.1).

#### 3.4.4.2 ATPase Activity

ATP turnover rates of NcKin433\_T273C\_S329C were 72-75  $\text{s}^{-1}$  under NEM and DTT conditions (Figure 3.14 and Table 3.1). They dropped to 33-34  $\text{s}^{-1}$  under oxidising and rescue conditions. Its  $K_{0.5,MT}$  ranged within normal values of 0.22-0.48  $\mu\text{M} \pm 0.34$ , but the values measured under oxidising and rescue conditions were twice as high.

The catalytic activity of the single mutant NcKin433\_T273C ranged between 42  $\text{s}^{-1}$  and 53  $\text{s}^{-1}$  for all but NEM conditions, where it came to 75  $\text{s}^{-1}$  (Figure 3.14 and Table 3.1).  $K_{0.5,MT}$  values were normal (0.40-0.42  $\mu\text{M}$ ), but rose to 0.97  $\mu\text{M}$  for DTNB measurements.

The same is true for the other single mutant NcKin433\_S329C. For NEM conditions a  $k_{cat}$  of 68  $\text{s}^{-1}$  was measured, for the remaining incubation methods 50-54  $\text{s}^{-1}$ . Normal  $K_{0.5,MT}$  values between 0.23-0.37  $\mu\text{M}$  were measured.

NcKin343\_T273C\_S329C's turnover rates were quite variable (Figure 3.14 and Table 3.1). The highest was the DTT value (222  $\text{s}^{-1}$ ), followed by the NEM value (160  $\text{s}^{-1}$ ), the rescue value (144  $\text{s}^{-1}$ ) and finally the DTNB value (95  $\text{s}^{-1}$ ).  $K_{0.5,MT}$  values greatly varied between the two measured protein preparations, causing extremely high standard deviations. The values overall were remarkably high (4.0-9.4  $\mu\text{M} \pm 100\%$ ), with a peak value for the rescue measurement (14.7  $\mu\text{M} \pm 5.7$ ).

The same holds for the single mutant NcKin343\_T273C (Figure 3.14 and Table 3.1). 261  $\text{s}^{-1}$  was measured for DTT, 203  $\text{s}^{-1}$  for rescue, 190  $\text{s}^{-1}$  for NEM and 95  $\text{s}^{-1}$  for DTNB conditions. Measurements under DTNB conditions were complicated by a dramatic loss of activity while performing the assay.  $K_{0.5,MT}$  ranged within normal values of 1.7-2.4  $\mu\text{M}$ .

By contrast, the other single mutant NcKin343\_S329C exhibited ATPase rates between 240-274  $\text{s}^{-1}$  for all conditions (Figure 3.14 and Table 3.1). Normal  $K_{0.5,MT}$  values between 2.1-3.0  $\mu\text{M}$  were measured.

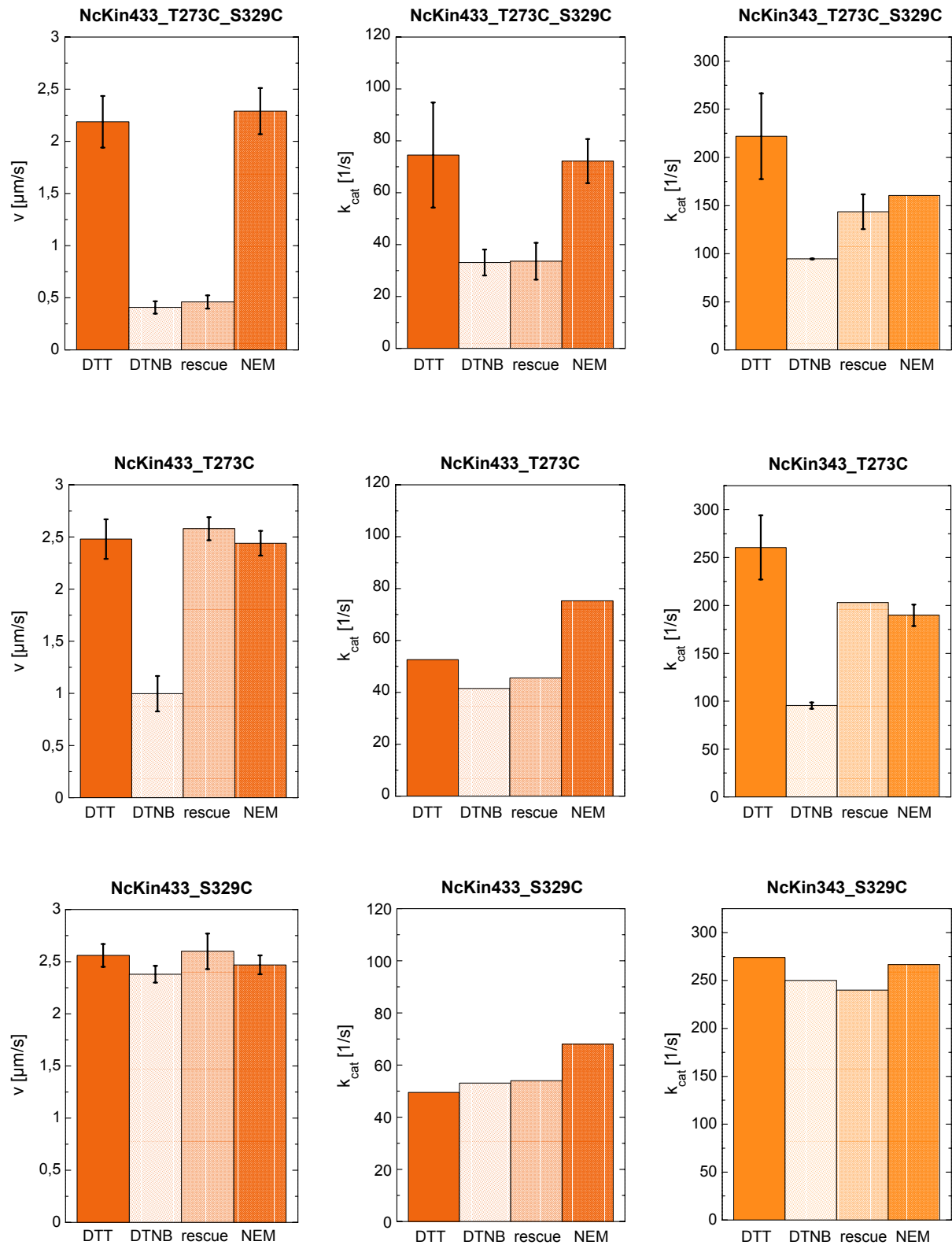


**Figure 3.14: Motility and ATPase properties of NcKin\_T273C\_S329C constructs.**

Bar charts of mean values and their standard deviations of gliding velocities and ATP turnover rates ( $k_{\text{cat}}$ ) of  $\alpha 4/\alpha 6$  crosslinking constructs.

### 3.4.4.3 Summary of NcKin\_T273C\_S329C

ATP turnover rates and gliding velocities have been measured for two independent preparations of NcKin433\_T273C\_S329C. Oxidation had a pronounced effect both on its gliding velocity and ATP turnover, and was not reversible. Its velocity and turnover rate were permanently reduced by 79-81% and 55-56%, respectively. This is reflected in the doubling of the  $K_{0.5,MT}$  under oxidising and rescue conditions.

Only one preparation of each single mutant was examined.

Oxidation also affected gliding velocity of the single mutant NcKin433\_T273C, decreasing it by 60%. The velocity dropped with increasing observation time. But these effects were fully reversible. Its ATPase activity was quite variable, showing normal activity only under NEM conditions. ATP turnover was 29-44% low for the other conditions. Furthermore oxidation doubled the  $K_{0.5,MT}$ .

Gliding velocity of single mutant NcKin433\_S329C was not influenced. However, it exhibited similar low ATPase activity for DTT, DTNB and rescue conditions (decrease by 21-26%) as the other single mutant.

Measurements of two independent preparations of NcKin343\_T273C\_S329C have been averaged for ATPase results. Oxidation led to a 57% decrease of ATP turnover, which could be rescued to 65% of the initial value. NEM values also lay 28% below DTT values. Values of  $K_{0.5,MT}$  were very variable and high, with the biggest value for rescue conditions.

Again, only one preparation of each single mutant was examined.

The catalytic activity of single mutant NcKin343\_T273C is comparable to the monomeric double mutant. Under rescue, NEM and DTNB conditions ATPase activity decreased by 22%, 27% and 63%, respectively. The decline of activity within the duration of the assay complicated the measurement for DTNB.

$K_{cat}$  values of the other single mutant NcKin343\_S329C were relatively constant.

These results are difficult to interpret but they suggest that although presumably no crosslink is formed between helices  $\alpha 4$  and  $\alpha 6$ , nevertheless their relative movement is limited to a degree which prevents normal chemomechanic cycling of NcKin.

## 3.4.5 Summary of All Constructs

construct	cond.	bands in SDS-gel [kD]	$k_{cat}$ [1/s]	$K_{0.5,MT}$ [ $\mu$ M]	$k_{bi,ATPase}$ [ $s^{-1}\mu$ M $^{-1}$ ]	gliding velocity [ $\mu$ m/s]	n
NcKin433_ wt	NEM		128	0.27	474	2.76 $\pm$ 0.16	1; 2
	DTT	60	74 $\pm$ 12	0.32 $\pm$ 0.27	231	2.63 $\pm$ 0.12	2
	DTNB	60	72 $\pm$ 9	0.35 $\pm$ 0.28	206	2.43 $\pm$ 0.23	2
	rescue	60	72 $\pm$ 15	0.34 $\pm$ 0.26	212	2.68 $\pm$ 0.27	2
	all		73 $\pm$ 10	0.33 $\pm$ 0.19	221	2.62 $\pm$ 0.24	
NcKin343_ wt	NEM		272	5.39	50		1
	DTT	40	303 $\pm$ 19	5.39 $\pm$ 1.76	56		2
	DTNB		261 $\pm$ 19	4.83 $\pm$ 0.93	54		2
	rescue		242 $\pm$ 10	4.83 $\pm$ 2.39	50		2
	all		269 $\pm$ 28	5.07 $\pm$ 1.30	53		
NcKin433_ S341C	NEM		82	0.33	248	2.36 $\pm$ 0.14	1
	DTT	60	68	0.17	400	2.13 $\pm$ 0.16	1
	DTNB	60, 200	61	0.27	226	1.69 $\pm$ 0.09	1
	rescue	60	56	0.18	311	1.77 $\pm$ 0.14	1
NcKin433_ P342C	NEM		63	0.32	197	2.53 $\pm$ 0.21	1; 2
	DTT	60	64 $\pm$ 5	0.30 $\pm$ 0.21	213	2.53 $\pm$ 0.16	2
	DTNB	200	66 $\pm$ 1	0.36 $\pm$ 0.25	183	2.12 $\pm$ 0.13	2
	rescue	60	63 $\pm$ 5	0.44 $\pm$ 0.21	143	2.49 $\pm$ 0.13	2
NcKin433_ S3C_A334C	NEM		94	0.17	553	1.66 $\pm$ 0.29	1; 2
	DTT	60	90 $\pm$ 30	0.21 $\pm$ 0.10	429	2.31 $\pm$ 0.23	2
	DTNB	60, 67, 70	97 $\pm$ 15	0.13 $\pm$ 0.10	746	0.07 $\pm$ 0.02	2
	rescue	60	86 $\pm$ 16	0.38 $\pm$ 0.26	226	2.20 $\pm$ 0.17	2
NcKin433_ S3C	NEM		70 <sup>1</sup>	0.22	318	2.74 $\pm$ 0.11 <sup>2</sup>	1
	DTT	60	99 <sup>1</sup>	0.22	450	2.74 $\pm$ 0.15	1
	DTNB	60, 120	67 <sup>1</sup>	0.32	209	2.10 $\pm$ 0.17 <sup>2</sup>	1
	rescue		81 <sup>1</sup>	0.24	338	2.62 $\pm$ 0.11	1
NcKin433_ A334C	NEM		92	0.52	177	2.17 $\pm$ 0.07 <sup>3</sup>	1
	DTT	60	96	0.70	137	2.74 $\pm$ 0.11	1
	DTNB	60	99	0.52	190	2.01 $\pm$ 0.17 <sup>3</sup>	1
	rescue		98	0.70	140	2.54 $\pm$ 0.09	1

NcKin343_ S3C_A334C	<b>NEM</b>		234	1.10	213		1
	<b>DTT</b>	40	283	2.10	135		1
	<b>DTNB</b>		231	1.72	134		1
	<b>rescue</b>		246	1.79	137		1
NcKin433_ A226C_E339C	<b>NEM</b>		26	0.35	74	2.42 ± 0.26	1; 2
	<b>DTT</b>	60	31 ± 7	0.28 ± 0.25	111	2.30 ± 0.26	2
	<b>DTNB</b>	<u>58</u> , 60	4.4 ± 1.2	0.99 ± 0.31	4	0.38 ± 0.14	2
	<b>rescue</b>	60	34 ± 6	0.20 ± 0.13	170	2.41 ± 0.21	2
NcKin433_ A226C	<b>NEM</b>		66	0.46	143	2.92 ± 0.11	1
	<b>DTT</b>	60	65	0.54	120	2.95 ± 0.15	1
	<b>DTNB</b>	60	61	1.03	59	2.52 ± 0.15	1
	<b>rescue</b>		64	0.54	119	2.90 ± 0.11	1
NcKin433_ E339C	<b>NEM</b>		70	0.40	175	2.35 ± 0.11	1
	<b>DTT</b>	60	95	0.37	257	2.48 ± 0.13	1
	<b>DTNB</b>	60, <u>200</u>	71	0.39	182	2.30 ± 0.11	1
	<b>rescue</b>		68	0.45	151	2.68 ± 0.26	1
NcKin343_ A226C_E339C	<b>NEM</b>		195	7.18	27		1
	<b>DTT</b>	40	205 ± 19	4.38 ± 0.88	47		2
	<b>DTNB</b>		6.8 ± 2.0	5.80 ± 2.92	1		2
	<b>rescue</b>		121 ± 52	7.73 ± 2.33	16		2
NcKin343_ A226C	<b>NEM</b>		263	2.79	94		1
	<b>DTT</b>	40	221	2.18	101		1
	<b>DTNB</b>		243	7.53	32		1
	<b>rescue</b>		199	2.58	77		1
NcKin343_ E339C	<b>NEM</b>		226	5.35	42		1
	<b>DTT</b>	40	258	4.26	61		1
	<b>DTNB</b>		144	22.99	6		1
	<b>rescue</b>		246	4.63	53		1
HsKin560_ K222C_E334C	<b>buffer</b>		30 ± 1	0.08 ± 0.02	390		1
	<b>DTT</b>	90	28 ± 3	0.08 ± 0.01	373		1
	<b>DTNB</b>		5.0 ± 0.3	0.25 ± 0.19	20		1
	<b>rescue</b>		7.3 ± 0.4	0.12 ± 0.06	61		1
HsKin339_ K222C_E334C	<b>buffer</b>		66 ± 2	0.40 ± 0.07	165		1
	<b>DTT</b>	40	56 ± 10	0.23 ± 0.21	243		1
	<b>DTNB</b>		3.6 ± 0.3	1.16 ± 0.11	3		1

	<b>rescue</b>		18 ± 4	0.37 ± 0.02	49		1
NcKin433_ T273C_S329C	<b>NEM</b>		72 ± 8	0.22 ± 0.13	327	2.29 ± 0.22	2
	<b>DTT</b>	60	75 ± 20	0.28 ± 0.19	268	2.19 ± 0.25	2
	<b>DTNB</b>	59	33 ± 5	0.48 ± 0.25	69	0.41 ± 0.06	2
	<b>rescue</b>	60	34 ± 7	0.47 ± 0.34	72	0.46 ± 0.06	2
NcKin433_ T273C	<b>NEM</b>		75	0.40	188	2.44 ± 0.12	1
	<b>DTT</b>	60	53	0.42	126	2.48 ± 0.19	1
	<b>DTNB</b>	59	42	0.97	43	1.00 ± 0.17 <sup>4</sup>	1
	<b>rescue</b>	60	46	0.40	115	2.58 ± 0.11	1
NcKin433_ S329C	<b>NEM</b>		68	0.32	213	2.47 ± 0.09	1
	<b>DTT</b>	60	50	0.23	217	2.56 ± 0.11	1
	<b>DTNB</b>	59	53	0.29	183	2.38 ± 0.08	1
	<b>rescue</b>	60	54	0.37	146	2.60 ± 0.17	1
NcKin343_ T273C_S329C	<b>NEM</b>		160	6.79	24		1
	<b>DTT</b>	40	222 ± 45	4.00 ± 4.86	56		2
	<b>DTNB</b>		95 ± 0.4	9.39 ± 9.14	10		2
	<b>rescue</b>		144 ± 18	14.74 ± 5.69	10		2
NcKin343_ T273C	<b>NEM</b>		190 ± 11	2.19 ± 0.05	87		2
	<b>DTT</b>	40	261 ± 33	2.37 ± 0.72	110		2
	<b>DTNB</b>		95 ± 3 <sup>5</sup>	2.03 ± 0.71	47		2
	<b>rescue</b>		203	1.72	118		1
NcKin343_ S329C	<b>NEM</b>		267	3.01	89		1
	<b>DTT</b>	40	274	2.79	98		1
	<b>DTNB</b>		250	2.44	102		1
	<b>rescue</b>		240	2.12	113		1

**Table 3.1: Summary of all investigated kinesin constructs.**

For all measuring conditions the inter- or intramolecular crosslinking state (underlined band sizes indicate prevailing band), mean values and their standard deviations for  $k_{cat}$ ,  $K_{0.5,MT}$  and gliding velocity, and values for  $k_{bi,ATPase} = k_{cat} / K_{0.5,MT}$  are listed. n = number of independent protein preparations measured (If there are two numbers given, the first applies for ATPase and the second for motility measurements. HsKin preparations were measured twice.), for the wild-type constructs the mean over all conditions is shown (the mean  $k_{cat}$  of NcKin433\_wt is calculated without the NEM value), superscripts 1-5 indicate problems with measurements: <sup>1</sup> within single ATPase assays the activity of the protein decreased, <sup>2</sup> gliding velocities slowed down at individual sites with time (to 0.7-1.6  $\mu\text{m/s}$  for DTNB and to 1.8-2.3  $\mu\text{m/s}$  for NEM), at a different site of the same slide fast gliding was observed again (light effect), <sup>3</sup> gliding velocities slowed down with time (to 0.8  $\mu\text{m/s}$  for DTNB and to 1.1-1.8  $\mu\text{m/s}$  for NEM), <sup>4</sup> gliding velocity slowed down with time (from 1.3 to 0.75  $\mu\text{m/s}$ ), <sup>5</sup> within one measurement ATPase activity dramatically decreased

### 3.5 Competitive Motility Assays

From results of motility measurements described above several questions concerning the neck-linker/motor core crosslinking constructs arose. First, why does the A226C/E339C crosslink, docking the whole neck-linker onto the motor tip, still allow slow movement at a speed of 0.4  $\mu\text{m/s}$ . Second, why does the S3C/E334C crosslink, restraining the movement of only part of the neck-linker, cause an even more severe decrease of gliding velocity to 0.07  $\mu\text{m/s}$ . Third, how can intermediate velocities between 1.7-2.2  $\mu\text{m/s}$  occurring for some control measurements be explained?

As the gliding velocity was measured under multiple motor conditions (2.3.9.2) and the crosslinking efficiency was not 100% (3.3.3), the observed velocities resulted from the superposition of the activities of crosslinked and noncrosslinked protein. Residual movement of the two neck-linker/motor core crosslinked proteins therefore could be caused by a small proportion of molecules that had not been crosslinked. The extent of residual movement then would depend on whether crosslinked or noncrosslinked protein dominates the gliding behaviour. Decisive for dominance is the proportion of uncrosslinked protein under oxidised conditions and the microtubule affinity of the immobile crosslinked protein. If it binds to microtubules in rigor, it profoundly hinders movement of microtubules by uncrosslinked protein. But if it shows no high affinity to microtubules, uncrosslinked protein can move microtubules extensively unhindered.

This assumption was tested by performing motility assays on mixtures of wild-type and mutant crosslinked protein under oxidising conditions. Neck-linker/motor core crosslinked proteins were mixed in different ratios with wild-type protein, which is not affected by oxidising conditions (3.4.1.1), and the resulting velocities were measured (2.3.9.2).

#### 3.5.1 Competition of NcKin433\_wt and NcKin433\_S3C\_A334C

Gliding velocities of mixtures of wild-type and S3C\_A334C crosslinked mutant with ratios of 100:1, 10:1, 1:1, 1:10 were measured. For mixtures containing 100x and 10x the amount of wild-type relatively to mutant (1-10% mutant protein) velocities were comparable to pure wild-type velocity (2.73  $\mu\text{m/s} \pm 0.13$  and 2.26  $\mu\text{m/s} \pm 0.52$  versus 2.43  $\mu\text{m/s} \pm 0.23$ ) (Figure 3.15). At a ratio of 1:1 (50% mutant protein) velocity of the mixture dropped to 0.96  $\mu\text{m/s} \pm 0.39$  (40% wild-type velocity). Mixtures containing 10x the amount of mutant relatively to wild-type (90% mutant protein) only exhibited 11% residual gliding velocity (0.27  $\mu\text{m/s} \pm 0.14$ ), which is slightly faster than pure crosslinked mutant protein (0.07  $\mu\text{m/s} \pm 0.02$ ).

### 3.5.2 Competition of NcKin433\_wt and NcKin433\_A226C\_E339C

Gliding velocities of mixtures of wild-type and A226C\_E339C crosslinked mutant with ratios of 1:1, 1:10, 1:100 and 1:1000 were measured. At ratios of 1:1 and 1:10 (50-90% mutant protein) velocities of the mixtures corresponded to pure wild-type velocity ( $2.43 \mu\text{m/s} \pm 0.20$  and  $2.29 \mu\text{m/s} \pm 0.11$  versus  $2.43 \mu\text{m/s} \pm 0.23$ ) (Figure 3.15). The gliding velocity for the first time dropped to  $1.44 \mu\text{m/s} \pm 0.38$  (60% wild-type velocity) for the mixture containing 100x the amount of mutant relatively to wild-type (99% mutant protein). Finally 14% residual velocity ( $0.33 \mu\text{m/s} \pm 0.11$ ) was reached for a 1000fold surplus of mutant over wild-type (99.9% mutant protein), which resembles the velocity measured for pure crosslinked mutant protein ( $0.38 \mu\text{m/s} \pm 0.14$ ).

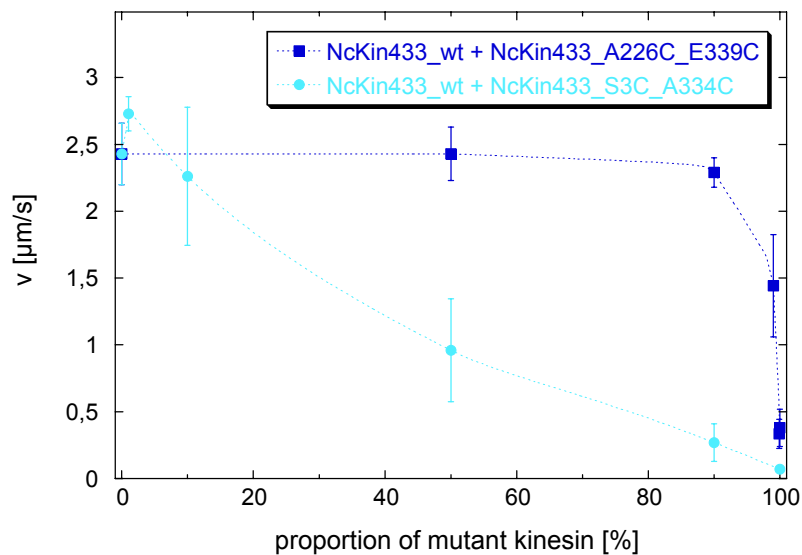


**Figure 3.15: Competitive motility assays.**

Mean gliding velocities and standard deviations of mixtures of wild-type and neck-linker/motor core crosslinked kinesin under oxidising conditions. NcKin433\_A226C\_E339C (fully immobilised neck-linker) starts to affect wild-type gliding if its in a ~100fold excess, while NcKin433\_S3C\_A334C (partly immobilised neck-linker) already influences wild-type gliding at the same concentration as wild-type.  $v$  = velocity

### 3.5.3 Summary of Competitive Motility Assays

Competitive motor gliding experiments demonstrated that the co-operation of crosslinked neck-linker/motor core mutant and uncrosslinked wild-type kinesin results in intermediate gliding velocities. Hence, residual gliding behaviour occurring in motility assays after oxidation of the pure neck-linker/motor core constructs may be due to incomplete oxidation that leads to a mixture of crosslinked and uncrosslinked protein causing intermediate velocities. As the vast majority of protein is crosslinked (3.3.3) and the uncrosslinked protein

behaves like wild-type (compare gliding velocities of neck-linker/motor core constructs under DTT conditions, 3.4.3.1.1 and 3.4.3.2.1), the situation is comparable to the above mixture experiments where only little wild-type is present.

The two mutants differ quantitatively in their ability to influence wild-type gliding behaviour under oxidising conditions. NcKin433\_S3C\_A334C affects gliding velocity, even if it is present at the same amount as wild-type, and only slight movement is left, when 10% wild-type is still present. To create such a dominant effect on wild-type gliding behaviour the proportion of NcKin433\_A226C\_E339C needs to be much higher. For this mutant only 10% wild-type protein is sufficient to generate wild-type velocity and even 1% wild-type protein reaches 60% wild-type velocity. Only at a 1000fold surplus of mutant motility almost completely ceases.

This allows conclusions on the microtubule affinity and crosslinking efficiency of these two mutants under oxidising conditions. The gliding velocities of the mixtures of wild-type and NcKin433\_S3C\_A334C indicate that the resulting velocity is influenced to the same extent by both proteins. From this it can be concluded that wild-type and crosslinked NcKin433\_S3C\_A334C have similar affinities for microtubules. Because in the presence of 90% mutant still a higher velocity has been measured than for pure mutant, the crosslinking efficiency of this mutant must be higher than 90%. Crosslinked NcKin433\_A226C\_E339C seems to exhibit only very weak microtubule affinity as it is not able to compete with wild-type protein unless it is in great excess. But this also means that the low gliding velocity of mutant protein under oxidising conditions requires a very high crosslinking efficiency of over 99%.

### 3.6 Sedimentation Assays

To confirm the low microtubule affinity of the crosslinked mutant NcKin\_A226C\_E339C (with completely immobilised neck-linker), co-sedimentation assays of tubulin and mutant kinesin were performed (2.3.12). This method allows to separate free and microtubule-bound kinesin based on the different sedimentation properties of polymerised tubulin and kinesin. The size of free kinesin is too low for sedimentation at 200000 g, while polymerised tubulin is pelleted. Therefore, kinesin is found in the pellet only when bound to microtubules. The amount of co-sedimenting kinesin depends on its affinity to microtubules. This affinity is influenced by the type of nucleotide bound to the head domain of kinesin. ATP and its nonhydrolysable analogue AMP-PNP cause strong binding to microtubules, ADP a weak

binding state [Crevel *et al.* 1996]. To evaluate the influence of a docked neck-linker on the microtubule affinity, sedimentation assays were carried out in the presence of ADP or AMP-PNP. Monomeric and dimeric NcKin\_A226C\_E339C were tested both under DTT and DTNB conditions. As the gliding velocity and microtubule-stimulated ATP turnover of the reduced mutants were indistinguishable from wild-type, it was expected that their affinity to microtubules did not differ from wild-type as well. On the contrary, from the competitive motility measurements (3.5.3) and the high  $K_{0.5,MT}$  values (Table 3.1) of the crosslinked mutants a dramatically reduced microtubule affinity was predicted. As a direct way of measuring the affinity of kinesin and microtubules, co-sedimentation assays were used to test the prediction.

Figure 3.16 shows typical gels of sedimentation assays for NcKin\_A226C\_E339C. With increasing microtubule concentration the fraction of kinesin found in the pellet rose. By plotting the fraction of microtubule-bound kinesin over microtubule concentration and fitting hyperbolas to the data points, the dissociation constants  $K_d$  of the microtubule-kinesin complex in the presence of AMP-PNP or ADP were determined (Figures 3.17 and 3.18).

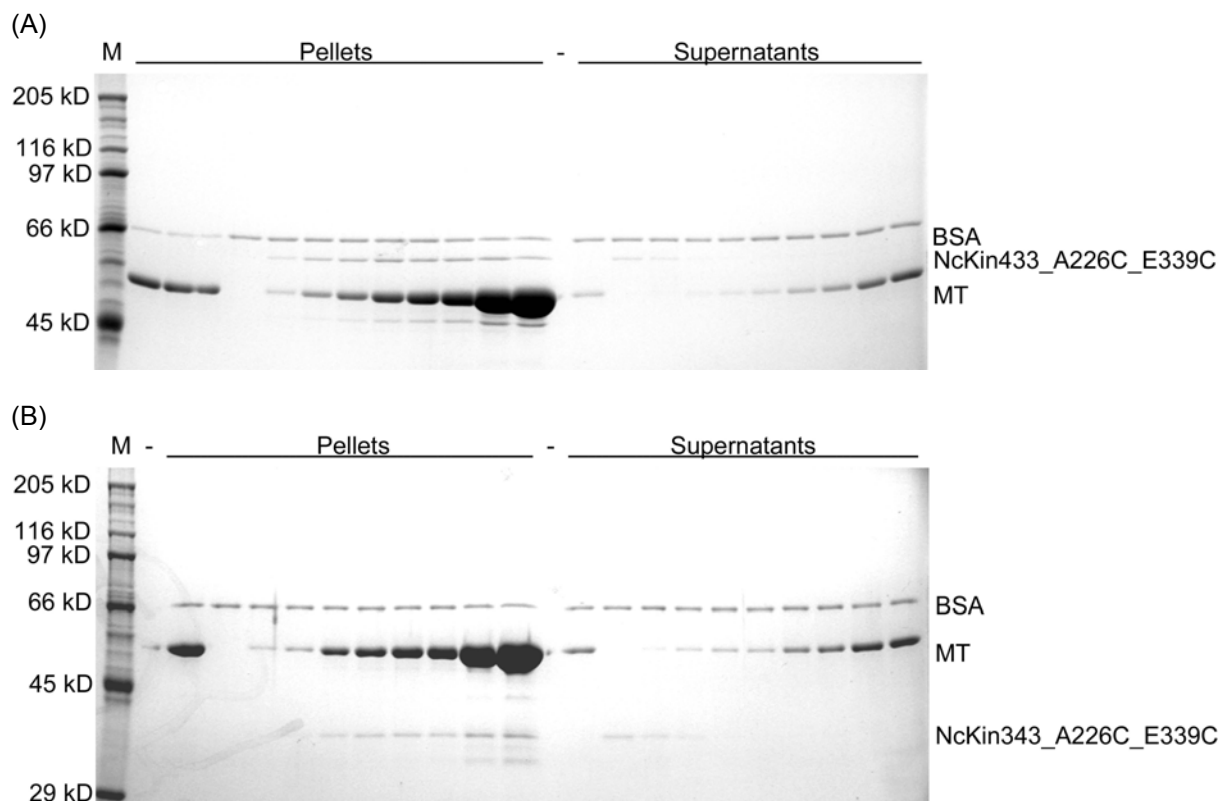


**Figure 3.16: Representative SDS-gels of sedimentation assays under reducing conditions with AMP-PNP. (A) NcKin433\_A226C\_E339C (B) NcKin343\_A226C\_E339C**

M = molecular mass standard, pellets and supernatants after ultracentrifugation: 1. lanes = control with 5  $\mu$ M microtubules without kinesin (in (A) the control has leaked to the first three lanes, all counted as one lane), 2. lanes = no microtubules, 3.-10. lanes = increasing amounts of microtubules, BSA bands were used for standardisation.

### 3.6.1 Microtubule Affinities of NcKin433\_A226C\_E339C

Microtubule concentrations of 0, 0.5, 1, 1.5, 2, 3, 4, 5, 7.5, 10  $\mu\text{M}$  and 0, 0.25, 0.5, 0.75, 1, 1.5, 2, 5, 10  $\mu\text{M}$  were used for sedimentation assays of 0.3  $\mu\text{M}$  NcKin433\_A226C\_E339C under reducing conditions in the presence of ADP and AMP-PNP, respectively. Under oxidising conditions much higher microtubule concentrations of 0, 0.5, 1, 2, 3.5, 5, 7.5, 10, 15, 20, 30  $\mu\text{M}$  were necessary for ADP and 0, 0.25, 0.5, 0.75, 1, 1.5, 2, 3.5, 5, 7.5, 10  $\mu\text{M}$  for AMP-PNP.

Under reducing conditions the dissociation constant was 0.18  $\mu\text{M}$  in the presence of AMP-PNP and 0.58  $\mu\text{M}$  for ADP (Table 3.2). Previous measurements on a NcKin460 construct came to a  $K_d$  of 0.09  $\mu\text{M}$  for AMP-PNP and 0.3  $\mu\text{M}$  for ADP [Crevel *et al.* 1999], which implies a 2fold higher microtubule affinity in the strong as well as the weak binding state.  $K_d$  values for the crosslinked NcKin433\_A226C\_E339C were approximately twice as high as for the uncrosslinked protein, namely 0.44  $\mu\text{M}$  and 1.1  $\mu\text{M}$  for AMP-PNP and ADP, respectively. This means that crosslinking of NcKin433\_A226C\_E339C reduces its affinity to microtubules by a factor of two (Figure 3.17 B). In fact, both the strong binding state (in the presence of AMP-PNP) and the weak binding state (with ADP bound) of the kinesin-microtubule complex are weakened equally by the formation of the crosslink.

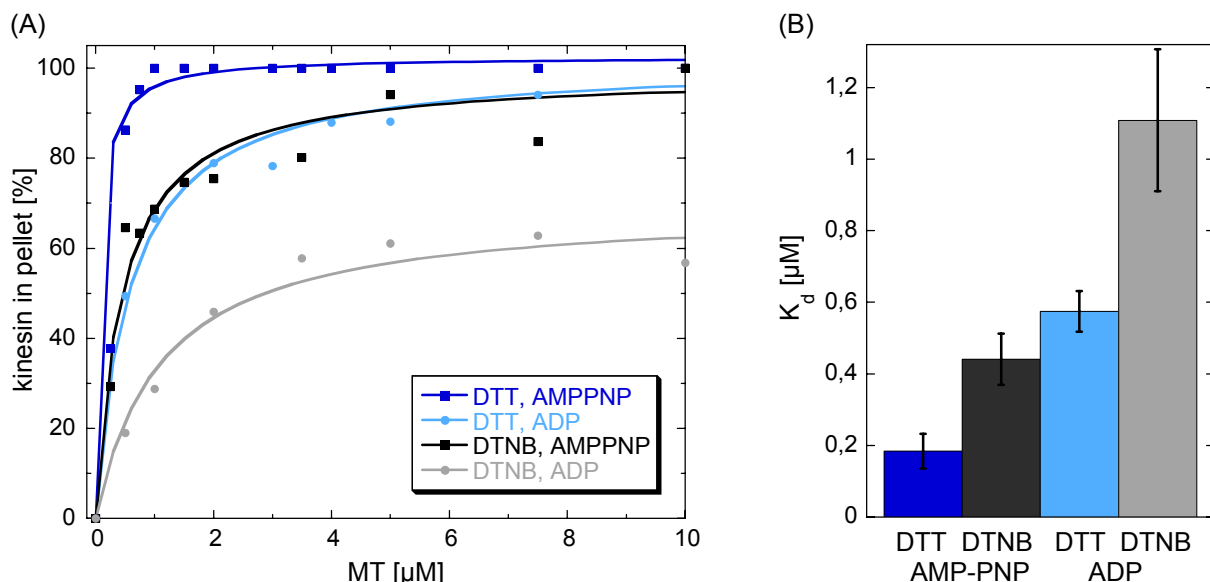


**Figure 3.17: Analysis of co-sedimentation gels of NcKin433\_A226C\_E339C. (A) Fraction of microtubule bound kinesin in dependence of microtubule concentration (B) calculated dissociation constants**

The curve fits to the following hyperbolic equation  $y = K1 * [MT] / (K_d + [MT])$  give the dissociation constants  $K_d$ . Under DTNB, ADP conditions even at 30  $\mu\text{M}$  microtubules some fraction of kinesin still is not pelleted.

### 3.6.2 Microtubule Affinities of NcKin343\_A226C\_E339C

For sedimentation assays of NcKin343\_A226C\_E339C under reducing conditions microtubule concentrations of 0, 1, 2, 3, 4, 5, 7.5, 10, 20  $\mu\text{M}$  and 0, 0.25, 0.5, 0.75, 1, 1.5, 2, 5, 10  $\mu\text{M}$  were used in the presence of ADP and AMP-PNP, respectively. Even higher microtubule concentrations of 0, 5, 10, 15, 20, 30, 50, 70  $\mu\text{M}$  were necessary for ADP and 0, 1, 2, 3.5, 5, 7.5, 10, 20, 50  $\mu\text{M}$  for AMP-PNP under oxidising conditions.

$K_d$  values for the monomer under reducing conditions were 0.5  $\mu\text{M}$  and 1.7  $\mu\text{M}$  in the presence of AMP-PNP and ADP, respectively (Table 3.2). Previously reported  $K_d$  values of a NcKin360 construct correspond quite well with 0.1  $\mu\text{M}$  for AMP-PNP and 1.82  $\mu\text{M}$  for ADP [Crevel *et al.* 1999]. These values mean that under reducing conditions the monomeric NcKin\_A226C\_E339C showed a 2-3fold lower microtubule affinity than the dimeric construct. Similar results for noncrosslinked proteins have been obtained by [Ma & Taylor 1997a] for human monomeric and dimeric kinesin constructs. They report a fivefold reduction of  $K_d$  of the monomer in the presence of ATP and ADP. Under oxidising conditions the  $K_d$  of NcKin343\_A226C\_E339C increased to 1.9  $\mu\text{M}$  for AMP-PNP and 11  $\mu\text{M}$  for ADP. The strong binding state of the kinesin-microtubule complex is influenced less by the formation of the crosslink (3.5fold reduction of microtubule affinity) than the weak binding state (6fold reduction of microtubule affinity) (Figure 3.18 B). Furthermore, the effect of crosslinking on microtubule affinity is much more pronounced for the monomer than the dimer.

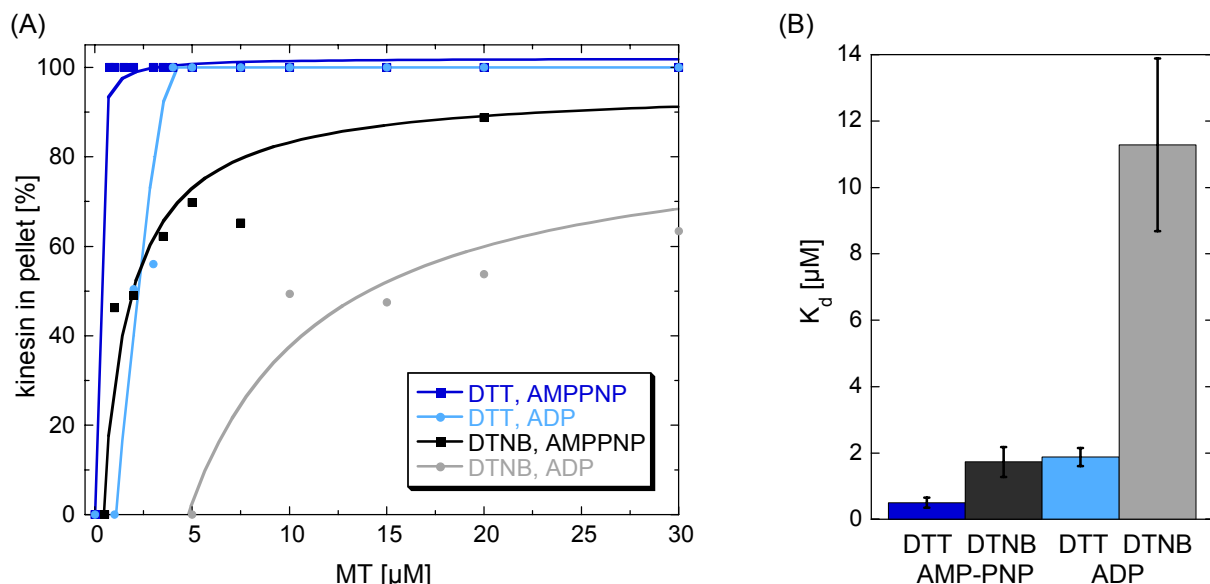


**Figure 3.18: Analysis of co-sedimentation gels of NcKin343\_A226C\_E339C. (A) Fraction of microtubule bound kinesin in dependence of microtubule concentration (B) calculated dissociation constants**

Curve fits to the hyperbolic equation  $y = K_1 * [MT] / (K_d + [MT])$  give the dissociation constants  $K_d$ . Under DTNB, ADP conditions even at 70  $\mu\text{M}$  microtubules some fraction of kinesin still is not pelleted.

conditions	NcKin433_A226C_E339C		NcKin343_A226C_E339C		NcKin460	NcKin360
	$K_d$ [ $\mu$ M]	diff.	$K_d$ [ $\mu$ M]	diff.	$K_d$ [ $\mu$ M]	$K_d$ [ $\mu$ M]
DTT, AMP-PNP	$0.18 \pm 0.05$	2.4 x	$0.50 \pm 0.15$	3.5 x	$0.09^*$	$0.10^*$
DTNB, AMP-PNP	$0.44 \pm 0.07$		$1.73 \pm 0.45$			
DTT, ADP	$0.58 \pm 0.06$	1.9 x	$1.88 \pm 0.27$	6.0 x	$0.30^*$	$1.82^*$
DTNB, ADP	$1.11 \pm 0.20$		$11.3 \pm 2.6$			

**Table 3.2: Influence of crosslinking on microtubule affinity.**

Dissociation constants  $K_d$  of NcKin\_A226C\_E339C constructs and their differences under reducing and oxidising conditions in the presence of AMP-PNP or ADP. \* data from [Crevel *et al.* 1999]

### 3.7 Basal ATPase Measurements

Kinesin's ATPase activity depends on microtubules. Nevertheless it hydrolyses ATP slowly in the absence of microtubules. This so-called basal ATPase activity gives information on whether the general catalytic mechanism works properly and to which degree the protein can be activated by microtubules. As the coupled ATPase assay is not sensitive enough to detect the low basal ATP turnover, the release of radioactive [ $\gamma$ - $^{32}$ P] over time was measured to determine the basal turnover rate  $k_0$  (2.3.10.1). The control measurements without kinesin exhibited no background by spontaneous ATP hydrolysis. Therefore, background hydrolysis was neglected.

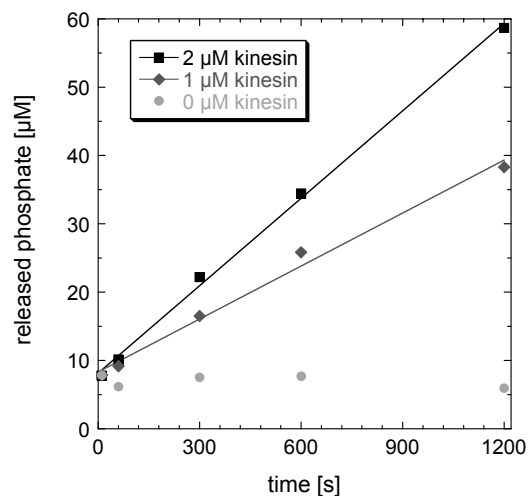


**Figure 3.19: Basal ATPase activity of NcKin433\_wt.**

Released [ $\gamma$ - $^{32}$ P] plotted against the reaction time. Measurements with no, 1  $\mu$ M and 2  $\mu$ M kinesin are depicted. Data points of measurements with kinesin were fitted to a line. The slope of the lines and the inserted amount of protein determines the specific basal ATPase activity of the construct.

### 3.7.1 NcKin\_wt

For the monomeric and dimeric wild-type constructs under DTT conditions basal ATP turnover rates between 0.016 and 0.038 s<sup>-1</sup> were measured, leading to a mean  $k_0$  of 0.027 s<sup>-1</sup> ± 0.009 (Figure 3.20 and Table 3.3). Its  $k_0$  was reduced by 25% under oxidising conditions. It ranged from 0.012 to 0.026 s<sup>-1</sup> with a mean value of 0.020 s<sup>-1</sup> ± 0.005. Because of the high standard deviations of 27-32% the difference between reducing and oxidising conditions is not significant. The variability of basal ATPase activity is quite high, but does not increase if wild-type monomer and dimer are averaged together, indicating that the catalytic mechanism of both constructs functions equally well. Previous studies also report similar basal ATPase rates for monomeric (0.014 s<sup>-1</sup>) and dimeric (0.022 s<sup>-1</sup>) NcKin constructs [Crevel *et al.* 1999] and monomeric (0.02 s<sup>-1</sup>) and dimeric (0.008 s<sup>-1</sup>) HsKin constructs [Ma & Taylor 1995b, 1997b]. ATP turnover is activated by microtubules by a factor of 13200-15000 for the monomer and by a factor of 2400-3100 for the dimer, regardless of the assay conditions. Comparable values have been reported for dimeric NcKin460 (3500) and HsKin379 (2500) constructs [Ma & Taylor 1995a; Crevel *et al.* 1999].

### 3.7.2 NcKin433\_S3C\_A334C

For NcKin433\_S3C\_A334C mean basal ATP turnover rates of 0.028 s<sup>-1</sup> ± 0.007 and 0.015 s<sup>-1</sup> ± 0.002 were measured under DTT and DTNB conditions, respectively (Figure 3.20 and Table 3.3). Accordingly,  $k_0$  was reduced by oxidation by 45%. Both measurements lie in the tolerance of the averaged wild-type values and the oxidation effect is only slightly higher than the variation within measurements under the same conditions. The ATPase activation factor for DTT (3200) corresponds to the one for wild-type dimer, while it doubled (6300) under oxidising conditions.

### 3.7.3 NcKin\_A226C\_E339C

The dimeric NcKin433\_A226C\_E339C construct exhibited extremely low basal ATPase activity values under reducing and oxidising conditions. The mean DTT value was only 0.006 s<sup>-1</sup> ± 0.0007 (Figure 3.20 and Table 3.3). This is roughly 4x less than expected from the values of the other constructs. The microtubule-activated ATPase activity of the nonoxidised construct was already less than half of the activity of other constructs (3.4.3.2.2). Possibly, reduction of the protein is not complete, leaving part of the protein in the inactive crosslinked state. Also, a considerable amount of protein may have been inactive for no apparent reason.

This leads to an overestimation of the active protein concentration and thereby to an underestimation of ATPase activity per kinesin head. However, this still does not explain why the basal ATPase activity was affected more severely than microtubule-stimulated ATPase activity. Oxidation further decreased the  $k_0$  to  $0.003 \text{ s}^{-1} \pm 0.0006$ . In contrast to the dimer the monomer showed a  $k_0$  of comparable size ( $0.017 \text{ s}^{-1} \pm 0.006$ ) to wild-type under DTT conditions (Figure 3.20 and Table 3.3). However, it matched the  $k_0$  of the dimer under DTNB conditions ( $0.003 \text{ s}^{-1} \pm 0.0009$ ). Oxidation of NcKin\_A226C\_E339C therefore led to an approximately 6-8 times reduced basal ATPase activity compared to wild-type under oxidising conditions ( $0.02 \text{ s}^{-1}$ , Table 3.3). Due to the unexpectedly low  $k_0$  for DTT measurements the activation factor of the dimer was relatively high (5500), while the factor of the monomer tallies with the average (11900). After crosslinking, activation factors for dimer and monomer were equally low (1700 and 2200, respectively). According to the activation factors that are normally much higher for monomers, the decrease of microtubule activation of ATPase by oxidation was more serious for the monomer (-84%) than for the dimer (-40%).

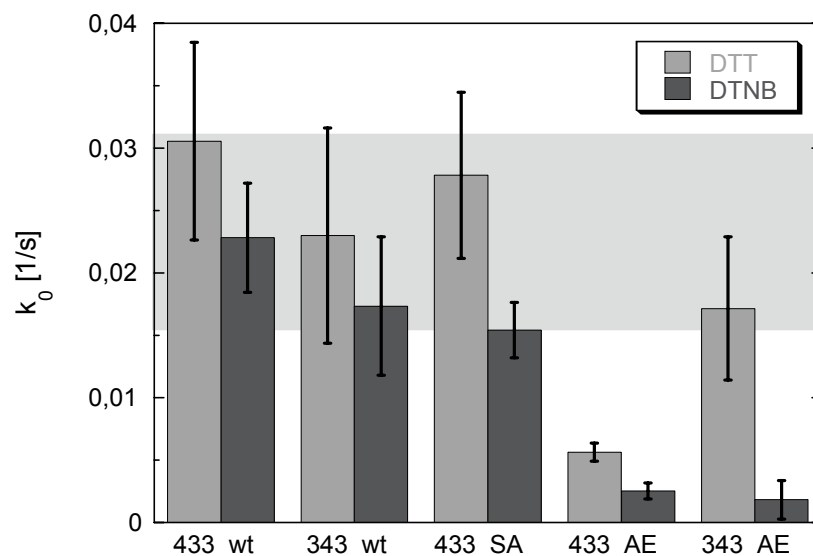


**Figure 3.20: ATPase activity in the absence of microtubules of NcKin433\_wt, NcKin343\_wt, NcKin433\_S3C\_A334C, NcKin433\_A226C\_E339C and NcKin343\_A226C\_E339C.**

Bar charts of mean values and their standard deviations of basal ATP turnover rates ( $k_0$ ) of some NcKin constructs. The grey background area indicates the standard deviation from the mean of all NcKin\_wt measurements.

construct	condition	$k_0$ [1/s]	$k_{cat}$ [1/s]	activation	n
NcKin433_wt	<b>DTT</b>	0.0306 ± 0.0079	74 ± 12	2400	2
	<b>DTNB</b>	0.0228 ± 0.0044	72 ± 9	3100	2
NcKin343_wt	<b>DTT</b>	0.0230 ± 0.0086	303 ± 19	13200	2
	<b>DTNB</b>	0.0174 ± 0.0055	261 ± 19	15000	2
both NcKin_wt	<b>DTT</b>	0.0268 ± 0.0087			
	<b>DTNB</b>	0.0201 ± 0.0055			
	<b>both</b>	0.0234 ± 0.0078			
NcKin433_ S3C_A334C	<b>DTT</b>	0.0278 ± 0.0067	90 ± 30	3200	2
	<b>DTNB</b>	0.0154 ± 0.0022	97 ± 15	6300	2
NcKin433_ A226C_E339C	<b>DTT</b>	0.0056 ± 0.0007	31 ± 7	5500	2
	<b>DTNB</b>	0.0025 ± 0.0006	4.4 ± 1.2	1700	2
NcKin343_ A226C_E339C	<b>DTT</b>	0.0172 ± 0.0057	205 ± 19	11900	2
	<b>DTNB</b>	0.0031 ± 0.0009	6.8 ± 2.0	2200	2

**Table 3.3: Comparison of basal and microtubule-activated ATP turnover rates and the resulting activation factors.**

Mean values and their standard deviations for basal ATPase turnover rates ( $k_0$ ) and microtubule-stimulated ATPase turnover rates ( $k_{cat}$ ), and resulting activation of turnover rates by microtubules. n = number of independent protein preparations measured. Dimeric and monomeric wild-type constructs have been averaged within each measuring condition and over both measuring conditions.

### 3.8 ADP Release Experiments

In the absence of microtubules kinesin exhibits only a slight basal ATPase activity (3.7). The rate-limiting step is the release of ADP after hydrolysis [Hackney 1988; Hackney *et al.* 1989; Hackney 1994b; Huang & Hackney 1994]. The ADP release is greatly enhanced by kinesin binding to microtubules [Hackney 1994a; Ma & Taylor 1995a]. Therefore, binding of kinesin to the microtubule can be observed by the immediately following ADP dissociation. For determination of the ADP release rates kinesin loaded with mantADP was used (2.3.11.1). MantADP fluoresces much stronger when bound to protein than free in solution. So, the dissociation of mantADP from kinesin heads can be followed by measuring the decrease of fluorescence in a fluorometer (2.3.11.3). Under substoichiometric microtubule concentration the ADP release rate shows a linear dependence on the microtubule concentration because

under these conditions the final rate is limited by microtubule binding instead of other rates in the ATP turnover cycle. The slope of this line determines the bimolecular binding rate  $k_{bi,ADP}$  of enzyme to substrate. For non-processive enzymes ATPase measurements give information about the bimolecular binding rate  $k_{bi}$ , which can be calculated as  $k_{cat} / K_m$ . But kinesin is a processive motor, meaning that it does not dissociate after each hydrolysis cycle from the microtubule. Therefore, its  $K_{0.5,MT}$  is much smaller than expected by kinesin's affinity to microtubules (3.4). This in turn results in a much higher ratio  $k_{bi,ATPase} = k_{cat} / K_{0.5,MT}$  than expected [Hackney 1995]. The ratio of apparent and measured bimolecular binding rates ( $k_{bi,ratio} = k_{bi,ATPase} / k_{bi,ADP}$ ) is called 'chemical processivity' and indicates the number of ATPase cycles performed by a kinesin molecule before detaching from the microtubule [Hackney 1995].

### 3.8.1 NcKin433\_A226C\_E339C

DTNB quenches the emission of mantADP fluorescence, therefore, after oxidation of the kinesin the DTNB had to be removed prior to the measurements in the fluorometer. This was achieved by DTNB or DTT treatment of the kinesin before the removal of unbound mantADP by the centrifuge column method (2.3.11.1), so that the oxidising and reducing reagents together with the unbound mantADP were retained in the sephadex resin. As crosslinking of NcKin433\_A226C\_E339C already affects the basal ATPase rate (3.7.3) and therefore also the loading with mantADP, the construct was incubated with mantATP first and crosslinked with DTNB thereafter. DTT incubation was carried out before loading with mantATP. Protein concentration after loading was approximately 20  $\mu$ M with a kinesin:mantADP stoichiometry of 1:1 for DTT and 1:2 for DTNB conditions. Some DTNB molecules still present probably lead to this increased absorption at 356 nm, which causes an overestimation of mantADP concentration. The decrease of mantADP fluorescence of 100 nM kinesin·mantADP complexes was measured over a period of 7 min for different substoichiometric microtubule concentrations (0-20 nM) under reducing and oxidising conditions (Figure 3.21 A). All resulting time traces of the oxidised protein and time traces with up to 2.5 nM of the reduced protein could be fitted by single exponential functions ( $y = B + A_1 \cdot \exp(-k_1 \cdot t)$ ). Whereas only double exponential functions ( $y = B + A_1 \cdot \exp(-k_1 \cdot t) + A_2 \cdot \exp(-k_2 \cdot t)$ ) produced proper fits to the curves with 5 nM or more of the reduced protein. This indicates that there are two mechanisms contributing to the fluorescence decay. One with a constant low rate ( $k_2$ ) and the other with a fast rate ( $k_1$ ) which is dependent on microtubule concentration (Figure 3.21 B).

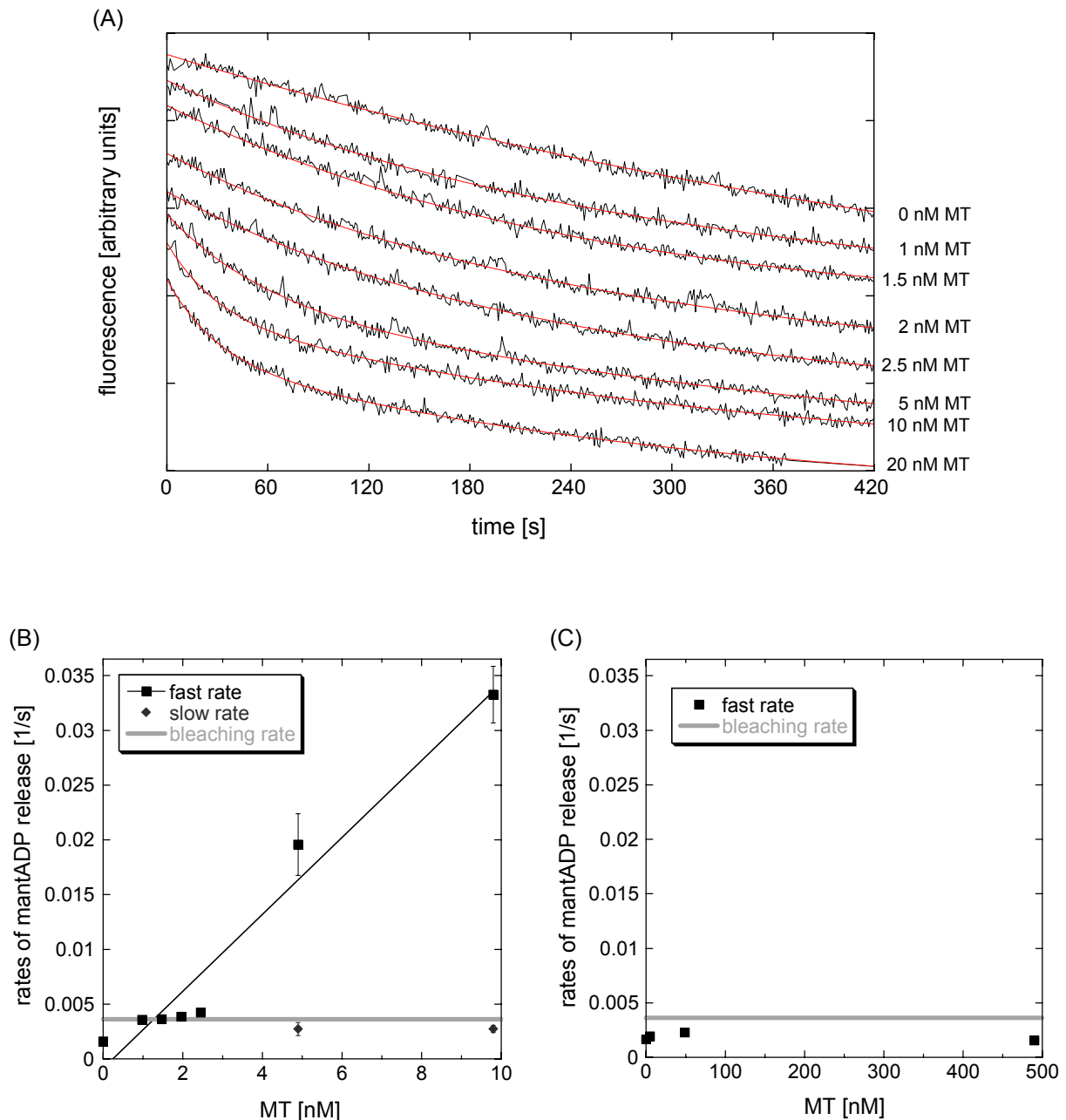


**Figure 3.21: MantADP release measurements for NcKin433\_A226C\_E339C under reducing and oxidising conditions.**

(A) Time traces of the decreasing fluorescence signal of 100 nM kinesin·mantADP measured for different substoichiometric microtubule concentrations (0, 1, 1.5, 2, 2.5, 5, 10, 20 nM) in the presence of 1mM ATP under reducing conditions. Single exponentials ( $y = B + A_1 \cdot \exp(-k_1 \cdot t)$ ) or double exponentials ( $y = B + A_1 \cdot \exp(-k_1 \cdot t) + A_2 \cdot \exp(-k_2 \cdot t)$ ) were fitted to the data traces.  $B$  = background,  $A_1, A_2$  = amplitude of the fast and slow phase,  $k_1, k_2$  = rate of the fast and slow phase (B) ADP release rates ( $k_1, k_2$ ) of the reduced protein plotted against the microtubule concentration. The fast rates ( $k_1$ ) show a linear dependence on the microtubule concentration, while the slow phase ( $k_2$ ) is constant. The slope of the line fitted to the fast rates gives the bimolecular binding constant  $k_{bi,ADP}$ . The slow rates are interpreted as bleaching of the mantADP. The rate constant of mantATP bleaching is indicated by the gray line. Error bars indicate the standard deviation of the curve fit. If they are not visible, they were too small. (C) as (B) but with oxidised protein. The fast rate ( $k_1$ ) is in the order of bleaching. Accordingly, no microtubule stimulation of ADP release could be detected and the bimolecular binding constant  $k_{bi,ADP}$  could not be determined.

The fast rates correspond to the microtubule binding which is synonymous with ADP release and the linear fit to these rates gives the measured bimolecular binding rate  $k_{bi,ADP}$ . However, the slow rates are difficult to understand. Mostly, only one rate is measured in such ADP release experiments [Ma & Taylor 1995a, 1997b; Kallipolitou *et al.* 2001; Schäfer *et al.* 2003] but others experienced the same problem with inaccurate fits to the fluorescence decay curves by single exponential functions [Hackney 2002; Hackney *et al.* 2003]. In one case, the fit was achieved by a single exponential plus a linear term [Hackney 2002], while in the other case double exponentials were fitted to the curves [Hackney *et al.* 2003]. Unfortunately, in both cases the authors did not interpret the linear and the slow exponential rates, respectively. Possibly, the slow rate represents the bleaching of mantADP fluorescence. As the observation time extends over seven minutes, the effect of bleaching must not be ignored. As a standard for bleaching, the decrease of fluorescence of 100 nM free mantATP was measured under the same settings without kinesin, microtubules and ATP. This reference curve for the bleaching property of mantATP was fitted by a single exponential function with a rate constant of  $0.0036 \text{ s}^{-1}$ , which is similar to the slow rates of the mantADP release experiments. This strongly supports the interpretation of the slow phase as a bleaching process.

For the experiments under reducing conditions a  $k_{bi,ADP}$  of  $3.5 \mu\text{M}^{-1}\text{s}^{-1}$  was determined (Figure 3.21 B). This value is in good agreement with previous measurements of bimolecular binding rates of dimeric conventional kinesins. For NcKin433  $4.2 \mu\text{M}^{-1}\text{s}^{-1}$  has been measured [Kallipolitou *et al.* 2001], for the *Drosophila* construct DKH405  $2 \mu\text{M}^{-1}\text{s}^{-1}$  [Hackney 2002], and for the human K379 construct  $2.1 \mu\text{M}^{-1}\text{s}^{-1}$  [Ma & Taylor 1995a]. The chemical processivity ( $k_{bi,ratio}$ ) of an enzyme is defined by dividing its apparent bimolecular binding rate ( $k_{bi,ATPase}$ ) by its measured bimolecular binding rate ( $k_{bi,ADP}$ ):

$$k_{bi,ratio} = k_{bi,ATPase} / k_{bi,ADP} = 111 \mu\text{M}^{-1}\text{s}^{-1} / 3.5 \mu\text{M}^{-1}\text{s}^{-1} = 32$$

The chemical processivity of non-crosslinked NcKin433\_A226C\_E339C therefore means that approximately 64 ATPase cycles are performed by one dimeric molecule (32 ATP hydrolysed per head) before it detaches from the microtubule. For DKH392 a  $k_{bi,ratio}$  of 60 has been reported [Hackney 1995], while for NcKin433 previous measurements resulted in the very high value of 726 [Kallipolitou *et al.* 2001]. The huge difference is mainly due to extremely low  $K_{0.5,MT}$  values measured by Kallipolitou. Accordingly, the chemical processivity is a rough indicator rather than an exact value of the number of ATP hydrolysed per microtubule encounter.

For the oxidised protein the bimolecular binding rate  $k_{bi,ADP}$  could not be determined. The ‘fast’ rates of the mantADP release were very low (Figure 3.21 C). They all were in the range

---

of the slow rates of the mantADP release of the reduced protein. Besides, the rates did not show a clear microtubule dependence. Accordingly, the observed rates correspond to bleaching and spontaneous ADP release. To exclude that the mantADP release reaction was too fast to measure manually, the amplitude of the reaction was analysed. The voltage output at the beginning of the measurements was always equivalent. Also, stopped-flow experiments in the ms-range failed to detect a fast reaction [J. Mergler, personal communication], indicating that the oxidised protein lacks a microtubule stimulation of the ADP release. This is a strong indication that the reduced ATPase turnover of NcKin433\_A226C\_E339C is due to a blocked pathway of stimulation of ADP release by microtubules.

---

## 4 Discussion

The central goal of this crosslinking study was to gain insight into the necessary degree of flexibility of certain parts of the kinesin molecule for its proper motor function. Two types of crosslinking mutants (neck/neck crosslinking constructs and neck-linker/motor core crosslinking constructs) were engineered to test two theories, which seek to explain how the two head domains of dimeric kinesin span the 8 nm distance between adjacent microtubule binding sites. The third type of crosslinking mutants ( $\alpha 4/\alpha 6$  crosslinking constructs) attempts to shed light onto the transmission of conformational changes from the nucleotide binding pocket to the neck-linker.

### 4.1 Evidence for Crosslinking

One of the main difficulties was the detection of crosslinks. The crosslinking state was deduced from the behaviour of constructs under reducing, oxidising or rescue conditions on nonreducing SDS-gels. Clues for crosslinking of the desired domains of the kinesin molecule will be discussed separately together with the observed effects for each class of construct in (4.3, 4.4, 4.5). As disulfide crossbridging could be deduced only from shifts of protein bands but could not be localised precisely, many control experiments were necessary. Thus single mutants of all constructs were examined to test whether the observed effects could indeed be assigned to the introduced cysteine residues. By and large, the single mutants showed that only both introduced cysteine residues together affected the characteristics of the oxidised construct. This confirmed that indeed crossbridges between the introduced cysteine residues were responsible for changes in protein properties.

Direct evidence for the formation of disulfide bridges between two introduced cysteine residues by for example mass spectrometry (see 4.6) would have been most convincing. In cooperation with Dr. Jörg Regula (Adolf Butenandt Institut, Zentrallabor für Proteinanalytik, LMU München) and Jörg Reinders and Dr. Albert Sickmann (Rudolf-Virchow-Zentrum, Universität Würzburg) this was attempted. Due to technical reasons, it was not possible to localise the disulfide bridges until now.

---

## 4.2 Validity of Wild-type Constructs

The constructs used here as ‘wild-type’ references differ from native *N. crassa* conventional kinesin in the following way. First, they are C-terminally truncated after amino acid 433 or 343, in order to increase expression and stability of the constructs and to prevent tail inhibition. Second, part of the human tail region (stopping far before the regulating region) is attached to the dimer to allow for motility assays since the construct without the hktail does not attach to the coverslip. Third, cysteine 307 was exchanged against alanine to minimise possible interactions of introduced cysteine residues with intrinsic cysteine residues. Cysteine residues 38 and 59 had to remain as the cysteine light construct was not expressed in *E. coli*. The presence of two intrinsic cysteine residues made several control experiments necessary.

The results of the different measurements show that in spite of these changes the wild-type control constructs NcKin433\_wt and NcKin343\_wt do not differ from wild-type full-length NcKin and wild-type NcKin truncated at amino acid 433 and 343, respectively and therefore serve as reliable references. Gliding velocity (3.4.1.1), microtubule-stimulated (3.4.1.2) and basal ATPase activities (3.7.1) of NcKin433\_wt and NcKin343\_wt were all in agreement with various previously reported values for full-length and truncated wild-type kinesins.

Both wild-type constructs are not affected by the different measuring conditions (reducing, oxidising, NEM and rescue conditions). The lack of band shifts on nonreducing gels for NcKin\_wt (3.3.1) indicate that upon oxidation no conformational change occurs. In addition incubation with DTT, DTNB or NEM had no influence at all on gliding velocity and microtubule-stimulated ATPase activity (3.4.1). In case of basal ATP turnover measured values under DTNB conditions are 25% below DTT values (3.7.1). As the turnover values generally fluctuate a lot, this difference is not significant.

## 4.3 Neck/Neck Crosslinking Constructs

### 4.3.1 Crosslinking Efficiency

Evidence for crosslinking of the neck/neck constructs should be clearly visible as the crosslink results in a doubling of the molecular mass by covalently connecting the two subunits of the kinesin molecule. As predicted by the positioning of the exchanged amino acids in the heptad repeat NcKin433\_P342C was more efficiently crosslinked than NcKin433\_S341C (3.3.2). Proline residue 342 occupies an ‘a’ position and the entire protein band of NcKin433\_P342C shifted upon oxidation while only a tiny fraction of oxidised

NcKin433\_S341C appeared in the higher band. The position of the shifted protein band was surprising since instead of the expected band near 120 kD the crosslinked product appeared at ~200 kD. The disulfide bridge probably connects the two subunits in a way that severely decreased their electrophoretic mobility. The formation of oligomers of more than two subunits is unlikely, especially as similar constructs just missing the hktail clearly run at the height corresponding to the molecular mass of two subunits when oxidised. The attached hktail did not contain any cysteine residues. Therefore, the constructs with and without hktail possess the same crosslinking options. Thus, most probably the oxidised NcKin433\_P342C mutant is crosslinked completely and unwinding of its neck coiled-coil is prevented.

#### 4.3.2 Characterisation of Motile and Hydrolysis Properties

As NcKin433\_S341C was hardly crosslinked at all, its measurements were of no significance for this investigation and are considered no further.

Motility assays revealed a slight impairment of gliding velocity for the crosslinked NcKin433\_P342C motor (3.4.2.1). Due to the rather high standard deviation this 16% reduction of average gliding velocity was not significant. Microtubule-stimulated ATP turnover rates were unaffected by oxidation, too (3.4.2.2). However, the multiple motor assays give little information about a possible influence of the crosslink on processivity. The crosslinked motor may be impaired in its processive movement while still leading to fast gliding velocities under multiple motor conditions. At any rate the results of motility and ATPase assays suggest that the fundamental force-generating process and the hydrolysis mechanism are not disturbed by preventing the unwinding of the neck coiled-coil.

#### 4.3.3 Comparison with other Neck/Neck Crosslinking Constructs

Tomishige and Vale [2000] investigated the human kinesin construct K560\_Cys337, that also could be crosslinked in the *a* position of the first heptad of the neck coiled-coil by oxidation. Their results for ATPase activity (unaffected) and multiple motor gliding velocity (-30%) are comparable to those reported here. Additionally, they performed single motor motility assays and found that single molecule velocity was unchanged after crosslinking while the run length decreased by 43%. They concluded for HsKin that neck coiled-coil unwinding does not need to occur during processive motion but may play a minor role in processivity.

Differences in the stability of the neck coiled-coil between *N. crassa* and animal kinesins made it necessary to investigate the NcKin neck separately. The C-terminal half of the neck

region of conventional animal kinesins exhibits a stable  $\alpha$ -helical coiled-coil that is sufficient for dimerisation [Jiang *et al.* 1997; Morii *et al.* 1997; Tripet *et al.* 1997]. In contrast, the neck region of NcKin requires additional amino acids from the hinge domain for the formation of a stable coiled-coil capable of dimerisation [Kallipolitou *et al.* 2001]. But, as stated above, the crosslinked NcKin construct behaved like the HsKin construct, revealing no difference concerning the necessity of the neck coiled-coil to melt during processive movement.

On the other hand, Hoenger *et al.* [2000] claimed that partial melting of the neck coiled-coil is essential for walking and ATP hydrolysis. They used the rat kinesin construct rK379-A339C (amino acid 339 in rat kinesin corresponds to amino acid 337 of human and amino acid 342 of *N. crassa* kinesin). Their conclusions need to be viewed with caution as they did not demonstrate the formation of the crosslink, and the ATPase activities of the reduced and oxidised variants were suppressed to the same extent. Therefore, the drop in ATPase activity cannot be linked unequivocally to a crosslink between the two neck domains. They also reported a 10fold increase of  $K_{0.5,MT}$  upon oxidation, inferring a loss of processivity. However,  $K_{0.5,MT}$  values of NcKin (Table 3.1) and HsKin [Tomishige & Vale 2000] crosslinked neck constructs were unchanged.

#### 4.3.4 Neck Coiled-Coil Unwinding Hypothesis

Different secondary structure prediction methods and secondary structure analyses of synthetic peptides corresponding to different parts of the neck of animal kinesins [Huang *et al.* 1994; Tripet *et al.* 1997] hinted at the instability of the middle two heptads of the neck coiled-coil due to ‘non-ideal’ residues destabilising the coiled-coil structure. Hoenger *et al.* [1998; 2000] interpret their three-dimensional reconstructions based on cryoelectron microscopy as the stable binding of both heads of a kinesin dimer to two adjacent binding sites on the microtubule. This controversial interpretation was used to argue for a different dimer configuration upon microtubule binding than in solution. On the basis of these observations the neck coiled-coil melting theory was suggested [E. Mandelkow & Hoenger 1999]. Unwinding of the coiled-coil is proposed to increase the distance between the heads to enable access to the microtubule of both heads (Figure 1.4 A). Shortly thereafter the neck coiled-coil was analysed in more detail, revealing that specific structural interactions (hydrophobic collar and helix capping motifs) compensate for the presence of coiled-coil destabilising hydrophilic and charged residues [Thormählen *et al.* 1998; Tripet & Hodges 2002]. This indicated that even the beginning of the neck coiled-coil is much more stable than thought before. In addition, Romberg *et al.* [1998] showed that replacing kinesin’s neck with

a highly stable artificial coiled-coil caused a decrease of processivity by only 45%. Furthermore, Hoenger et al. [2000] reported double-headed binding of kinesin dimers to the microtubule while its neck coiled-coil was crosslinked. Owing to an increased  $K_{0.5,MT}$  they concluded that melting of the neck coiled-coil is necessary for processivity but not simultaneous binding of both heads. However, this contrasts with results reported here for NcKin (3.4.2) and by Tomishige and Vale [2000] for HsKin, confirming wild-type ATPase activity and  $K_{0.5,MT}$ , slightly reduced multiple motor velocity and only 43% reduced processivity. Thus, preventing the melting of the coiled-coil neck either by crosslinking or by the insertion of a highly stable coiled-coil sequence approximately halves the run length but does not abolish processivity [Romberg *et al.* 1998; Tomishige & Vale 2000]. Further evidence against an unwinding of the neck coiled-coil during double-headed binding has been obtained recently by cryoelectron microscopy and image reconstruction of dimeric kinesin constructs complexed to microtubules [Skiniotis *et al.* 2003]. The authors engineered a Spectrin SH3 domain into the transition between neck-linker and neck coiled-coil in order to enhance the visibility of this region. The close proximity of the SH3 tags from the trailing and leading heads, both bound to the microtubule, suggests that the neck coiled-coil remains completely folded.

The overall picture emerges that unwinding of the neck coiled-coil is not essential for double-headed binding and proper motor functions, including processive movement.

## 4.4 Neck-Linker/Motor Core Crosslinking Constructs

### 4.4.1 Crosslinking Efficiency

Evidence for crosslinking of the neck-linker/motor core constructs is much more difficult to obtain from band shifts on nonreducing gels as the crosslink does not change the molecular mass of the constructs. Therefore, only tiny differences in the running behaviour of crosslinked proteins can be expected. This is the case for NcKin433\_S3C\_A334C (partly immobilised neck-linker construct) and NcKin433\_A226C\_E339C (completely immobilised neck-linker construct) (3.3.3), indicating crosslinking efficiencies of 90% and 75%, respectively. Unpredicted extra bands occurred for the single mutants NcKin433\_S3C and NcKin433\_E339C, while the electrophoretic properties of the other single mutants were not influenced by oxidation. NcKin433\_S3C exhibited a negligible tendency to an interchain crosslink. But NcKin433\_E339C was crosslinked to 60% presumably by an intermolecular

disulfide bridge between residues 339. These intermolecular crosslinks do not occur in the double mutants, showing the dominance of the desired intramolecular crosslink. Nonetheless all single mutants show no evidence for the formation of an intramolecular crosslink involving one of the intrinsic cysteine residues. Thus, the observed intramolecular crosslinks of the double mutants clearly depend on both inserted cysteine residues, leading to a partly or totally immobilised neck-linker.

#### 4.4.2 Characterisation of Motility, Hydrolysis and Binding Properties

##### 4.4.2.1 NcKin\_S3C\_A334C Constructs

The partly immobilised neck-linker of NcKin\_S3C\_A334C completely, but reversibly abolished motility while hydrolysis in the presence and absence of microtubules of the dimeric and monomeric constructs were largely unaffected (3.4.3.1 and 3.7.2). Thus, ATP turnover and stepping process have been uncoupled by permanently docking the C-terminal half of the neck-linker onto the motor core. It seems as if the binding of NEM to residue 334 in the neck-linker produces sterical clashes interfering with the stepping mechanism but not hydrolysis. Competitive motility assays indicated that microtubule affinity of the crosslinked protein was comparable to that of wild-type (3.5).

The single mutant controls show that S3C and A334C are both required to exhibit the defect in motility (3.4.3.1.3). However, they also show some strange behaviour. Gliding velocity and hydrolysis were affected differently by inactivation of the proteins during measuring. There is no straightforward explanation for this phenomenon.

##### 4.4.2.2 NcKin\_A226C\_E339C Constructs

The totally immobilised neck-linker of NcKin433\_A226C\_E339C caused a reduction of motility and microtubule-stimulated ATPase activity by 85%, which was fully reversible (3.4.3.2). Considering the estimated amount of crosslinking by gel electrophoresis (75%, see 3.3.3) and the results of the competitive motility assay (mixture of active and inactive protein leads to intermediate velocities, see 3.5), all motor functions tested appear to be fully inactivated by docking the neck-linker onto the motor core. This was supported by a 97% decrease in ATP turnover of the crosslinked monomeric construct. However, the monomeric mutant, NcKin343\_A226C\_E339C, differed from the dimeric construct in its partial rescue capacity. Reasons for this are not obvious.

The single mutant controls confirm that both introduced cysteine residues are required for inactivation of the dimeric and monomeric constructs by oxidation (3.4.3.2.3). Both dimeric single mutants showed no effects upon oxidation although NcKin433\_E339C developed a prominent intermolecular crosslink (3.3.3). The monomeric single mutant NcKin343\_A226C was not influenced by oxidation either. However, the ATPase activity of the other monomeric single mutant, NcKin343\_E339C, was reduced by 40% upon oxidation and reverted to 100% after rescue. This effect is probably due to an intramolecular crosslink between cysteine 339 and one of the remaining intrinsic cysteine residues. Additionally, the extremely high  $K_{0.5,MT}$  of NcKin343\_E339C under oxidising conditions suggested a dramatically reduced microtubule affinity. Possibly, the reduced ATPase activity results from an improper ATPase stimulation by microtubules caused by poor microtubule binding of the crosslinked construct. The formation of this undesirable crosslink cannot be excluded for the monomeric double mutant, though the effect of crosslinking the double mutant is much more pronounced than the effect of crosslinking the single mutant. Therefore, NcKin343\_A226C\_E339C is at least partly crosslinked via residues 339 and 226. Possibly, different effects of both intramolecular crosslinks superimpose. Nevertheless, the observed effect of the double mutant can at least partially be assigned to docking of the neck-linker. Interestingly, the monomeric and dimeric single mutants E339C develop different undesirable crosslinks that are linked to the absence or presence of the coiled-coil neck domain and cause or do not cause effects. In the dimer the C-terminal parts of the neck-linker are held close together by the neck coiled-coil, while in the monomer the neck-linkers are freely movable.

Microtubule-stimulated and basal ATP turnover rates (Table 3.3) for uncrosslinked NcKin433\_A226C\_E339C were less than half of the wild-type mean values (42% of  $73 \text{ s}^{-1}$  and 24% of  $0.023 \text{ s}^{-1}$ ), which either might hint at a considerable amount of inactive protein or may be the result of the concurrent occurrence of both mutations. This did not apply to the monomeric construct. Here, the ATP turnover in the presence and absence of microtubules of uncrosslinked NcKin343\_A226C\_E339C was only slightly lower than the wild-type mean values (76% of  $269 \text{ s}^{-1}$  and 75% of  $0.023 \text{ s}^{-1}$ ). This suggests that the double mutation per se does not reduce the enzymatic activity.

In contrast to this difference between dimer and monomer, the basal ATPase activities of crosslinked dimer and monomer were indistinguishable (3.7.3). Docking of the neck-linker diminished it to 11-13% of mean wild-type values. Notwithstanding an overall 25% decrease of basal ATPase activity, this is a significant effect. In addition, microtubule activation of ATP turnover rates diminished to 60% and 16% for the dimer and monomer, respectively.

Therefore, most of the crosslinking effect observed for the dimer can be attributed to the dramatic reduction of basal ATPase activity. In contrast to the dimer, the basal ATP turnover and the microtubule stimulation of ATP turnover of the monomer are reduced to the same extent by crosslinking. Hence, a permanently docked neck-linker inhibits normal basal enzymatic activity. It cannot be decided whether hydrolysis, nucleotide exchange or phosphate release are responsible.

Competitive motility assays (3.5) and sedimentation assays (3.6) clearly displayed a dramatically reduced affinity for microtubules when the neck-linker was permanently docked. The microtubule affinity of the dimer was twofold reduced by crosslinking both in the strong (AMP-PNP) and weak (ADP) binding state. Crosslinking of the monomer lowered microtubule affinity by a factor of 5 or 10 in the strong and weak binding state, respectively. As both binding states are affected, a docked neck-linker prevents strong binding to microtubules no matter whether AMP-PNP or ADP is in the nucleotide pocket. Possibly though, the nucleotide was not exchanged completely, thereby reducing microtubule affinity. However, as the dissociation constants of crosslinked monomeric and dimeric constructs differ for AMP-PNP and ADP, they still must be able to sense which nucleotide is bound and pass this information on to the microtubule binding site.

The low microtubule affinity observed in the motility assay (very weak attachment of microtubules on kinesin-coated coverslips, see 3.4.3.2.3) indicates that the crosslinked protein predominantly is in the weak binding state, which is the ADP state.

ADP release experiments of NcKin433\_A226C\_E339C (3.8) revealed a chemical processivity of 32 for the uncrosslinked protein. This value implies that like wild-type NcKin this construct hydrolyses many ATP molecules during one productive microtubule encounter. However, ADP release rates of the crosslinked construct were very slow and indistinguishable from mantADP bleaching. This suggests that upon docking of the neck-linker, activation of ADP release by microtubules is suppressed which, in turn, causes very low ATPase activity. As microtubule binding and ADP release are mutually dependent (ADP release requires microtubule binding and tight binding requires ADP release) it is impossible to decide between cause and effect.

#### 4.4.2.3 HsKin\_K222C\_E334C Constructs

With respect to the position of the crosslink HsKin\_K222C\_E334C constructs correspond to NcKin\_A226C\_E339C constructs in sequence and structural alignments of human and *N. crassa* conventional kinesin. Docking of the neck-linker over its entire length led to total

loss of enzymatic activity of dimeric and monomeric HsKin\_K222C\_E334C. Crosslinking was irreversible. Furthermore, immobilisation of the neck-linker considerably increased  $K_{0.5,MT}$  values of both constructs, pointing to reduced microtubule affinity or chemical processivity. These results conflict with previously reported ATP turnover rates of a dimeric human kinesin construct identical to HsKin560\_K222C\_E334C [Tomishige & Vale 2000]. The authors report a more than 50% decrease of ATPase activity for the noncrosslinked protein compared with wild-type and a further 50% decrease upon crosslinking. They did not investigate the monomeric construct.

#### 4.4.3 Comparison of Neck-Linker/Motor Core Crosslinking Constructs

The neck-linker/motor core crosslinking constructs discussed here can be divided into two classes, namely, (i) constructs with fully docked neck-linker (dimeric and monomeric NcKin\_A226C\_E339C and corresponding HsKin constructs) and (ii) constructs with partially docked neck-linker (dimeric and monomeric NcKin\_S3C\_A334C and corresponding HsKin constructs Cys330/Cys4 [Tomishige & Vale 2000]). Regarding sequence alignment and structural positioning, amino acids 4 and 330 in HsKin correspond to amino acids 3 and 334 in NcKin, resulting in identically located crosslinks. Although fungal and human constructs develop crosslinks at identical positions, the effects caused by these crosslinks differ.

The discrepancy is most evident in constructs with a partially immobilised neck-linker. Crosslinking NcKin abolished motility while enzymatic activity was unaffected (4.4.2.1). Tomishige and Vale [2000] also observed hardly any movement for the crosslinked HsKin dimer, but this effect was accompanied by a 50% reduction of ATP turnover. However, the ATP turnover of the monomer was unaffected by the crosslink. As a result, they attributed the slow residual motility and the decrease in ATPase activity to an inactivation of the second head of the dimer due to an inability of both heads to access the microtubule. In other words, they suggested a loss of head-head coordination instead of an alteration of the catalytic mechanism. NcKin constructs instead show an uncoupling of enzymatic and mechanical processes which is intrinsic to each head.

Inconsistencies of the effects of immobilising the whole neck-linker already occur with one and the same construct, namely the HsKin construct measured by Tomishige and Vale [2000] and in this study (4.4.2.3). Complete loss of motility concurrently has been shown for crosslinked *N. crassa* and human constructs. In principle, the same is true of the reduced ATPase activity and increased  $K_{0.5,MT}$  after crosslinking. Primarily, conclusions from the different extent of effects are contradictory. Although they did not check influences of

---

crosslinking on the single headed construct, Tomishige and Vale [2000] considered the disruption of double headed binding to microtubules to be the cause for their observed 50% decreased ATP turnover of the crosslinked dimer. As they already measured a 50% reduced ATPase activity of the mutant under reducing conditions compared to wild-type, the crosslinking effect could be as high as 75% if some of the protein was crosslinked even in the 'reduced' state. They assumed that only one head of the dimer has its ATPase cycle stimulated as the other head is prevented from binding to the microtubule by the docked neck-linker. However, the alternating head model does not predict a 50% reduced ATP turnover for dimers with one inactive head. By contrast, the current study revealed that also in monomeric HsKin and NcKin constructs, ATP turnover is severely inhibited. Additionally, the decrease of ATPase activity of the human and *N. crassa* dimer found here was much more pronounced than 50% in the study of Tomishige and Vale [2000]. These findings strongly argue against one fully functional and one inactive head of a dimer but for the complete shut down of all motor functions. Furthermore, the observed weak microtubule affinity of NcKin constructs with a fully docked neck-linker (3.6) conflicts with the reported microtubule binding of the crosslinked human construct [Tomishige & Vale 2000], which is said to be unaffected.

#### 4.4.4 Neck-Linker Unzippering Hypothesis

The necessity of a two-heads bound intermediate for processive movement is widely accepted, as is the fact that this requires a conformational change in the observed crystal structure [Block 1998]. Romberg et al. [1998] elaborated the theory that a reorientation of the neck-linker during the hydrolysis cycle temporarily enables double-headed binding. It involves breaking of the bonds holding the neck-linker to the catalytic core, whereupon the neck-linker adopts a flexible conformation and folds to the opposite end of the catalytic core (Figure 1.4 B). In favor of this model, Rice et al. [1999] detected an ATP-dependent conformational change of the neck-linker using electron paramagnetic resonance, fluorescence resonance energy transfer, and cryoelectron microscopy. They found that the neck-linker is docked onto the catalytic core when kinesin is bound to microtubules and ATP is in the active site, but becomes unzipped in the ADP or nucleotide-free state. These findings, together with cryoelectron microscopy work that reveals the docking orientation of kinesin on the microtubule, suggest that the two kinesin heads can span the distance between tubulin binding sites if the neck-linker of the rear head is docked and pointing forward and the neck-linker on the forward head is detached and pointing backward [Vale & Milligan 2000]. Sindelar et al. [2002] showed that the docked conformation of the neck-linker visible in some

---

crystal structures is comparable to the docking observed by electron paramagnetic resonance spectroscopy. The authors explained the crystallisation of docked and disordered neck-linker structures with ADP in the active site by the absence of microtubules. They concluded that only in the presence of microtubules is neck-linker flexibility dependent on the nucleotide state. The results of Rice *et al.* [1999] and Sindelar *et al.* [2002] were obtained on monomeric constructs and have been questioned to be applicable to dimers [Schief & Howard 2001]. A recent study applied cryoelectron microscopy and image reconstruction to investigate the location of the kinesin neck in dimeric and monomeric constructs complexed with microtubules [Skiniotis *et al.* 2003]. They confirmed the states of neck-linker mobility for monomers and showed that in dimers the neck-linker behaved identically, namely being flexible in the absence of nucleotide and ordered in the presence of AMP-PNP. Furthermore, the opposite orientation of the two neck-linkers when both heads are bound was demonstrated. Sugata *et al.* [2004] reached a different conclusion. The authors investigated dimeric kinesin by electron spin resonance to determine the conformation of the neck-linker in the absence and presence of microtubules. As in the studies on monomeric constructs, without microtubules the neck-linkers of dimers co-existed in both docked and disordered conformations. In all nucleotide states, however, the neck-linkers were well ordered when dimeric kinesin is bound to microtubules. These data do not support the nucleotide-dependent 'flexibility switch' model developed for monomeric kinesin [Rice *et al.* 1999] and applicable to dimeric kinesin [Skiniotis *et al.* 2003]. Instead a different mechanism is suggested: when both motor domains are bound to the microtubule, the neck-linkers of each motor core are fixed in different orientations. In the presence of microtubules the neck-linker does not change the degree of flexibility during the ATPase cycle, but changes its orientation between two fixed conformations. However, the authors do not comment on the difficulties to interpret the overlapping signal of two spin labels in a dimer and the slight differences in spectra observed for different nucleotides in the presence of microtubules. Whatever mechanism is correct, the key aspect of both models is the opposing orientation of the neck-linker when both motor domains are bound to the microtubule.

How do the results of the present crosslinking study fit into the current understanding of neck-linker motility?

The inability of the crosslinked neck-linker/motor core constructs to produce motility suggests that the position of the neck-linker plays a crucial role in the mechanical transducer process. Already a partial immobilisation of the neck-linker prevents movement even in the multiple motor gliding assay (4.4.2.1). This confirms the notion that it is not the coordination

---

of the motor domains that is impeded, but the function of the heads themselves. Monomeric kinesin constructs cannot move processively as they have only a single motor domain, but still many molecules can act in concert to move microtubules at a reduced velocity of 0.7-1  $\mu\text{m/s}$  for NcKin [Kallipolitou *et al.* 2001]. The minimal kinesin construct exhibiting microtubule motor activity contains only the conserved motor domain and neck-linker, although the efficiency with which ATP hydrolysis is coupled to microtubule movement declines dramatically with increasing truncation [Stewart *et al.* 1993]. These observations clearly support the absolute requirement of a flexible neck-linker for any kind of motility and not just for processive movement. Hence, this crosslinking study confirms the neck-linker as the essential transducer element, but it does not give a direct clue on the validity of the neck-linker unzipping model.

Some results of this crosslinking study seem to conflict with certain aspects of the model. First, the low microtubule affinity of the construct with the fully docked neck-linker was unexpected. In wild-type kinesin nucleotide state and microtubule affinity are mutually dependent, as was shown also for the fully docked neck-linker mutant, although its microtubule affinity was reduced dramatically. Kinesin binds tightly to microtubules only when no nucleotide or ATP is bound. On the other hand, MT binding is necessary for kinesin to release ADP. The position of the neck-linker is independent of the nucleotide state as long as kinesin is in solution [Sindelar *et al.* 2002]. Once kinesin is bound to microtubules, the conformation and orientation of the neck-linker and nucleotide state are tightly coupled [Rice *et al.* 1999]. Upon ATP binding the neck-linker docks onto the catalytic core, while in the ADP state the neck-linker is mobile. These results predict that in the docked neck-linker state (with bound ATP), kinesin exhibits tight microtubule binding. However, the construct with the fully docked neck-linker exhibited very weak microtubule binding (4.4.2.2). It is unclear whether the crosslinked construct does indeed contain ATP in its nucleotide pocket. As the ADP release is not activated by microtubules, probably ADP is bound predominantly to the crosslinked protein, preventing tight microtubule binding. Nevertheless, the conflict remains that even in the AMP-PNP state microtubule affinity is weak. This implies that docking of the neck-linker generally weakens the interactions with microtubules instead of resulting in a tight binding state. These contradictory observations can be reconciled only by the assumption that for the initial weak microtubule encounter leading to ADP release an undocked neck-linker is a prerequisite, while docking of the neck-linker is not an obstacle in the following tight binding state. Hence, this would mean that for initiation and continuation of tight binding different positions of the neck-linker are mandatory.

---

The second apparent discrepancy relates to the dramatically reduced ATP turnover in the absence of microtubules observed also for the fully docked neck-linker construct (4.4.2.2). Electron paramagnetic resonance analyses showed that the neck-linker freely exchanges between docked and disordered conformations when microtubules are absent [Sindelar *et al.* 2002]. The conformational equilibrium of the neck-linker is not affected by nucleotide exchange. But this does not allow to conclude the opposite. If nucleotide exchange does not define the position of the neck-linker, its immobilisation may certainly hinder nucleotide exchange. A second possibility how these observations may fit is that in the crosslinked mutant, inhibition of either hydrolysis itself or phosphate release leads to the low ATP turnover, leaving nucleotide exchange unaffected by the position of the neck-linker.

## 4.5 $\alpha 4/\alpha 6$ Crosslinking Constructs

### 4.5.1 Crosslinking Efficiency

The desired crosslink could not be confirmed by nonreducing SDS-PAGE analysis as no definite band shift occurred in both the double and single mutants (3.3.4). Nevertheless, oxidation affected their motile and catalytic properties to various extents (3.4.4). These effects, unfortunately, cannot be ascribed clearly to the formation of a disulfide bridge since they are not reversible and since they are also observed in some of the single mutants. However, they are unambiguously linked to oxidation. Thus, something must be happening with the introduced cysteine residues but exactly what is difficult to determine. Crosslinks between the introduced and one of the intrinsic cysteine residues can be ruled out due to their spatial separation.

### 4.5.2 Characterisation of Motile and Hydrolysis Properties

While the monomeric and dimeric single mutants S329C were unaffected by oxidation, the other single mutants T273C exhibited similar effects as the double mutants. The latter two types of mutants differed mainly in their rescue behaviour. Upon oxidation these constructs showed only about 20-55% motile and catalytic activity and a twofold increase in the half maximal activation constant, indicating a loss of processivity. While under rescue conditions the effects remained largely unchanged in the double mutants, the single mutants displayed 80-100% activity and a normal  $K_{0.5,MT}$ . The NEM controls were normal for the dimeric constructs and revealed about 70% activity in the monomeric constructs. These results are

difficult to interpret. As the effects in the T273C and the double mutants are very similar, it can be assumed that they are caused by the attachment of a DTNB molecule to cysteine residue 273. However, it remains unclear why this attachment is reversible only in the single mutants and why the effects are not also induced by NEM. Probably, the DTNB molecule, when attached to helix  $\alpha 4$ , sterically clashes with side chains protruding from helix  $\alpha 6$ . This may prevent conformational changes taking place between these two helices, resulting in an inhibition of protein activity. Thus, although presumably no crosslink forms between helices  $\alpha 4$  and  $\alpha 6$ , their relative movement is hindered in such a way that both ATPase and motor activity are impaired profoundly. Because ATP turnover of monomers and dimers is affected equally, the conformational change thus prevented is necessary for the catalytic cycle of a single motor domain. Hence, the loss of ATPase activity is intrinsic to each motor domain and not due to disturbed head-head coordination. However, motility is affected to a much higher extent than ATP turnover. This and the doubled half maximal activation constants of the oxidised dimers suggest that the observed slow velocity is accompanied by a reduced or abolished processivity. Processivity is dependent on the tight coupling of both motor domains. Their ATPase cycles and therefore their microtubule affinities must be kept out of phase, and additionally, attachment of one head must precede detachment of the other head. As helix  $\alpha 4$  is involved in microtubule binding, motor-microtubule association likely is affected. To decide whether processivity is altered, further experiments are necessary.

#### 4.5.3 Rotation of Helix $\alpha 4$ against the Motor Core

During the hydrolysis cycle of kinesin, nucleotide-dependent conformational changes occur in the motor domain. Small conformational changes at the active site are transmitted to the microtubule binding site (loop L12), coupling the nucleotide state to microtubule affinity [Vale *et al.* 2000]. Conserved amino acid residues of the switch regions interact with the  $\gamma$ -phosphate of the nucleotide when ATP or ADP $\cdot$ P<sub>i</sub> is bound. These interactions are disrupted for  $\gamma$ -phosphate release, causing conformational changes in switches I and II. In KIF1A, a monomeric kinesin sharing 43% amino acid sequence identity with the motor domain of conventional kinesin and having the same overall architecture of the catalytic core, restructuring of switch II causes conformational rearrangements of the consecutive structural elements loop L11, helix  $\alpha 4$ , loop L12, helix  $\alpha 5$  and loop L13 [Kikkawa *et al.* 2001]. This ‘switch II cluster’ rotates by 20° relative to the core. These nucleotide-dependent movements of the switch II cluster result in docking and undocking of the neck-linker on the catalytic

---

core. Kikkawa et al. [2001] suggest that the positioning of the neck-linker depends on the rotation of the switch II cluster, containing helix  $\alpha_4$ , relative to the rest of the motor core, including helix  $\alpha_6$ . Here it was tried to inhibit this putative rotation by crosslinking helices  $\alpha_4$  and  $\alpha_6$ . Unfortunately, the desired crosslink could not be demonstrated unambiguously. However, the attachment of a DTNB molecule to the cysteine residue at the C-terminal end of helix  $\alpha_4$  produced a pronounced loss of catalytic and mechanic motor activity. It is not known, with which structural element the attached molecule interferes and whether this sterical clash inhibits a rotational or translational rearrangement. But by simulating DTNB attachment in the three-dimensional structure of NcKin only few residues in  $\beta$ -sheet 1 or  $\alpha$ -helix 6 are likely affected. Therefore, it can be concluded that for normal chemomechanic cycling of NcKin the movement of  $\alpha_4$  relative to  $\beta_1$  or  $\alpha_6$  is indispensable. If processivity indeed is abolished, this could be caused by a restriction of the neck-linker's freedom to move between a docked and a flexible position. But this is highly speculative. With the experiments carried out so far, Kikkawa's model of the dependence of neck-linker docking on the nucleotide-dependent rotation of the switch II cluster can neither be confirmed nor dismissed.

## 4.6 Future Prospects

This study is based on the formation of disulfide crosslinks to investigate the significance of conformational changes between structural parts of NcKin. The interpretation of the results depends on the reliability of crosslinking the desired residues. The most direct evidence for crosslinking at the expected positions is the isolation and characterisation of cysteine-containing proteolytic peptides from NcKin. However, so far all attempts to identify tryptic peptides by mass spectrometry failed for technical reasons.

All motility data presented here are based on multiple motor assays. The surface is densely coated with kinesin dimers such that a microtubule is moved by thousands of motors. Under these circumstances no details about the motile behaviour of a single dimeric kinesin molecule can be derived. For example, many nonprocessive monomeric kinesins together are able to move microtubules, while each motor by itself cannot produce movement [Vale *et al.* 1996]. Single motor tests are necessary to make statements about processivity and run length of kinesin constructs. One such assay is total internal reflection fluorescence (TIRF) microscopy whereby single fluorescence-labeled kinesin molecules can be observed moving

---

along the microtubule [Vale *et al.* 1996]. It would be important to assay for the processivity of several constructs studied here, but two of them are of particular interest.

One is the crosslinked neck construct P342C to determine whether an unwinding of the neck coiled-coil may be required for normal run length behaviour.

The second is the  $\alpha 4/\alpha 6$  crosslinking construct. If processivity is reduced or abolished, as indicated here, a further kinetic characterisation might reveal which of the prerequisites for processive movement is affected. A kinesin construct with an intact neck dimerisation domain which nonetheless is unprocessive but still exhibits multiple motor movement would be very illuminating. Until now, there are dimeric constructs which either are motile and processive or do not have any motor activity left. With such a construct, one could distinguish between basal necessities for motility and advanced requirements for processive movement.

From the complete loss of motility of the neck-linker crosslinking constructs it can be concluded that for chemomechanical coupling the neck-linker needs to undock from the motor core over its entire length. It is likely that complete undocking of the neck-linker also is required for processive movement. In order to confirm the direct influence of the neck-linker on the binding of both heads, constructs are needed that are not processive but still generate movement when acting in concert. A possible candidate is NcKin433\_E339C. This single mutant partly develops an intermolecular disulfide bridge. If the efficiency of the crosslink can be increased by longer oxidation time or by using spacer crosslinkers, effects due to the shortening of the effective length of the neck-linker may appear. Another approach to a motile but nonprocessive kinesin construct could be the generation of deletion mutants in which amino acid residues from the N-terminal end of the neck-linker are removed successively. At some stage the increasingly shortened neck-linker does not suffice to span the 8 nm distance between two adjacent  $\beta$ -tubulin binding sites, but the remaining part of the neck-linker may still promote movement.

Another very interesting aspect is the exact step in the ATPase cycle that is affected by the completely docked neck-linker. The determination of the nucleotide state of the kinesin constructs with a docked neck-linker would allow to draw conclusions about the step that is slowed down. The assumption is that ADP is retained in the nucleotide pocket, as ADP release is reduced dramatically. Alternatively, hydrolysis could be slowed down, leading to the retention of ATP in the nucleotide pocket.

The same is true for the reduced basal ATPase activity of the constructs with completely docked neck-linkers. Is it hydrolysis, phosphate release or nucleotide exchange that is affected?

---

## 5 Summary

### 5.1 Summary

Conventional kinesin of the filamentous fungus *N. crassa* (NcKin) moves processively along microtubules as its animal counterparts. It is able to take many steps without falling off the microtubule. In this process the trailing head does not detach before the leading head has attached to the microtubule. However, the positioning of the two motor domains visible in the three-dimensional crystal structure of the kinesin dimer prevents simultaneous binding of both heads to adjacent tubulin subunits. To achieve double-headed binding, a conformational change in the neck region, consisting of the neck-linker and the neck coiled-coil, is necessary. Two theories, how this conformational change might be accomplished, have been advanced: First, the unwinding of the  $\alpha$ -helical coiled-coil in the neck, and second, the reorientation of the neck-linker.

The goal of the present work was to decide between these two hypotheses. For that purpose, the kinetic and motile properties of NcKin mutants were examined. In the mutants introduced cysteine residues could reversibly be crosslinked via disulfide bridges preventing certain conformational changes.

A dimeric construct with a neck coiled-coil that could not unwind displayed normal ATP turnover and gliding velocity. This excludes that the melting of the neck coiled-coil is essential for proper mechano-chemical coupling of the two motor domains.

However, dimeric constructs with a partially or completely immobilised neck-linker did not move. Hence, a completely flexible neck-linker is indispensable for motility. Kinetic studies on these and corresponding monomeric constructs showed furthermore that docking of the whole neck-linker onto the catalytic core led to a dramatically reduced basal and microtubule-stimulated ATPase activity as well as a considerably diminished microtubule affinity. The weak microtubule binding probably fails to activate ADP release and consequently the ATP turnover rate. By contrast, the partially immobilised neck-linker did not influence ATP turnover either in the presence or absence of microtubules. Also, it did not affect microtubule affinity. Thus, enzymatic and motile activities of kinesin are uncoupled if the flexibility of the neck-linker is restricted.

Attempts to prevent the putative rotation of helix  $\alpha 4$ , which is involved in microtubule binding, against the rest of the motor core failed to provide straightforward results. The formation of the desired disulfide bridge could not be shown directly and the observed effects could not be ascribed unambiguously to the two introduced cysteine residues. Nevertheless, the results suggest that mobility of helix  $\alpha 4$  is important for proper motor function.

## 5.2 Zusammenfassung

Das konventionelle Kinesin aus dem filamentösen Pilz *N. crassa* (NcKin) bewegt sich wie die tierischen Vertreter prozessiv entlang von Mikrotubuli, kann also viele einzelne Schritte nacheinander durchführen, ohne sich vom Mikrotubulus zu lösen. Dies ist nur möglich, wenn immer mindestens eine der beiden Motordomänen an den Mikrotubulus gebunden ist. Das heißt, der hintere Kopf darf sich erst vom Mikrotubulus lösen, wenn der vordere bereits gebunden hat. In der dreidimensionalen Struktur des Kinesin Dimers erlaubt die relative Lage der beiden Motordomänen zueinander jedoch nicht die gleichzeitige Bindung an benachbarte  $\beta$ -Tubulin Untereinheiten. Dazu muß eine Konformationsänderung im Bereich der Halsregion, die aus der Halsverbindung und dem superhelikalen Hals besteht, stattfinden. Zwei Theorien, wie diese Konformationsänderung aussehen könnte, wurden aufgestellt: Erstens, Aufschmelzen des  $\alpha$ -helikalen Doppelstranges in der Halsregion und zweitens, Umorientierung der Halsverbindung.

Ziel der vorliegenden Arbeit war es, zwischen diesen beiden Hypothesen zu entscheiden. Hierzu wurden Mutanten auf ihre kinetischen und motilen Eigenschaften hin untersucht. In diesen Mutanten konnten eingeführte Cysteine reversibel zu Disulfidbrücken verbunden werden, so daß bestimmte Konformationsänderungen verhindert wurden.

Ein dimeres Konstrukt, dessen Hals-Superhelix sich nicht entwinden konnte, zeigte normalen ATP Umsatz und Gleitgeschwindigkeit. Daher kann ausgeschlossen werden, daß das Aufschmelzen des superhelikalen Halses für die ungestörte mechano-chemische Kopplung beider Motordomänen erforderlich ist.

Dimere Konstrukte, deren Halsverbindung entweder teilweise oder vollständig an die Motordomäne gekoppelt war, erzeugten hingegen keine Bewegung. Somit ist die vollständige Bewegungsfreiheit der Halsverbindung für die Motilität unentbehrlich. Kinetische Untersuchungen an diesen und entsprechenden monomeren Konstrukten zeigten, daß die Anheftung der gesamten Halsverbindung an die Motordomäne außerdem zu einer drastischen

---

Verringerung der basalen und Mikrotubuli-stimulierten ATPase Aktivität, sowie einer stark verringerten Mikrotubuli Affinität führte. Wahrscheinlich kann durch die schwache Mikrotubuli Bindung die ADP Freisetzung nicht beschleunigt werden und somit auch nicht die ATP Umsatzrate. Dagegen beeinflusste die Immobilisierung des proximalen Teils der Halsverbindung den ATP Umsatz in Ab- und Anwesenheit von Mikrotubuli nicht. Auch die Affinität zu Mikrotubuli war nicht verringert. Bei eingeschränkter Bewegungsfreiheit der Halsverbindung werden also enzymatische und motile Aktivität des Proteins entkoppelt.

Versuche, die mutmaßliche Rotation der Mikrotubuli bindenden  $\alpha$ -Helix 4 gegen die restliche Motordomäne zu unterbinden, lieferten keine eindeutig interpretierbaren Ergebnisse. Es konnte nicht direkt gezeigt werden, ob die gewünschte Disulfidbrücke gebildet wurde, und die beobachteten Effekte ließen sich nicht eindeutig auf die Einführung beider Cysteine zurückführen. Dennoch deuten die Ergebnisse darauf hin, daß Helix  $\alpha$ 4 für eine normale Motorfunktion beweglich sein muß.

---

## 6 References

**Asbury CL, Fehr AN & Block SM** (2003) "Kinesin moves by an asymmetric hand-over-hand mechanism." *Science* 302: 2130-2134.

**Berliner E, Young EC, Anderson K, Mahtani HK & Gelles J** (1995) "Failure of a single-headed kinesin to track parallel to microtubule protofilaments." *Nature* 373: 718-721.

**Block SM** (1998) "Kinesin: what gives?" *Cell* 93: 5-8.

**Bradford MM** (1976) "A rapid and sensitive method for the quantitation of microgram quantities of protein utilizing the principle of protein-dye binding." *Anal Biochem* 72: 248-253.

**Brady ST** (1985) "A novel brain ATPase with properties expected for the fast axonal transport motor." *Nature* 317: 73-75.

**Case RB, Rice S, Hart CL, Ly B & Vale RD** (2000) "Role of the kinesin neck linker and catalytic core in microtubule-based motility." *Curr Biol* 10: 157-160.

**Coy DL, Hancock WO, Wagenbach M & Howard J** (1999) "Kinesin's tail domain is an inhibitory regulator of the motor domain." *Nat Cell Biol* 1: 288-292.

**Crevel IM, Lockhart A & Cross RA** (1996) "Weak and strong states of kinesin and ncd." *J Mol Biol* 257: 66-76.

**Crevel IM, Carter N, Schliwa M & Cross R** (1999) "Coupled chemical and mechanical reaction steps in a processive *Neurospora* kinesin." *Embo J* 18: 5863-5872.

**Dagenbach EM & Endow SA** (2004) "A new kinesin tree." *J Cell Sci* 117: 3-7.

**de Cuevas M, Tao T & Goldstein LS** (1992) "Evidence that the stalk of *Drosophila* kinesin heavy chain is an alpha-helical coiled coil." *J Cell Biol* 116: 957-965.

**Deluca D, Woehlke G & Moroder L** (2003) "Synthesis and conformational characterization of peptides related to the neck domain of a fungal kinesin." *J Pept Sci* 9: 203-211.

**Diefenbach RJ, Mackay JP, Armati PJ & Cunningham AL** (1998) "The C-terminal region of the stalk domain of ubiquitous human kinesin heavy chain contains the binding site for kinesin light chain." *Biochemistry* 37: 16663-16670.

**Endow SA** (1999) "Determinants of molecular motor directionality." *Nat Cell Biol* 1: E163-167.

**Endow SA & Barker DS** (2003) "Processive and nonprocessive models of kinesin movement." *Annu Rev Physiol* 65: 161-175.

**Enos AP & Morris NR** (1990) "Mutation of a gene that encodes a kinesin-like protein blocks nuclear division in *A. nidulans*." *Cell* 60: 1019-1027.

- 
- Friedman DS & Vale RD** (1999) "Single-molecule analysis of kinesin motility reveals regulation by the cargo-binding tail domain." *Nat Cell Biol* 1: 293-297.
- Gho M, McDonald K, Ganetzky B & Saxton WM** (1992) "Effects of kinesin mutations on neuronal functions." *Science* 258: 313-316.
- Gilbert SP, Moyer ML & Johnson KA** (1998) "Alternating site mechanism of the kinesin ATPase." *Biochemistry* 37: 792-799.
- Gindhart JG, Jr., Desai CJ, Beushausen S, Zinn K & Goldstein LS** (1998) "Kinesin light chains are essential for axonal transport in *Drosophila*." *J Cell Biol* 141: 443-454.
- Goldstein LS & Philp AV** (1999) "The road less traveled: emerging principles of kinesin motor utilization." *Annu Rev Cell Dev Biol* 15: 141-183.
- Grummt M, Pistor S, Lottspeich F & Schliwa M** (1998) "Cloning and functional expression of a 'fast' fungal kinesin." *FEBS Lett* 427: 79-84.
- Hackney DD** (1988) "Kinesin ATPase: rate-limiting ADP release." *Proc Natl Acad Sci U S A* 85: 6314-6318.
- Hackney DD, Malik AS & Wright KW** (1989) "Nucleotide-free kinesin hydrolyzes ATP with burst kinetics." *J Biol Chem* 264: 15943-15948.
- Hackney DD** (1994a) "Evidence for alternating head catalysis by kinesin during microtubule-stimulated ATP hydrolysis." *Proc Natl Acad Sci U S A* 91: 6865-6869.
- Hackney DD** (1994b) "The rate-limiting step in microtubule-stimulated ATP hydrolysis by dimeric kinesin head domains occurs while bound to the microtubule." *J Biol Chem* 269: 16508-16511.
- Hackney DD** (1995) "Highly processive microtubule-stimulated ATP hydrolysis by dimeric kinesin head domains." *Nature* 377: 448-450.
- Hackney DD & Stock MF** (2000) "Kinesin's IAK tail domain inhibits initial microtubule-stimulated ADP release." *Nat Cell Biol* 2: 257-260.
- Hackney DD** (2002) "Pathway of ADP-stimulated ADP release and dissociation of tethered kinesin from microtubules. Implications for the extent of processivity." *Biochemistry* 41: 4437-4446.
- Hackney DD, Stock MF, Moore J & Patterson RA** (2003) "Modulation of kinesin half-site ADP release and kinetic processivity by a spacer between the head groups." *Biochemistry* 42: 12011-12018.
- Hancock WO & Howard J** (1998) "Processivity of the motor protein kinesin requires two heads." *J Cell Biol* 140: 1395-1405.
- Hildebrandt ER & Hoyt MA** (2000) "Mitotic motors in *Saccharomyces cerevisiae*." *Biochim Biophys Acta* 1496: 99-116.

- 
- Hirokawa N, Pfister KK, Yorifuji H, Wagner MC, Brady ST & Bloom GS (1989)** "Submolecular domains of bovine brain kinesin identified by electron microscopy and monoclonal antibody decoration." *Cell* 56: 867-878.
- Hirokawa N (1998)** "Kinesin and dynein superfamily proteins and the mechanism of organelle transport." *Science* 279: 519-526.
- Hoenger A, Sack S, Thormählen M, Marx A, Müller J, Gross H & Mandelkow E (1998)** "Image reconstructions of microtubules decorated with monomeric and dimeric kinesins: comparison with x-ray structure and implications for motility." *J Cell Biol* 141: 419-430.
- Hoenger A, Thormählen M, Diaz-Avalos R, Doerhoefer M, Goldie KN, Müller J & Mandelkow E (2000)** "A new look at the microtubule binding patterns of dimeric kinesins." *J Mol Biol* 297: 1087-1103.
- Howard J, Hudspeth AJ & Vale RD (1989)** "Movement of microtubules by single kinesin molecules." *Nature* 342: 154-158.
- Hua W, Young EC, Fleming ML & Gelles J (1997)** "Coupling of kinesin steps to ATP hydrolysis." *Nature* 388: 390-393.
- Hua W, Chung J & Gelles J (2002)** "Distinguishing inchworm and hand-over-hand processive kinesin movement by neck rotation measurements." *Science* 295: 844-848.
- Huang TG & Hackney DD (1994)** "*Drosophila* kinesin minimal motor domain expressed in *Escherichia coli*. Purification and kinetic characterization." *J Biol Chem* 269: 16493-16501.
- Huang TG, Suhan J & Hackney DD (1994)** "*Drosophila* kinesin motor domain extending to amino acid position 392 is dimeric when expressed in *Escherichia coli*." *J Biol Chem* 269: 32708.
- Inoue H, Nojima H & Okayama H (1990)** "High efficiency transformation of *Escherichia coli* with plasmids." *Gene* 96: 23-28.
- Jiang W, Stock MF, Li X & Hackney DD (1997)** "Influence of the kinesin neck domain on dimerization and ATPase kinetics." *J Biol Chem* 272: 7626-7632.
- Kallipolitou A, Deluca D, Majdic U, Lakämper S, Cross R, Meyhofer E, Moroder L, Schliwa M & Woehlke G (2001)** "Unusual properties of the fungal conventional kinesin neck domain from *Neurospora crassa*." *Embo J* 20: 6226-6235.
- Kaseda K, Higuchi H & Hirose K (2003)** "Alternate fast and slow stepping of a heterodimeric kinesin molecule." *Nat Cell Biol* 5: 1079-1082.
- Kikkawa M, Sablin EP, Okada Y, Yajima H, Fletterick RJ & Hirokawa N (2001)** "Switch-based mechanism of kinesin motors." *Nature* 411: 439-445.
- Kim AJ & Endow SA (2000)** "A kinesin family tree." *J Cell Sci* 113 Pt 21: 3681-3682.
- Kirchner J, Seiler S, Fuchs S & Schliwa M (1999a)** "Functional anatomy of the kinesin molecule in vivo." *Embo J* 18: 4404-4413.

- 
- Kirchner J, Woehlke G & Schliwa M** (1999b) "Universal and unique features of kinesin motors: insights from a comparison of fungal and animal conventional kinesins." *Biol Chem* 380: 915-921.
- Kozielski F, Sack S, Marx A, Thormählen M, Schonbrunn E, Biou V, Thompson A, Mandelkow EM & Mandelkow E** (1997) "The crystal structure of dimeric kinesin and implications for microtubule-dependent motility." *Cell* 91: 985-994.
- Kull FJ, Sablin EP, Lau R, Fletterick RJ & Vale RD** (1996) "Crystal structure of the kinesin motor domain reveals a structural similarity to myosin." *Nature* 380: 550-555.
- Kull FJ & Endow SA** (2002) "Kinesin: switch I & II and the motor mechanism." *J Cell Sci* 115: 15-23.
- Laemmli UK** (1970) "Cleavage of structural proteins during the assembly of the head of bacteriophage T4." *Nature* 356: 722-725.
- Lawrence CJ, Malmberg RL, Muszynski MG & Dawe RK** (2002) "Maximum likelihood methods reveal conservation of function among closely related kinesin families." *J Mol Evol* 54: 42-53.
- Lehmler C, Steinberg G, Snetselaar KM, Schliwa M, Kahmann R & Bolker M** (1997) "Identification of a motor protein required for filamentous growth in *Ustilago maydis*." *Embo J* 16: 3464-3473.
- Ma YZ & Taylor EW** (1995a) "Mechanism of microtubule kinesin ATPase." *Biochemistry* 34: 13242-13251.
- Ma YZ & Taylor EW** (1995b) "Kinetic mechanism of kinesin motor domain." *Biochemistry* 34: 13233-13241.
- Ma YZ & Taylor EW** (1997a) "Interacting head mechanism of microtubule-kinesin ATPase." *J Biol Chem* 272: 724-730.
- Ma YZ & Taylor EW** (1997b) "Kinetic mechanism of a monomeric kinesin construct." *J Biol Chem* 272: 717-723.
- Majdic U** (1999) "*Untersuchungen zur Geschwindigkeits- und Polaritätsdetermination bei Kinesinen.*" PhD thesis, Adolf-Butenandt-Institut für Zellbiologie, Ludwig-Maximilians-Universität München.
- Mandelkow E & Johnson KA** (1998) "The structural and mechanochemical cycle of kinesin." *Trends Biochem Sci* 23: 429-433.
- Mandelkow E & Hoenger A** (1999) "Structures of kinesin and kinesin-microtubule interactions." *Curr Opin Cell Biol* 11: 34-44.
- Mandelkow E-M, Herrmann M & Rühl U** (1985) "Tubulin domains probed by limited proteolysis and subunit-specific antibodies." *J Mol Biol* 185: 311-327.
- Miki H, Setou M, Kaneshiro K & Hirokawa N** (2001) "All kinesin superfamily protein, KIF, genes in mouse and human." *Proc Natl Acad Sci U S A* 98: 7004-7011.

- 
- Morii H, Takenawa T, Arisaka F & Shimizu T** (1997) "Identification of kinesin neck region as a stable alpha-helical coiled coil and its thermodynamic characterization." *Biochemistry* 36: 1933-1942.
- O'Connell MJ, Meluh PB, Rose MD & Morris NR** (1993) "Suppression of the bimC4 mitotic spindle defect by deletion of klpA, a gene encoding a KAR3-related kinesin-like protein in *Aspergillus nidulans*." *J Cell Biol* 120: 153-162.
- Paschal BM & Vallee RB** (1993) "Microtubule and axoneme gliding assays for force production by microtubule motor proteins." *Methods Cell Biol* 39: 65-74.
- Patel N, Thierry-Mieg D & Mancillas JR** (1993) "Cloning by insertional mutagenesis of a cDNA encoding *Caenorhabditis elegans* kinesin heavy chain." *Proc Natl Acad Sci U S A* 90: 9181-9185.
- Reddy AS & Day IS** (2001) "Kinesins in the *Arabidopsis* genome: A comparative analysis among eukaryotes." *BMC Genomics* 2: 1-13.
- Requena N, Alberti-Segui C, Winzenburg E, Horn C, Schliwa M, Philippsen P, Liese R & Fischer R** (2001) "Genetic evidence for a microtubule-destabilizing effect of conventional kinesin and analysis of its consequences for the control of nuclear distribution in *Aspergillus nidulans*." *Mol Microbiol* 42: 121-132.
- Rice S, Lin AW, Safer D, Hart CL, Naber N, Carragher BO, Cain SM, Pechatnikova E, Wilson-Kubalek EM, Whittaker M, Pate E, Cooke R, Taylor EW, Milligan RA & Vale RD** (1999) "A structural change in the kinesin motor protein that drives motility." *Nature* 402: 778-784.
- Riddles PW, Blakeley RL & Zerner B** (1983) "Reassessment of Ellman's reagent." *Methods Enzymol* 91: 49-60.
- Romberg L, Pierce DW & Vale RD** (1998) "Role of the kinesin neck region in processive microtubule-based motility." *J Cell Biol* 140: 1407-1416.
- Sablin EP & Fletterick RJ** (2001) "Nucleotide switches in molecular motors: structural analysis of kinesins and myosins." *Curr Opin Struct Biol* 11: 716-724.
- Sack S, Müller J, Marx A, Thormählen M, Mandelkow EM, Brady ST & Mandelkow E** (1997) "X-ray structure of motor and neck domains from rat brain kinesin." *Biochemistry* 36: 16155-16165.
- Sakowicz R, Farlow S & Goldstein LS** (1999) "Cloning and expression of kinesins from the thermophilic fungus *Thermomyces lanuginosus*." *Protein Sci* 8: 2705-2710.
- Sambrook J, Fritsch EF & Maniatis T** (1989) "*Molecular cloning: a laboratory manual*." Cold Spring Harbor Laboratory Press.
- Saxton WM, Hicks J, Goldstein LS & Raff EC** (1991) "Kinesin heavy chain is essential for viability and neuromuscular functions in *Drosophila*, but mutants show no defects in mitosis." *Cell* 64: 1093-1102.

- 
- Schäfer F, Deluca D, Majdic U, Kirchner J, Schliwa M, Moroder L & Woehlke G** (2003) "A conserved tyrosine in the neck of a fungal kinesin regulates the catalytic motor core." *Embo J* 22: 450-458.
- Schief WR & Howard J** (2001) "Conformational changes during kinesin motility." *Curr Opin Cell Biol* 13: 19-28.
- Schief WR, Clark RH, Crevenna AH & Howard J** (2004) "Inhibition of kinesin motility by ADP and phosphate supports a hand-over-hand mechanism." *Proc Natl Acad Sci U S A* 101: 1183-1188.
- Schliwa M** (1989) "Head and tail." *Cell* 56: 719-720.
- Schliwa M & Woehlke G** (2003) "Molecular motors." *Nature* 422: 759-765.
- Schnitzer MJ & Block SM** (1997) "Kinesin hydrolyses one ATP per 8-nm step." *Nature* 388: 386-390.
- Schoch CL, Aist JR, Yoder OC & Gillian Turgeon B** (2003) "A complete inventory of fungal kinesins in representative filamentous ascomycetes." *Fungal Genet Biol* 39: 1-15.
- Seeberger C, Mandelkow E & Meyer B** (2000) "Conformational preferences of a synthetic 30mer peptide from the interface between the neck and stalk regions of kinesin." *Biochemistry* 39: 12558-12567.
- Seiler S, Nargang FE, Steinberg G & Schliwa M** (1997) "Kinesin is essential for cell morphogenesis and polarized secretion in *Neurospora crassa*." *Embo J* 16: 3025-3034.
- Seiler S, Plamann M & Schliwa M** (1999) "Kinesin and dynein mutants provide novel insights into the roles of vesicle traffic during cell morphogenesis in *Neurospora*." *Curr Biol* 9: 779-785.
- Seiler S, Kirchner J, Horn C, Kallipolitou A, Woehlke G & Schliwa M** (2000) "Cargo binding and regulatory sites in the tail of fungal conventional kinesin." *Nat Cell Biol* 2: 333-338.
- Shimizu T, Thorn KS, Ruby A & Vale RD** (2000) "ATPase kinetic characterization and single molecule behavior of mutant human kinesin motors defective in microtubule-based motility." *Biochemistry* 39: 5265-5273.
- Sindelar CV, Budny MJ, Rice S, Naber N, Fletterick R & Cooke R** (2002) "Two conformations in the human kinesin power stroke defined by X-ray crystallography and EPR spectroscopy." *Nat Struct Biol* 9: 844-848.
- Skiniotis G, Surrey T, Altmann S, Gross H, Song YH, Mandelkow E & Hoenger A** (2003) "Nucleotide-induced conformations in the neck region of dimeric kinesin." *Embo J* 22: 1518-1528.
- Song YH, Marx A, Müller J, Woehlke G, Schliwa M, Krebs A, Hoenger A & Mandelkow E** (2001) "Structure of a fast kinesin: implications for ATPase mechanism and interactions with microtubules." *Embo J* 20: 6213-6225.

- 
- Steinberg G & Schliwa M** (1995) "The *Neurospora* organelle motor: a distant relative of conventional kinesin with unconventional properties." *Mol Biol Cell* 6: 1605-1618.
- Steinberg G** (1997) "A kinesin-like mechanoenzyme from the zygomycete *Syncephalastrum racemosum* shares biochemical similarities with conventional kinesin from *Neurospora crassa*." *Eur J Cell Biol* 73: 124-131.
- Stenoien DL & Brady ST** (1997) "Immunochemical analysis of kinesin light chain function." *Mol Biol Cell* 8: 675-689.
- Stewart RJ, Thaler JP & Goldstein LS** (1993) "Direction of microtubule movement is an intrinsic property of the motor domains of kinesin heavy chain and *Drosophila* ncd protein." *Proc Natl Acad Sci U S A* 90: 5209-5213.
- Studier FW, Rosenberg AH, Dunn JJ & Dubendorff JW** (1990) "Use of T7 RNA polymerase to direct expression of cloned genes." *Methods Enzymol* 185: 60-89.
- Sugata K, Nakamura M, Ueki S, Fajer PG & Arata T** (2004) "ESR reveals the mobility of the neck linker in dimeric kinesin." *Biochem Biophys Res Commun* 314: 447-451.
- Svoboda K, Schmidt CF, Schnapp BJ & Block SM** (1993) "Direct observation of kinesin stepping by optical trapping interferometry." *Nature* 365: 721-727.
- Tanaka Y, Kanai Y, Okada Y, Nonaka S, Takeda S, Harada A & Hirokawa N** (1998) "Targeted disruption of mouse conventional kinesin heavy chain, kif5B, results in abnormal perinuclear clustering of mitochondria." *Cell* 93: 1147-1158.
- Thormählen M, Marx A, Sack S & Mandelkow E** (1998) "The coiled-coil helix in the neck of kinesin." *J Struct Biol* 122: 30-41.
- Tomishige M & Vale RD** (2000) "Controlling kinesin by reversible disulfide cross-linking. Identifying the motility-producing conformational change." *J Cell Biol* 151: 1081-1092.
- Tripet B, Vale RD & Hodges RS** (1997) "Demonstration of coiled-coil interactions within the kinesin neck region using synthetic peptides. Implications for motor activity." *J Biol Chem* 272: 8946-8956.
- Tripet B & Hodges RS** (2002) "Helix capping interactions stabilize the N-terminus of the kinesin neck coiled-coil." *J Struct Biol* 137: 220-235.
- Vale RD, Reese TS & Sheetz MP** (1985) "Identification of a novel force-generating protein, kinesin, involved in microtubule-based motility." *Cell* 42: 39-50.
- Vale RD** (1996) "Switches, latches, and amplifiers: common themes of G proteins and molecular motors." *J Cell Biol* 135: 291-302.
- Vale RD, Funatsu T, Pierce DW, Romberg L, Harada Y & Yanagida T** (1996) "Direct observation of single kinesin molecules moving along microtubules." *Nature* 380: 451-453.
- Vale RD & Fletterick RJ** (1997) "The design plan of kinesin motors." *Annu Rev Cell Dev Biol* 13: 745-777.

- 
- Vale RD, Case R, Sablin E, Hart C & Fletterick R** (2000) "Searching for kinesin's mechanical amplifier." *Philos Trans R Soc Lond B Biol Sci* 355: 449-457.
- Vale RD & Milligan RA** (2000) "The way things move: looking under the hood of molecular motor proteins." *Science* 288: 88-95.
- Verhey KJ, Lizotte DL, Abramson T, Barenboim L, Schnapp BJ & Rapoport TA** (1998) "Light chain-dependent regulation of Kinesin's interaction with microtubules." *J Cell Biol* 143: 1053-1066.
- Verhey KJ & Rapoport TA** (2001) "Kinesin carries the signal." *Trends Biochem Sci* 26: 545-550.
- Vetter IR & Wittinghofer A** (2001) "The guanine nucleotide-binding switch in three dimensions." *Science* 294: 1299-1304.
- Woehlke G, Ruby AK, Hart CL, Ly B, Hom-Booher N & Vale RD** (1997) "Microtubule interaction site of the kinesin motor." *Cell* 90: 207-216.
- Woehlke G & Schliwa M** (2000) "Walking on two heads: the many talents of kinesin." *Nat Rev Mol Cell Biol* 1: 50-58.
- Woehlke G** (2001) "A look into kinesin's powerhouse." *FEBS Lett* 508: 291-294.
- Wu Q, Sandrock TM, Turgeon BG, Yoder OC, Wirsal SG & Aist JR** (1998) "A fungal kinesin required for organelle motility, hyphal growth, and morphogenesis." *Mol Biol Cell* 9: 89-101.
- Xiang X & Plamann M** (2003) "Cytoskeleton and motor proteins in filamentous fungi." *Curr Opin Microbiol* 6: 628-633.
- Yang JT, Saxton WM, Stewart RJ, Raff EC & Goldstein LS** (1990) "Evidence that the head of kinesin is sufficient for force generation and motility in vitro." *Science* 249: 42-47.
- Yildiz A, Tomishige M, Vale RD & Selvin PR** (2004) "Kinesin Walks Hand-Over-Hand." *Science* 303: 676-678.
- Young EC, Mahtani HK & Gelles J** (1998) "One-headed kinesin derivatives move by a nonprocessive, low-duty ratio mechanism unlike that of two-headed kinesin." *Biochemistry* 37: 3467-3479.
- Zhou NE, Kay CM & Hodges RS** (1993) "Disulfide bond contribution to protein stability: positional effects of substitution in the hydrophobic core of the two-stranded  $\alpha$ -helical coiled-coil." *Biochemistry* 32: 3178-3187.

## Acknowledgements

I thank Prof. Dr. Manfred Schliwa for his guidance and support during my time in his laboratory.

I thank Prof. Dr. Charles N. David for advocating my thesis in the biology faculty.

I thank PD Dr. Günther Woehlke for his support and assistance with laboratory and computational problems and his willingness to discuss strange or confusing results.

I thank PD Dr. Ralph Gräf for many very helpful tips and tricks around laboratory and computational work.

I thank Athina Kallipolitou and Friederike Bathe for many important discussions and active assistance concerning kinesins and life in general.

The girls from room #315 (Athina Kallipolitou, Friederike Bathe, Sarah Adio, Judith Mergler) helped a lot to keep going, to forget disappointments, to overcome trouble, to enjoy a good lunch or cake, and to improve music in the lab.

I thank my husband Ingo for his patience and understanding during hard times when experiments just did not work and his continuous support, motivation and appreciation of my work.

---

## Curriculum vitae

### personal data

name: Katrin Hahlen  
day of birth: 3.5.1972  
birth place: Köln  
nationality: german

### school education

1978-1982 primary school in Wesseling-Urfeld  
1982-1991 high school in Bornheim-Hersel  
1991 graduation from high school (Abitur)

### university education

1991-1998 studies of computer science at the University of Bonn  
1994 prediploma exams in computer science (Vordiplom)  
1993-1999 studies of biology at the University of Bonn  
1995 prediploma exams in biology (Vordiplom)  
March-Dec. 1996 scholarship of the DAAD for two terms of biological studies at the University of New South Wales, Sydney  
1998 diploma exams in biology (Diplom)  
Sept.-Dec. 1998 research for the biology diploma thesis in the laboratory of Prof. Dr. David Sandeman at the University of New South Wales, Sydney, supported by the Flora Immerschitt Stiftung  
Jan.-Aug. 1999 biology diploma thesis in the laboratory of Prof. Dr. Hans-Georg Heinzel at the University of Bonn. Title: "Beeinflussung der stomatogastrischen neuronalen Netzwerke durch die Sensorik des Kopfes beim australischen Flußkrebs"  
Jan. 2000-July 2004 PhD thesis in the laboratory of Prof. Dr. Manfred Schliwa at the University of Munich. Title: "Crosslinking studies on the conventional kinesin of *Neurospora crassa*"